

ผลของการปรับปรุงพื้นผิวเส้นใยเคลือบข้าวต่อสมบัติทางกายภาพของ
คอมโพสิทระหว่างเส้นใยเคลือบข้าวกับยางธรรมชาติ

นางสาวดดาวรรณ ศรีสุวรรณ

วิทยานิพนธ์นี้เป็นส่วนหนึ่งของการศึกษาตามหลักสูตรปริญญาวิศวกรรมศาสตรมหาบัณฑิต
สาขาวิชาวิศวกรรมพอลิเมอร์
มหาวิทยาลัยเทคโนโลยีสุรนารี
ปีการศึกษา 2555

**EFFECT OF RICE HUSK FIBER SURFACE TREATMENT
ON PHYSICAL PROPERTIES OF RICE HUSK
FIBER/NATURAL RUBBER COMPOSITES**

Ladawan Srisuwan

**A Thesis Submitted in Partial Fulfillment of the Requirements for the
Degree of Master of Engineering in Polymer Engineering**

Suranaree University of Technology

Academic Year 2012

**EFFECT OF RICE HUSK FIBER SURFACE TREATMENT
ON PHYSICAL PROPERTIES OF RICE HUSK
FIBER/NATURAL RUBBER COMPOSITES**

Suranaree University of Technology has approved this thesis submitted in partial fulfillment of the requirements for a Master's Degree.

Thesis Examining Committee

(Asst. Prof. Dr. Wimonlak Sutapun)

Chairperson

(Asst. Prof. Dr. Nitinat Suppakarn)

Member (Thesis Advisor)

(Asst. Prof. Dr. Kasama Jarukumjorn)

Member

(Asst. Prof. Dr. Pranee Chumsamrong)

Member

(Assoc. Prof. Dr. Yupaporn Ruksakulpiwat)

Member

(Prof. Dr. Sukit Limpijumnong)

Vice Rector for Academic Affairs

(Assoc. Prof. Flt. Lt. Dr. Kontorn Chamniprasart)

Dean of Institute of Engineering

ดศาวรรณ ศรีสุวรรณ : ผลของการปรับปรุงพื้นผิวเส้นใยเคลือบข้าวต่อสมบัติทางกายภาพของคอมโพสิตระหว่างเส้นใยเคลือบข้าวกับยางธรรมชาติ (EFFECT OF RICE HUSK FIBER SURFACE TREATMENT ON PHYSICAL PROPERTIES OF RICE HUSK FIBER/ NATURAL RUBBER COMPOSITES) อาจารย์ที่ปรึกษา : ผู้ช่วยศาสตราจารย์ ดร.นิธินาถ ศุภกาญจน์, 156 หน้า.

ในวิทยานิพนธ์นี้ เส้นใยเคลือบข้าวซึ่งเป็นผลผลิตพลอยได้จากกระบวนการสีข้าวถูกใช้เป็นส่วนตัวเติมเสริมแรงสำหรับการเตรียมคอมโพสิตยางธรรมชาติ เส้นใยเคลือบข้าวที่ใช้มีขนาดระหว่าง 150-300 ไมโครเมตร การปรับปรุงพื้นผิวเส้นใยเคลือบข้าวได้แก่ การปรับปรุงพื้นผิวด้วยสารละลายกรด การปรับปรุงพื้นผิวด้วยสารละลายด่าง และการปรับปรุงพื้นผิวด้วยสารคู่ควบไซเลน ถูกนำมาใช้เพื่อปรับปรุงความเข้ากันได้ระหว่างเส้นใยเคลือบข้าวและยางธรรมชาติ

ผลของปริมาณเส้นใยเคลือบข้าวต่อสมบัติการคงรูป สมบัติทางกล และต้นทุนวิทยาของคอมโพสิตระหว่างเส้นใยเคลือบข้าวกับยางธรรมชาติได้ถูกตรวจสอบ จากผลการศึกษาพบว่า เมื่อเพิ่มปริมาณเส้นใยเคลือบข้าว ค่ามอดูลัสที่ 100 เปอร์เซนต์การดึงยืด และค่ามอดูลัสที่ 300 เปอร์เซนต์การดึงยืดของคอมโพสิตของยางธรรมชาติมีค่าเพิ่มขึ้น ในขณะที่ค่าการทนทานต่อแรงดึง ค่าเปอร์เซนต์การยืดตัวก่อนขาด และค่าการทนทานต่อการฉีกขาดมีค่าลดลง อย่างไรก็ตาม ปริมาณเส้นใยเคลือบข้าวไม่มีผลต่อเวลาการสกรอชและเวลาการคงรูปของคอมโพสิตระหว่างเส้นใยเคลือบข้าวและยางธรรมชาติ ภาพจากกล้องจุลทรรศน์อิเล็กตรอนแบบส่องกราดของคอมโพสิตระหว่างเส้นใยเคลือบข้าวและยางธรรมชาติแสดงให้เห็นการเกาะกลุ่มของเส้นใยเคลือบข้าวในยางธรรมชาติ เมื่อพิจารณาจากสมบัติทางกลและราคาต้นทุนของคอมโพสิตของยางธรรมชาติ ปริมาณเส้นใยเคลือบข้าวที่เหมาะสมคือ 40 ส่วนใน 100 ส่วนของยางธรรมชาติ

เส้นใยเคลือบข้าวถูกปรับปรุงพื้นผิวด้วยสารละลายกรดหรือสารละลายด่างที่เวลาการปรับปรุงพื้นผิวต่างๆ และเส้นใยที่ผ่านการปรับปรุงพื้นผิวถูกนำไปตรวจสอบ เมื่อเปรียบเทียบกับผลของเส้นใยเคลือบข้าวที่ไม่ผ่านการปรับปรุงพื้นผิว รูปแบบการเสื่อมสลายทางความร้อนและผลอินฟราเรดสเปกโตรสโคปีของเส้นใยเคลือบข้าวที่ผ่านการปรับปรุงพื้นผิวด้วยสารละลายกรดไม่เปลี่ยนแปลง ในทางตรงกันข้าม ผลของการวิเคราะห์เทอร์โมกราวิเมตริกและอินฟราเรดสเปกโตรสโคปีของเส้นใยเคลือบข้าวที่ผ่านการปรับปรุงพื้นผิวด้วยสารละลายด่างแสดงการหายไปของเฮมิเซลลูโลสและลิกนิน เวลาการปรับปรุงพื้นผิวไม่ส่งผลอย่างมีนัยสำคัญต่อสมบัติของเส้นใยเคลือบข้าวที่ผ่านการปรับปรุงพื้นผิวด้วยสารละลายกรดและสารละลายด่าง หลังจากนั้น เส้นใยเคลือบข้าวที่ผ่านการปรับปรุงพื้นผิวถูกนำมาใช้เป็นส่วนตัวเติมสำหรับการเตรียมคอมโพสิตของยางธรรมชาติ

เวลาการสกอร์ชของคอมโพสิตของยางธรรมชาติที่เดิมเส้นใยเคลือบขาวที่ผ่านการปรับปรุงพื้นผิวด้วยสารละลายต่างมีค่ามากกว่าเวลาการสกอร์ชของคอมโพสิตของยางธรรมชาติที่เดิมเส้นใยเคลือบขาวที่ผ่านการปรับปรุงพื้นผิวด้วยสารละลายกรด เมื่อเวลาการปรับปรุงพื้นผิวเพิ่มขึ้น เวลาการสกอร์ชของคอมโพสิตของยางธรรมชาติที่เดิมเส้นใยเคลือบขาวที่ผ่านการปรับปรุงพื้นผิวด้วยสารละลายกรด และคอมโพสิตของยางธรรมชาติที่เดิมเส้นใยเคลือบขาวที่ผ่านการปรับปรุงพื้นผิวด้วยสารละลายต่างเปลี่ยนแปลงเล็กน้อย ในขณะที่เวลาการคงรูปของคอมโพสิตทั้งสองชนิดมีค่าคงที่ ค่ามอดูลัสที่ 100 เปอร์เซนต์การดึงยืด ค่ามอดูลัสที่ 300 เปอร์เซนต์การดึงยืด และค่าการทนทานต่อการฉีกขาดของคอมโพสิตของยางธรรมชาติที่เดิมเส้นใยเคลือบขาวที่ผ่านการปรับปรุงพื้นผิวด้วยสารละลายกรด และคอมโพสิตของยางธรรมชาติที่เดิมเส้นใยเคลือบขาวที่ผ่านการปรับปรุงพื้นผิวด้วยสารละลายต่างไม่มีความแตกต่างกันอย่างมีนัยสำคัญ การปรับปรุงพื้นผิวเส้นใยเคลือบขาวด้วยสารละลายต่างแสดงประสิทธิภาพในการปรับปรุงสมบัติทางกลของคอมโพสิตของยางธรรมชาติมากกว่าการปรับปรุงพื้นผิวเส้นใยเคลือบขาวด้วยสารละลายกรด เมื่อเปรียบเทียบระหว่างคอมโพสิตของยางธรรมชาติที่เดิมเส้นใยเคลือบขาวที่ผ่านการปรับปรุงพื้นผิวด้วยสารละลายต่าง คอมโพสิตของยางธรรมชาติที่เดิมเส้นใยเคลือบขาวที่ผ่านการปรับปรุงพื้นผิวด้วยสารละลายต่างที่เวลา 2 ชั่วโมงแสดงสมบัติทางกลที่เหมาะสมที่สุด

เส้นใยเคลือบขาวที่ถูกปรับปรุงพื้นผิวด้วยสารละลายต่างเป็นเวลา 2 ชั่วโมงถูกนำไปปรับปรุงพื้นผิวด้วยสารคู่ควบไซเลน 69 ที่ปริมาณต่างๆ เมื่อปริมาณสารคู่ควบไซเลน 69 เพิ่มขึ้นรูปแบบการเสื่อมสลายทางความร้อนของเส้นใยที่ผ่านการปรับปรุงพื้นผิวด้วยสารคู่ควบไซเลนไม่เปลี่ยนแปลง อินฟราเรดสเปกโตรสโคปีสเปกตรัมของเส้นใยที่ผ่านการปรับปรุงพื้นผิวด้วยสารคู่ควบไซเลนยืนยันการติดอยู่ของสารคู่ควบไซเลนที่พื้นผิวของเส้นใยเคลือบขาว สำหรับคอมโพสิตของยางธรรมชาติ เวลาการสกอร์ชของคอมโพสิตของยางธรรมชาติที่เดิมเส้นใยเคลือบขาวที่ผ่านการปรับปรุงด้วยสารคู่ควบไซเลนมีค่ามากกว่าเวลาการสกอร์ชของคอมโพสิตของยางธรรมชาติที่เดิมเส้นใยเคลือบขาวที่ผ่านการปรับปรุงด้วยสารละลายต่าง เมื่อปริมาณสารคู่ควบไซเลน 69 เพิ่มขึ้นไม่มีการเปลี่ยนแปลงของเวลาการสกอร์ชของคอมโพสิตของยางธรรมชาติ คอมโพสิตของยางธรรมชาติที่เดิมเส้นใยเคลือบขาวที่ผ่านการปรับปรุงด้วยสารคู่ควบไซเลนที่ปริมาณ 5 เปอร์เซนต์ โดยน้ำหนักแสดงค่าสูงสุดของค่ามอดูลัสที่ 100 เปอร์เซนต์การดึงยืด และค่ามอดูลัสที่ 300 เปอร์เซนต์การดึงยืดค่าการทนทานต่อแรงดึง และค่าการทนทานต่อการฉีกขาด

สาขาวิชา วิศวกรรมพอลิเมอร์

ปีการศึกษา 2555

ลายมือชื่อนักศึกษา _____

ลายมือชื่ออาจารย์ที่ปรึกษา _____

ลายมือชื่ออาจารย์ที่ปรึกษาร่วม _____

LADAWAN SRISUWAN : EFFECT OF RICE HUSK FIBER SURFACE
TREATMENT ON PHYSICAL PROPERTIES OF RICE HUSK FIBER/
NATURAL RUBBER COMPOSITES. THISIS ADVISOR : ASST. PROF.
NITINAT SUPPAKARN, Ph.D., 156 PP.

RICE HUSK FIBER/NATURAL RUBBER COMPOSITES/ACID
TREATMENT/ALKALI TREATMET/SILANE TREATMENT

In this study, rice husk fiber (RHF), as a byproduct from a rice milling process, was used as reinforcing filler for preparing natural rubber (NR) composites. RHF retained in sieve size ranging between 150-300 μm was used. RHF surface treatments, *i.e.*, acid treatment, alkali treatment and silane treatment, were used to improve compatibility between RHF and NR matrix.

Effect of RHF content on cure characteristics, mechanical properties and morphological properties of RHF/NR composites was investigated. With increasing RHF content, modulus at 100% strain (M100) and modulus at 300% strain (M300) of the NR composites increased while elongation at break, tensile strength and tear strength decreased. Nonetheless, scorch time and cure time of RHF/NR composites were not affected by RHF content. SEM micrographs of RHF/NR composites showed RHF agglomeration in NR matrix. Based on the mechanical properties and material cost of the NR composites, the optimum content of RHF was 40 phr.

RHF was treated with acid or alkali solutions at various treatment times and the treated RHF was characterized. As compared with the corresponding results of untreated RHF (UT), thermal decomposition patterns and FTIR results of acid treated

RHF (ACT) were not changed. On the other hand, TGA and FTIR results of alkali treated RHF (ALT) showed the disappearance of hemicellulose and lignin. Treatment time insignificantly affected the properties of ACT and ALT. Then, the treated RHF was used as filler for producing NR composites. Scorch time of ALT/NR composites was longer than that of ACT/NR composites. With increasing treatment time, scorch time of ACT/NR and ALT/NR composites slightly changed whereas their cure time remained constant. M100, M300 and tear strength of ACT/NR and ALT/NR composites were insignificant difference. Alkali treatment showed more effective improvement in the mechanical properties of the NR composites than acid treatment. Among the ALT/NR composites, the NR composite containing ALT at 2 h treatment time showed the optimum mechanical properties.

RHF was pretreated with alkali solution for 2 h before treating RHF surface with Si69 at various Si69 contents. With increasing Si69 content, thermal decomposition patterns of silane treated RHF (ST) were not changed. FTIR spectra of ST confirmed that ST was attached on RHF surface. For NR composites, scorch time of ST/NR composites was longer than that of ALT/NR composites. With increasing Si69 content, there was no change in scorch time of NR composites. ST/NR composites showed the maximum values of M100, M300, tensile strength and tear strength at Si69 content of 5 wt%.

School of Polymer Engineering

Academic Year 2012

Student's Signature _____

Advisor's Signature _____

Co-advisor's Signature _____

ACKNOWLEDGEMENTS

I am grateful for the supported of Suranaree University of Technology and the Center of Excellence on Petrochemical and Materials Technology.

I would like to deeply thank my thesis advisor, Asst. Prof. Dr. Nitinat Suppakarn, for her suggestion, advice, encouragement and support throughout the period of the study. In addition, my gratitude is expressed to the thesis co-advisor, Asst. Prof. Dr. Kasama Jarukumjorn, for her valuable suggestions. My appreciation goes to Asst. Prof. Dr. Wimonlak Sutapun, Asst. Prof. Dr. Pranee Chumsamrong and Assoc. Prof. Dr. Yupaporn Raksakulpiwat, for their valuable suggestions and guidance as committee members.

I am sincerely grateful to Chanel Chemical, Co., Ltd. for rubber chemical support and Louis T. Leonowens (Thailand) Co., Ltd. for supplying Si69. Furthermore, I would especially like to thank lecturers, staff members, and my friends in the School of Polymer Engineering.

Finally, I would also like to thank my parents, Mr. Manut and Mrs. Potchana Srisuwan and my sister, Mrs. Thasani Kongsuwan, for their support and encouragement throughout my life.

Ladawan Srisuwan

TABLE OF CONTENTS

	Page
ABSTRACT (THAI)	I
ABSTRACT (ENGLISH)	III
ACKNOWLEDGEMENTS	V
TABLE OF CONTENTS.....	VI
LIST OF TABLES	XI
LIST OF FIGURES	XIII
SYMBOLS AND ABBREVIATIONS.....	XVIII
CHAPTER	
I INTRODUCTION.....	1
1.1 Background.....	1
1.2 Research objectives.....	4
1.3 Scope and limitation	4
II LITERATURE REVIEW	6
2.1 Rice husk.....	6
2.1.1 Thermal properties	8
2.1.2 Chemical functional analysis	11
2.1.3 Morphological properties.....	12
2.2 RH/polymer composites.....	15
2.3 RH/rubber composites	17

TABLE OF CONTENTS (Continued)

	Page
2.4 Compatibility improvement between RH and polymer matrices	20
2.4.1 RH surface treatment	21
2.4.1.1 Physical method	21
2.4.1.2 Chemical method	24
2.4.2 Addition of compatibilizer	31
2.4.3 Matrix modification	39
III EXPERIMENTAL	40
3.1 Material	40
3.2 Experimental	41
3.2.1 Preparation of RHF	41
3.2.2 Surface treatment of RHF	41
3.2.2.1 Acid treatment.....	41
3.2.2.2 Alkali treatment	41
3.2.2.3 Silane treatment	42
3.2.3 Characterization of untreated and surface treated RHF	42
3.2.3.1 Thermal properties	42
3.2.3.2 Functional group analysis	42
3.2.3.3 Morphological properties.....	43

TABLE OF CONTENTS (Continued)

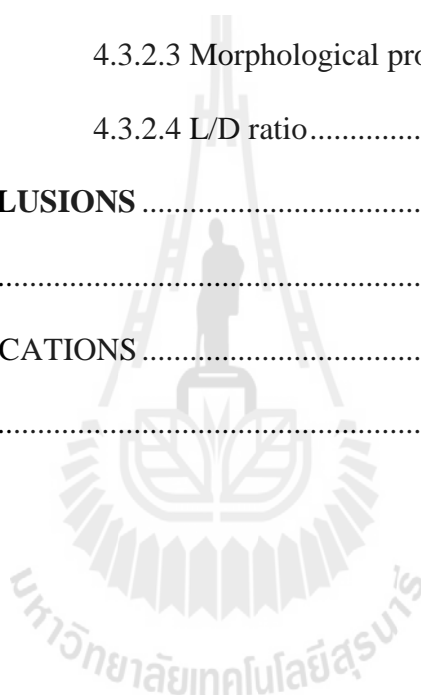
	Page
3.2.3.4 Fiber dimension	43
3.2.4 Preparation of RHF/NR composites	43
3.2.5 Characterization of RHF/NR composites	45
3.2.5.1 Cure characteristics	45
3.2.5.2 Mechanical properties	45
3.2.5.3 Morphological properties	46
3.2.5.4 Crosslink density	46
3.2.5.5 Fiber length and diameter	47
VI RESULTS AND DISCUSSION	48
4.1 Effect of rice husk fiber content on physical properties of RHF/NR composites	48
4.1.1 Cure characteristics	48
4.1.2 Mechanical properties and crosslink density	53
4.1.2.1 Tensile properties	53
4.1.2.2 Tear properties	58
4.1.2.3 Crosslink density	59
4.1.3 Morphological properties	62
4.2 Effect of acid and alkali treatments on physical properties of RHF and RHF/NR composites	64
4.2.1 Fiber characterization	64
4.2.1.1 Thermal properties	64

TABLE OF CONTENTS (Continued)

	Page
4.2.1.2 Functional group analysis	70
4.2.1.3 Morphological properties	75
4.2.1.4 Length/diameter (L/D) ratio	81
4.2.2 Composite characterization	83
4.2.2.1 Cure characteristics	83
4.2.2.2 Mechanical properties and crosslink density	91
4.2.2.2.1 Tensile properties	91
4.2.2.2.2 Tear properties	96
4.2.2.2.3 Crosslink density	97
4.2.2.3 Morphological properties	99
4.3 Effect of bis (triethixysislypropyl) tetrasulfide (Si69) content on physical properties of RHF and RHF/NR composites	103
4.3.1 Fiber characterization	103
4.3.1.1 Thermal properties	103
4.3.1.2 Functional group analysis	106
4.3.1.3 Morphological properties	109
4.3.2 Composite characterization	112
4.3.2.1 Cure characteristics	112
4.3.2.2 Mechanical properties and crosslink density	118

TABLE OF CONTENTS (Continued)

	Page
4.3.2.2.1 Tensile properties.....	118
4.3.2.2.2 Tear properties	122
4.3.2.2.3 Crosslink density.....	123
4.3.2.3 Morphological properties.....	126
4.3.2.4 L/D ratio.....	128
V CONCLUSIONS	130
REFERENCES.....	133
APPENDIX A PUBLICATIONS	146
BIOGRAPHY	156



LIST OF TABLES

Table	Page
2.1 Chemical compositions of RH reported by several research groups	8
3.1 Formulation of RHF/NR composites	44
4.1 Cure characteristics of gum NR and NR composites at various RHF contents	52
4.2 Mechanical properties and crosslink density of gum NR and NR composites at various RHF contents	61
4.3 Thermal decomposition temperatures of UT, ACT and ALT at various treatment times	69
4.4 FTIR peak positions of UT, ACT and ALT at various treatment times	74
4.5 L/D ratio of UT, ACT and ALT at various treatment times	82
4.6 Cure characteristics of UT/NR, ACT/NR and ALT/NR composites at various treatment times	90
4.7 Mechanical properties and crosslink density of UT/NR, ACT/NR and ALT/NR composites at various treatment times	98
4.8 Thermal decomposition temperatures of ALT and ST at various Si69 contents	105
4.9 FTIR peak positions of 2ALT and ST at various Si69 contents	108
4.10 Cure characteristics of ALT/NR and ST/NR composites at various Si69 contents	117

LIST OF TABLES (Continued)

Table	Page
4.11 Mechanical properties and crosslink density of ALT/NR and ST/NR composites at various Si69 contents	125
4.12 L/D ratio before and after mixing of UT/NR, 2ALT/NR and 5ST/NR composites.....	129



LIST OF FIGURES

Figure	Page
2.1 Structures of rice grain and RH	6
2.2 Cross sectional structure of RH	8
2.3 SEM micrographs of (a) RH structure and (b) silica profile in RH.....	12
2.4 SEM micrographs of (a) RH and (b) protuberance, outer epidermis and silica in RH.....	13
2.5 SEM micrographs of (a) outer surface and (b) cross-section of RH.....	14
2.6 FE-SEM micrograph of outer surface of RH	14
3.1 Chemical structures of (a) Bis (triethoxysilylpropyl) tetrasulfide (Si69) and (b) N-cyclohexyl-2-benzothiazole-2-sulphenamide (CBS)	40
4.1 Scorch time and cure time of gum NR and NR composites at various RHF contents	49
4.2 Minimum and maximum torques of NR and NR composites at various RHF contents	50
4.3 Torque difference of gum NR and NR composites at various RHF contents	52
4.4 Stress-strain curve of gum NR and NR composites at various RHF contents	54
4.5 Modulus at 100% strain (M100) of gum NR and NR composites at various RHF contents	55

LIST OF FIGURES (Continued)

Figure	Page
4.6 Modulus at 300% strain (M300) of gum NR and NR composites at various RHF contents.....	56
4.7 Elongation at break of gum NR and NR composites at various RHF contents	57
4.8 Tensile strength of gum NR and NR composites at various RHF contents	58
4.9 Tear strength of gum NR and NR composites at various RHF contents	59
4.10 Crosslink density of gum NR and NR composites at various RHF contents	60
4.11 SEM micrographs of (a) gum NR, (b) 10RHF/NR, (c) 20RHF/NR, (d) 30RHF/NR, (e) 40RHF/NR and (f) 50RHF/NR composites	63
4.12 TGA (a) and DTGA (b) thermograms of UT and ACT at various treatment times.....	66
4.13 TGA (a) and DTGA (b) thermograms of UT and ALT at various treatment times.....	68
4.14 FTIR spectra of UT and ACT at various treatment times.....	71
4.15 FTIR spectra of UT and ALT at various treatment times	73
4.16 SEM micrographs of outer surfaces of (a) UT, (b) 1ACT, (c) 2ACT, (d) 6ACT, (e) 12ACT and (f) 24ACT.....	76
4.17 SEM micrographs of inner surfaces of (a) UT, (b) 1ACT, (c) 2ACT, (d) 6ACT, (e) 12ACT and (f) 24ACT.....	77

LIST OF FIGURES (Continued)

Figure	Page
4.18 SEM micrographs of the outer surfaces of (a) UT, (b) 1ALT, (c) 2ALT, (d) 6ALT, (e) 12ALT and (f) 24ALT	79
4.19 SEM micrographs of inner surfaces of (a) UT, (b) 1ALT, (c) 2ALT, (d) 6ALT, (e) 12ALT and (f) 24ALT	80
4.20 Scorch time of UT/NR, ACT/NR and ALT/NR composites at various treatment times.....	85
4.21 Cure time of UT/NR, ACT/NR and ALT/NR composites at various treatment times.....	85
4.22 Minimum torque of UT/NR, ACT/NR and ALT/NR composites at various treatment times	87
4.23 Maximum torque of UT/NR, ACT/NR and ALT/NR composites at various treatment times	88
4.24 Torque difference of UT/NR, ACT/NR and ALT/NR composites at various treatment times	89
4.25 Modulus at 100% strain (M100) of UT/NR, ACT/NR and ALT/NR composites at various treatment times	92
4.26 Modulus at 300% strain (M300) of UT/NR, ACT/NR and ALT/NR composites at various treatment times	92
4.27 Elongation at break of UT/NR, ACT/NR and ALT/NR composites at various treatment times	94

LIST OF FIGURES (Continued)

Figure	Page
4.28 Tensile strength of UT/NR, ACT/NR and ALT/NR composites at various treatment times	95
4.29 Tear strength of UT/NR, ACT/NR and ALT/NR composites at various treatment times	96
4.30 Crosslink density of UT/NR, ACT/NR and ALT/NR composites at various treatment times	97
4.31 SEM micrographs of (a) UT/NR, (b) 1ACT/NR, (c) 2ACT/NR, (d) 6ACT/NR, (e) 12ACT/NR and (f) 24ACT/NR composites	100
4.32 SEM micrographs of (a) UT/NR, (b) 1ALT/NR, (c) 2ALT/NR, (d) 6ALT/NR, (e) 12ALT/NR and (f) 24ALT/NR composites	102
4.33 TGA (a) and DTGA (b) thermograms of ALT and ST at various Si69 contents	104
4.34 FTIR spectra of 2ALT and ST at various Si69 contents.....	107
4.35 SEM micrographs of outer surfaces of (a) 2ALT, (b) 2ST, (c) 5ST and (d) 10ST	110
4.36 SEM micrographs of inner surfaces of (a) 2ALT, (b) 2ST, (c) 5ST and (d) 10ST	111
4.37 Scorch time of ALT/NR and ST/NR composites at various Si69 contents	113
4.38 Cure time of ALT/NR and ST/NR composites at various Si69 contents	113

LIST OF FIGURES (Continued)

Figure	Page
4.39 Minimum torque of ALT/NR and ST/NR composites at various Si69 contents	115
4.40 Maximum torque of ALT/NR and ST/NR composites at various Si69 contents	115
4.41 Torque difference of ALT/NR and ST/NR composites at various Si69 contents	117
4.42 Modulus at 100% strain (M100) of ALT/NR and ST/NR composites at various Si69 contents	119
4.43 Modulus at 300% strain (M300) of ALT/NR and ST/NR composites at various Si69 contents	119
4.44 Elongation at break of ALT/NR and ST/NR composites at various Si69 contents	120
4.45 Tensile strength of ALT/NR and ST/NR composites at various Si69 contents	121
4.46 Tear strength of ALT/NR and ST/NR composites at various Si69 contents	122
4.47 Crosslink density of ALT/NR and ST/NR composites at various Si69 contents	124
4.48 SEM micrographs of (a) 2ALT/NR, (b) 2ST/NR, (c) 5ST/NR and 10ST/NR composites	127

SYMBOLS AND ABBREVIATIONS

NR	=	Natural rubber
RH	=	Rice husk
RHF	=	Rice husk fiber
HCl	=	Hydrochloric acid
NaOH	=	Sodium hydroxide
Si69	=	Bis (triethoxysilylpropyl) tetrasulfide
ACT	=	Acid treated rice husk fiber
ALT	=	Alkali treated rice husk fiber
ST	=	Silane treated rice husk fiber
TGA	=	Thermogravimetric analyzer
FTIR	=	Fourier transform infrared spectrometer
OM	=	Optical microscope
SEM	=	Scanning electron microscope
MDR	=	Moving die rheometer
UTM	=	Universal testing machine
CBS	=	N-cyclohexyl-2-benzothiazole-2-sulphenamide
dNm	=	Deci Newton meter

CHAPTER I

INTRODUCTION

1.1 Background

Nowadays, Thailand is the main producer and exporter of natural rubber (NR) in the world. About 90 percents of the exported NR are in raw forms such as ribbed sheet, block rubber and concentrated latex and the rest is utilized in the country to produce NR products. NR has several interesting properties, *e.g.* high tear strength, high abrasion resistance, high resilience, strain-induced crystallization (Muniandy, Ismail and Ohtman, 2012; Ostad-Movahed, Yasin, Ansarifar, Song and Hameed, 2008). Due to the good properties, NR is used in several industrial applications, *i.e.*, tire, hose, belting and bridge bearing. In order to expand the applications of NR products, the improvement of mechanical properties of the rubber products is very important.

Generally, properties of NR products can be adjusted or enhanced by several approaches, *e.g.* vulcanization system and addition of reinforcing filler. For mechanical properties improvement, carbon black and silica are conventional reinforcing fillers mostly used in NR industries. Carbon black is made from nonrenewable resources. It causes environmental pollution and gives black color products. Silica is generally used in light color products but it needs surface modification to reduce agglomeration leading to the high cost in silica production (Kohjiya and Ikeda, 2000). Recently, there are numerous efforts to use natural fibers

from agricultural sources, such as sisal, jute, banana, flax, wheat straw, wood flour, rice husk, as alternative fillers for NR. The use of natural fibers as reinforcing fillers for NR is interesting because of their high specific strength and high stiffness. In addition, the natural fibers have advantages over the conventional fillers in the view of renewability, biodegradability, environmental safety and low cost (Nordin, Said and Ismail, 2007; Sarkawi and Aziz, 2003).

One of the interesting natural fibers is rice husk (RH). RH is abundantly available in Thailand as a byproduct from the rice milling process. Only a minor portion of the RH is used as animal feed, bedding material or household fuel while the huge quantities are burned in fields leading to environmental pollution. Various researchers attempt to expand the utilization of RH in industries, *e.g.* as pozzolanic material to enhance the lime treatment of degraded soil, as a filler to increase compressive strength in cement, as particleboard materials and as activated carbon (Vempati, Musthyala, Mollah and Cocke, 1995). Another way to increase the application of RH is to use RH as a reinforcing filler for NR. RH contains 45% cellulose, 19% hemicelluloses, 19.5% lignin and 15% silica by weight (Marti-Ferrer, Vilaplana, Ribes-Greus, Benedito-Borras and Sanz-Box, 2006; Panthapulakkal, Law and Sain, 2005). Besides cellulose, RH has high silica content as compared with other natural fibers. The presence of these two components in RH may help improving mechanical properties of NR composites such as tensile strength, tear strength, modulus and hardness. In addition, RH has many advantages similar to other natural fibers such as biodegradability, low density, low cost, high strength, high stiffness and non abrasiveness (Nordin, Said and Ismail, 2007; Panthapulakkal, *et al.*, 2005). The utilization of RH as a reinforcing filler for NR is an approach to obtain value added

products from an agricultural waste. Moreover, this approach also helps reducing material cost of producing NR composites as well as helps improving mechanical properties of the obtained products.

However, hydrophilic RH is incompatible with hydrophobic NR leading to the poor interfacial adhesion between these two components. The compatibility between NR and RH can be improved by several approaches such as addition of compatibilizer, matrix modification and surface treatment of rice husk (Bera and Kale, 2008; Yang, Kim, Park, Lee and Hwang, 2007). Surface treatment of RH can be made via physical and chemical methods. Physical method, *e.g.* electron beam (EB) irradiation, plasma treatment, water treatment and chemical method, *e.g.* acid treatment, alkali treatment, silane treatment, are widely used to modify RH surface (Lane, Ahmad, Dahlan and Abdullah, 2010; Kim, Kim and Kim, 2006; Kim, Kim, Kim and Yang, 2006).

Both acid and alkali treatments increase porosity on RH surface by elimination of hemicellulose, lignin and impurities from RH surface leading to the increase in surface roughness of RH (Li, Tabil and Panigrahi, 2007; Ndazi, Karlsson, Tesha and Nyahumwa, 2007). The treatments improve interfacial adhesion between RH and NR matrix through mechanical interlocking. However, this interaction is only physical interaction. To increase the chemical interaction between two materials, silane treatment is used after pretreating RH with acid or alkali treatments. The surface roughness after pretreatment increases the penetration of silane into the micropores on RH surface. Silane coupling has the bi-functional groups. One functional group of silane reacts with hydroxyl groups of RH and forms a covalent bond onto RH surface whereas another functional group of silane interacts with polymer matrix by hydrogen

bond or entanglement. Therefore, silane coupling agent acts as a bridge between hydrophilic RH and hydrophobic polymer matrix leading to the enhancement of interfacial adhesion between them (Maziad, El-Nashar and Sadek, 2009; Li *et al.*, 2007).

In this study, rice husk fiber (RHF)/NR composites were prepared. Acid treatment, alkali treatment and silane treatment were used to treat RHF surface to improve compatibility between RHF and NR matrix.

1.2 Research objectives

The aims of this research are as follows:

- (i) To determine effect of RHF content on cure characteristics, mechanical properties and morphological properties of RHF/NR composites.
- (ii) To determine effect of acid and alkali treatments on cure characteristics, mechanical properties and morphological properties of RHF/NR composites.
- (iii) To determine effect of silane content on cure characteristics, mechanical properties and morphological properties of RHF/NR composites.

1.3 Scope and limitation of the study

Rice husk fiber (RHF) retained in sieve size ranging between 150-300 μm was used. The RHF was surface treated with hydrochloric acid (HCl), sodium hydroxide (NaOH), or a silane coupling agent, bis (triethoxysilylpropyl) tetrasulfide (Si69). For RHF surface treatment using acid or alkali, treatment times were varied, *i.e.*, 1, 2, 6, 12 and 24 h. For silane treatment, RHF surface was pretreated with acid or alkali at

optimum treatment time before treating with silane. Silane concentrations were varied, *i.e.*, 2, 5 and 10 wt% based on content of RHF. Three types of treated RHF were designated as acid treated RHF (ACT), alkali treated RHF (ALT) or silane treated RHF (ST), according to the treatment method. RHF and treated RHF were characterized using a thermogravimetric analyzer (TGA), a Fourier transform infrared spectrometer (FTIR), an optical microscope (OM) and a scanning electron microscope (SEM).

RHF or treated RHF were incorporated into NR on a two-roll mill. Conventional sulfur vulcanization was used. Variables in the preparation of RHF/NR composites were RHF content and RHF surface treatment. Cure characteristics, mechanical properties and morphological properties of the NR composites were investigated using a moving die rheometer (MDR), a universal testing machine (UTM) and a scanning electron microscope (SEM), respectively.

CHAPTER II

LITERATURE REVIEW

2.1 Rice husk

Rice husk (RH) or rice hull is the outer component of rice grain which has about 20 wt% of the rice grain (Juliano and Bechtel, 1985). The structures of rice grain and RH are shown in Figure 2.1. The main function of RH is to prevent rice grain from insect infestation and fungal damage during storage. RH is removed from the rice grain during rice milling process.

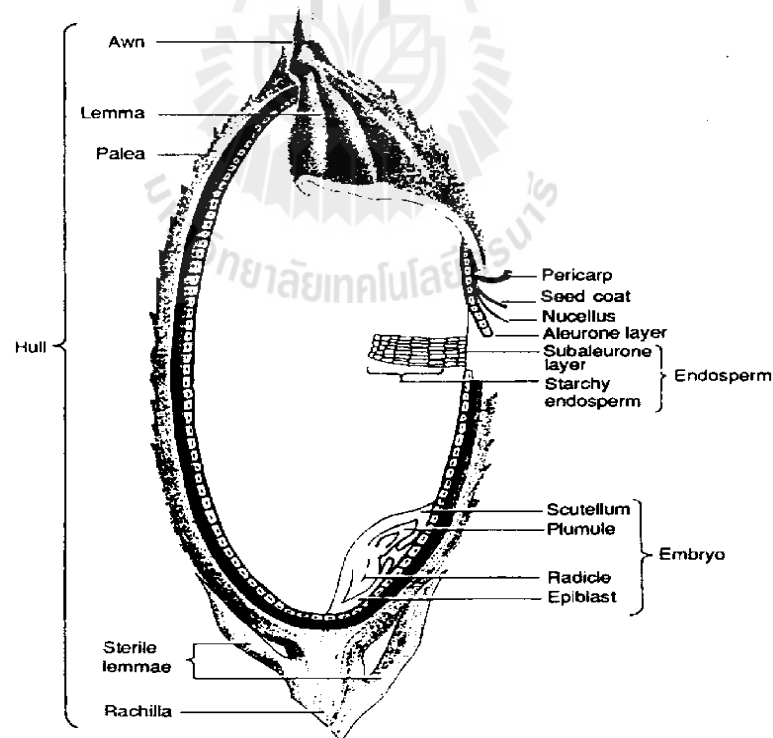


Figure 2.1 Structures of rice grain and RH (Juliano *et al.*, 1985).

The structure of RH has been studied by many researchers (Juliano *et al.*, 1985; Luh, 1991; Yoshida, Ohnishi and Kitagishi, 1962). The main structure of RH is lemma and palea which coexist together in form of tightness hooklike structures. A cross sectional structure of RH is shown Figure 2.2. The lemma and palea in RH have four structural layers. The first layer is epidermis and silica layers. The outer epidermis is sinuous structures covering with thick cuticle cell which has trichomes between the structures. The silica in this layer is largely accumulated under the thick cuticle in form of cuticle-silica (Yoshida *et al.*, 1962). The second layer is sclerenchyma having two or three layers thick and is a lignified cell wall. The third and forth layers are a spongy parenchyma and inner epidermis (Juliano *et al.*, 1985). The major compositions of RH are hemicellulose, cellulose, lignin and silica. The chemical compositions of RH depend on types of paddy, crop year, geographical conditions, climatic variation, soil chemistry and fertilizers used in the paddy growth (Chandrasekhar, Satyanrayana, Pramada and Raghavan, 2003). The chemical compositions of RH have been reported by several research works and shown in Table 2.1.

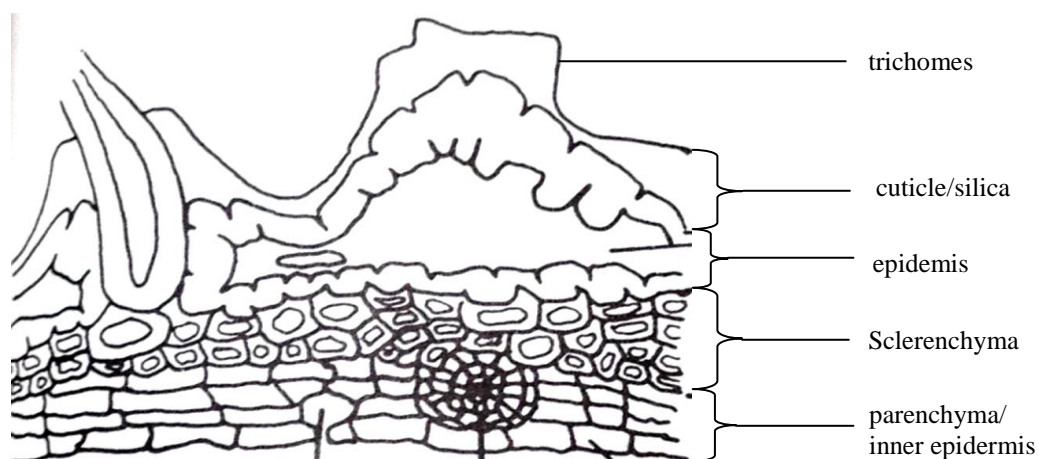


Figure 2.2 Cross sectional structure of RH (Juliano, 1985).

Table 2.1 Chemical compositions of RH reported by several research groups.

Chemical compositions (wt%)				References
Hemicellulose	Cellulose	Lignin	Ash	
12	28-36	9-20	18.8-22.3	Luh (1991)
22.3	35.5	13.6	16.1	Rahman, Ismail and Osman (1997)
25	35	20	17	Mustapa, Hassan and Rahmant (2005)
19.0	45.0	19.5	15.0	Martí'-Ferrer <i>et al</i> (2006)
63.66	30.42	22.53	20.44	Adel, El-Wahab, Ibrahim and Al-Shemy (2010)
8-21	25-35	26-31	15-17	Morsi, Pakzad, Amin, Yassar and Hediden (2011)

2.1.1 Thermal properties

Thermal properties of RH have been reported by several research groups. Mansaray and Ghaly, (1998) observed thermal properties of RH from different states of USA, *i.e.*, Broussard Rice Mills (Lemont LG), West African Rice

Research Station (POK 14), Rokupr (CP 4) and Sierra Leone (Pa Potho) using thermogravimetric analyzer (TGA) under nitrogen atmosphere from room temperature to 700°C at three heating rates, *i.e.*, 10°C/min, 20°C/min and 50°C/min. They found that with increasing heating rate, thermal degradation rate and residue at 700°C of RH samples increased meanwhile their initial decomposition temperature decreased. Pa Potho RH showed higher thermal degradation rate and initial decomposition temperature than Lemont, ROK 14 and CP 4 RH due to its higher hemicellulose and cellulose contents. CP 4 RH revealed the higher residue at 700°C than other RH samples. The result suggested that pyrolysis at higher heating rate was not completely achieved due to insufficient reaction time. In addition, Mansaray and Ghaly (1999) also studied thermal properties of Lemont LG, POK 14, CP 4 and Pa Potho RH under oxygen atmosphere at a heating rate of 20°C/min. They suggested that RH showed two thermal decomposition zones, *i.e.*, hemicellulose decomposition (203-295°C) and cellulose decompositions (295-467°C). Patho RH showed higher thermal degradation rate than Lemont LG, ROK 14 and CP 4 in the first reaction zone because of its higher volatile matter and lower ash contents. ROK 14 RH showed higher degradation rate in the second reaction than other RH samples. CP 4 RH had the highest residual weight at 700°C. The difference in thermal properties of RH from different states was due to the different chemical compositions in RH. The chemical compositions in RH depended on types of paddy, crop year, geographical conditions, climatic variation, soil chemistry and fertilizers used in the paddy growth (Chandrasekhar *et al.*, 2003).

Similar work has been reported by Kim and Eom (2003). They studied thermal properties of RH having four different particle sizes, *i.e.*, under 324 mesh, under 200 mesh, 100-200 mesh and 50-100 mesh. RH having larger particle size

(under 324 and 200 mesh) was easily decomposed between 350 to 800°C due to the lower hemicellulose, cellulose and lignin content in RH. However, RH having larger particle size showed higher ash content at 800°C indicating higher silica content in this RH.

Markovska and Lybuche (2007) studied thermal degradation of RH under air atmosphere from room temperature to 1000°C at a heating rate of 10°C/min. They found that thermal decomposition of RH started at 220°C and finished at 640°C. This was attributed to hemicellulose, cellulose and lignin decomposition. The residue at 1000°C was silica in RH and its content was 26%.

Luduen, Fasce, Alvarez and Stefani (2011) studied thermal properties of RH using TGA from 25°C to 750°C at a heating rate of 10°C/min under nitrogen and air atmospheres. In the nitrogen atmosphere, RH revealed hemicellulose and glycosidic links decomposition (300°C), cellulose decomposition (360°C) and lignin decomposition (200-500°C). Residue at 700°C in nitrogen atmosphere was silica and carbonaceous products. On the other hand, RH showed the third thermal decomposition around 366-410°C in the air atmosphere because of oxidation of products from the second decomposition stage. In addition, the residual weight of RH at 700°C in this atmosphere was silica.

Similar work was reported by Yin and Goh (2012). They investigated thermal degradation of RH under nitrogen and air atmospheres. RH was heated from 25 to 1000°C at a rate of 10°C/min. RH exhibited two decomposition stages. The first decomposition stage of RH in nitrogen atmosphere occurred at around 230-380°C while that in air atmosphere occurred at around 230-390°C. This was attributed to hemicellulose and cellulose decomposition. The second decomposition of RH in two

systems revealed at around 380-640°C and 390-540°C involving the decomposition of lignin and lignin conversion as char in RH.

2.1.2 Chemical functional analysis

Markovska *et al.*, (2007) studied RH structure using Fourier transform infrared spectroscopy (FTIR) in the interval of 4000-400 cm^{-1} at a resolution of 1 cm^{-1} . RH showed several absorption bands due to chemical composition of RH. The absorption band about 3430 cm^{-1} ascribed the vibration of -OH groups of hemicellulose, cellulose, lignin and water molecules. The absorption bands at 2930 and 2850 cm^{-1} involved the vibration of -C-H bond in -CH₃ and -CH₂ groups of lignin, cellulose and hemicellulose. The triplet absorption band appeared at 1000-1200 cm^{-1} attributing to the vibration of C-O-H bonds and Si-O bonds in siloxane groups. The weak bands of RH showed at 780 and 460 cm^{-1} indicating the silicon-oxygen component.

Similar result was reported by Luduena *et al.*, (2011). They studied chemical characteristics of RH using FTIR. They observed that the absorption band at 3560 to 3200 cm^{-1} was attributed to OH groups of hemicellulose, cellulose, lignin and water molecules. The peaks around 1732 and 1640 cm^{-1} were related to C=O groups of cellulose and OH groups of adsorbed water in RH, respectively. The small peaks at 1420, 1375 and 1270 cm^{-1} ascribed the CH₂ and CH groups of cellulose. The absorption bands of aromatic groups of RH appeared at 1606 and 1515 cm^{-1} which related to lignin in RH. In addition, RH showed the three adsorption bands at 1100-1070, 799 and 465 cm^{-1} involving Si-O-Si bonds in RH.

2.1.3 Morphological properties

Jauberthie, Rendell, Tamba and Cisse (2000) studied morphological properties of RH and silica profile in RH using a scanning electron microscope (SEM). RH showed the irregular surface with needle-like protuberances as shown in Figure 2.3 (a) and (b). The researchers found that the external surface of RH had higher silica concentration than the internal surface of RH. Moreover, they suggested that silica was not presented within the husk.

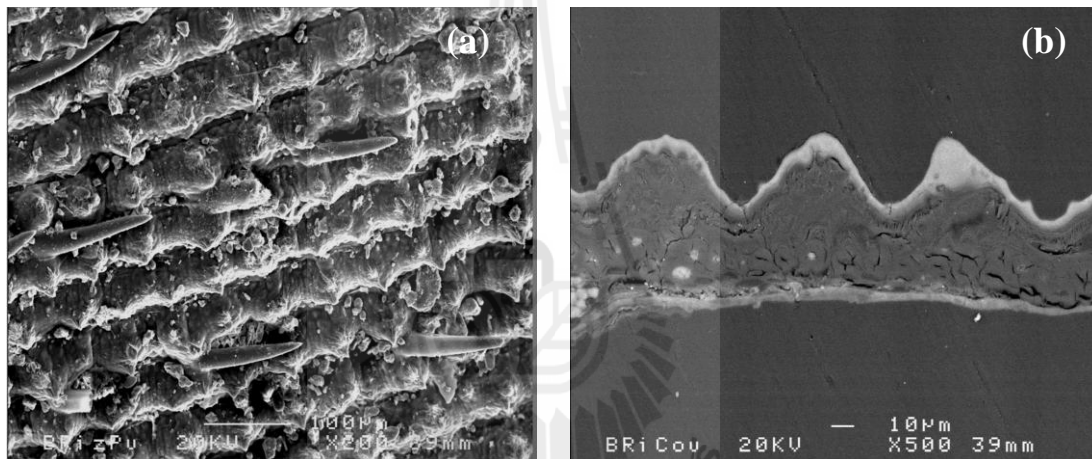


Figure 2.3 SEM micrographs of (a) RH structure and (b) silica profile in RH (Jauberthie *et al.*, 2004).

Chandrasekhar, Satyanayana, Pramada and Raghavan (2003) reported morphologies of RH using a scanning electron microscope (SEM). They suggested that RH was fibrous material which composed of silica and organic material. Silica was mainly found on protuberance and trichomes on the outer epidermis surface which was adjacent to the rice kernel. Morphologies of RH and protuberance, outer epidermis and silica are shown in Figure 2.4 (a) and (b).

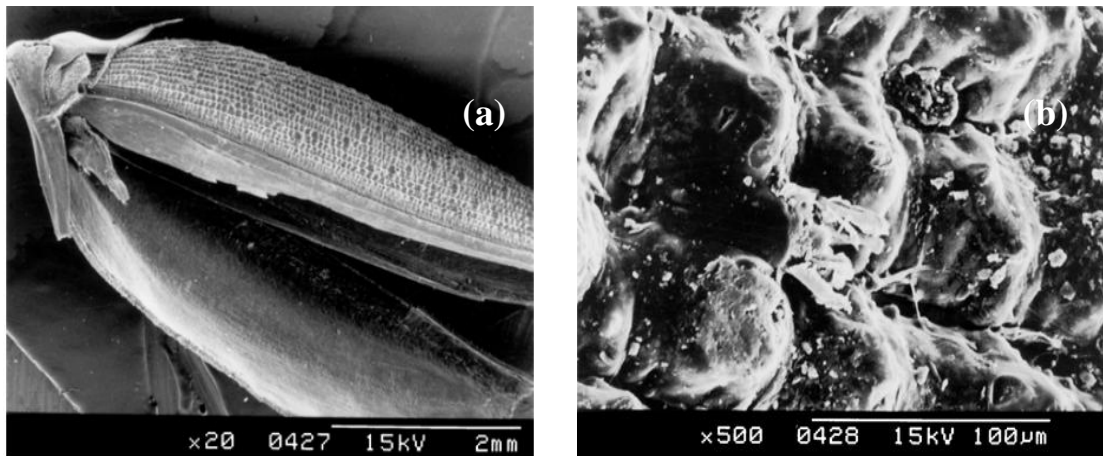


Figure 2.4 SEM micrographs of (a) RH and (b) protuberance, outer epidermis and silica in RH (Chandrasekhar *et al.*, 2003).

Park, Wi, Lee, Sigh, Yoon and Kim (2003) investigated surface morphology of RH and silica distribution in RH using a scanning electron microscope (SEM) and field-emission SEM (FE-SEM). SEM micrograph of outer surface and cross section of RH is shown Figure 2.5(a). The main composition of RH was lemma and palea. Lemma and palea are found on the outer epidermis of RH. The outer surface of RH showed the linear ridge and furrow structure. The ridge was separated with prominent conical protrusion. SEM micrograph of cross section of outer epidermis of RH is shown in Figure 2.5 (b). The outer epidermis of RH revealed two layers of thick wall fibers. Between two layers of tissues, it had xylem and phloem which evolved by bundle sheath. In addition, they used FE-SEM to study the silica distribution in RH. The outer surface of lemma showed brightness and less brightness regions in Figure 2.6. The brightness region represented the presence of silica and the high brightness indicated the high silica concentration. The less brightness region presented the low silica concentration. The high brightness region was found at tip of

dome and dome shoulders. In contrast, FE-SEM image of the cross-section of lemma showed little brightness implying low silica concentration in this region.

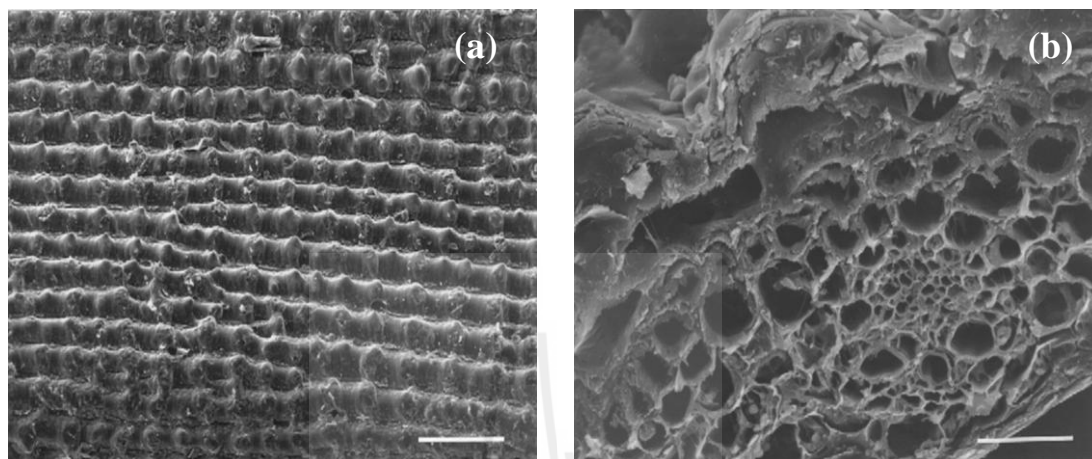


Figure 2.5 SEM micrographs of (a) outer surface and (b) cross-section of RH (Park *et al.*, 2003).

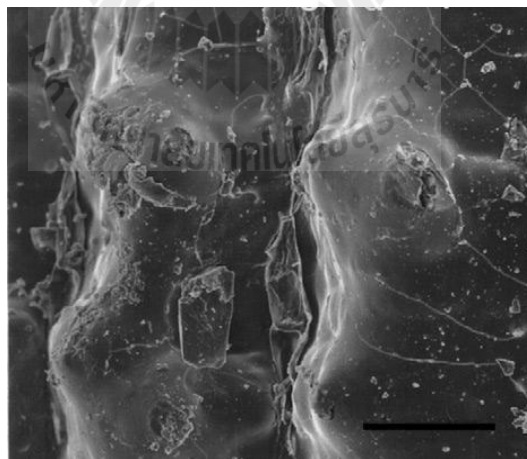


Figure 2.6 FE-SEM micrograph of outer surface of RH (Park *et al.*, 2003).

From the result of various research groups, RH contains hemicellulose, cellulose and lignin. Besides organic components, RH has inorganic component which is silica. The high cellulose and silica contents in RH result in the use of RH as reinforcing filler for polymer composites. In addition, RH has low density, high strength, stiffness, non abrasiveness, renewability, biodegradability, environmental safety, and low cost.

2.2 RH/polymer composites

Due to its high contents of cellulose and silica, RH is received attention to be used as reinforcing filler for polymers. Various forms of RH were used as reinforcing filler for thermoplastics and rubbers. Effects of RH content and RH particle size on properties of RH/polymer composites were studied.

Yang, Kim, Son, Park, Lee and Hwang (2004) studied effect of rice husk flour (RHF) content on mechanical and morphological properties of RHF/polypropylene (PP) composites. PP was mixed with RHF at various contents, *i.e.*, 10, 20, 30 and 40 wt%. Tensile strength of RHF/PP composites decreased with increasing RHF content whereas tensile modulus of the composites increased. Tensile modulus of RHF/PP composites showed the optimum value at RHF content of 40 wt%. Moreover, SEM micrographs of tensile fracture surface of RHF/PP composites showed numerous of holes in the matrix resulting from RHF pull out. This implied the poor compatibility between RHF and PP matrix.

Kim, Yang and Kim, (2005) studied effects of RHF particle size and content on mechanical properties and biodegradability of RHF/polybutylene succinate (PBS) composites. The RHF with different particle sizes, *e.g.*, 80-100 and 200 meshes, and

various RHF contents, *i.e.*, 10, 20, 30 and 40 wt%, were added into PBS. With decreasing particle size of RHF, tensile strength of RHF/PBS composites increased while impact strength of the composites decreased. This was because the smaller RHF had good particle dispersion in PBS matrix leading to the good adhesion between RHF and PBS matrix. In contrast, tensile strength and impact strength of RHF/PBS composites decreased with increasing RHF content due to the poor interfacial adhesion between RHF and polymer matrix. As RHF particle size and RHF content increased, percentage weight loss of RHF/PBS composites increased. The result was because the increase in RHF particle size and RHF content in PBS composites enhanced the degradation rate of the PBS composites.

Rozman, Musa and Abubakar (2005) studied effects of RH particle size and RH content on mechanical properties of RH/unsaturated polyester (USP) composites. Three filler particle sizes, *i.e.*, 35-60, 60-80 and 100-140 μm and various RH contents, *i.e.*, 42%, 57% and 72% were incorporated into USP. With decreasing RH particle size, tensile, flexural and impact properties of RH/USP composites increased. This was because of the larger surface area of RH leading to the good interaction between OH groups on RH surface and C=O groups of polyester matrix. However, tensile, flexural and impact properties of the composites decreased with increasing RH content. This was attributed to the weak interaction between RH and matrix.

Zhao, Tao, Yam, Mok, Li and Song, (2008) investigated effect of RH content on crystallization and biodegradation behaviors of RH/polycaprolactone (PCL) composites in simulated soil medium. PCL composites were prepared with RH at various contents, *i.e.*, 10, 20, 30, 40 and 50 wt%. The crystallization and biodegradation behavior of RH/PCL composites were characterized using differential

scanning calorimetry (DSC) and quantitative analysis from modification of TGA method, respectively. The melting temperature (T_m) and crystallinity of RH/PCL composites decreased as RH content increased. This result was because RH hindered the arrangement of PCL molecule into its lattice resulting in the reduction of the crystallization of PCL and the melting temperature of RH/PCL composites. In addition, the percentage of weight retention of RH/PCL decreased with increasing RH content. The result was explained that the high hydrophilicity of RH led to the high penetration of water molecules into PCL matrix resulting in the increase in degradation of PCL matrix.

2.3 RH/rubber composites

RH was also used as filler for rubbers, *i.e.*, styrene butadiene rubber (SBR), natural rubber (NR), epoxidized natural rubber (ENR) and thermoplastic elastomers.

Ismail, Mohamad, and Bakar, (2004) studied effect of dynamic vulcanization on mechanical properties, water adsorption and morphological properties of rice husk powder (RHP)/ polystyrene (PS)/styrene butadiene rubber (SBR) composites. PS was mixed with SBR and RH of various contents, *i.e.*, 15, 30, 45 and 60 wt%. As RHP content increased, tensile strength and elongation at break of uncured and cured RHP/PS/SBR composites decreased whereas Young's modulus and percentage of water absorption of the composites increased. The result was attributed to the weak interfacial adhesion between RHP and matrix and the high polarity of the composites as the filler content increased. Cured RHP/PS/SBR composites showed higher tensile strength but lower elongation at break, Young's modulus and percentage of water absorption than uncured RHP/PS/SBR composites. These results were because the

dynamic vulcanization enhanced interfacial adhesion between RHP and matrix leading to the improvement of mechanical properties and the reduction of penetration of the water molecule into the cure composites. Moreover, SEM micrograph of tensile fracture surface of the cured composites presented embedded RHP in PS/SBR matrices and little RHP pull-out. The result supported the mechanical properties of cured RHP/PS/SBR composites.

Sarkawi and Aziz, (2003) studied effects of RHP particle size and RHP content on cure characteristics and physical properties of RHP/natural rubber (NR) vulcanizates. RHP with two particle sizes, *i.e.*, 300 μm and 180 μm , were varied from 0 to 50 phr in NR composites. The rubber compounds containing different RHP particle sizes exhibited similar scorch time and cure time. With increasing RHP content, scorch time and cure time of both systems insignificant changed. Tensile strength, elongation at break and abrasion resistance of NR composites containing RHP of 180 μm were higher than those of NR composites containing RHP of 300 μm . This result was because the smaller particle size of RHP offered the larger surface area leading to the increase in interfacial adhesion between RHP and NR matrix. However, tensile strength, elongation at break and abrasion resistance of the NR composites decreased as RHP content increased. The result ascribed that the increase in RHP content led to the poor interaction between RHP and NR matrix and the RHP agglomeration in NR matrix. In addition, both NR composites showed the maximum in tensile strength and elongation at break values at 10 phr of RHP. Mechanical properties results of RHP/NR composites were confirmed by SEM micrographs of cross section of the composites. The composites with lower RHP content presented better RHP dispersion in NR matrix than those with higher RHP content.

Nordin, Said and Ismail, (2007) studied effect of rice husk powder (RHP) content on cure characteristics and mechanical properties of RHP/NR composites. NR composites were prepared at various RHP contents, *i.e.*, 10, 20, 30 and 50 phr. Scorch time and cure time of RHP/NR composites decreased with increasing RHP content. This result was because the long mixing time initiated premature vulcanization of rubber compound during compounding. Tensile strength of the composites showed the maximum value at RHP content of 20 phr. Tensile strength and elongation at break of NR composites decreased with increasing RHP content whereas their modulus at 100% elongation (M100), modulus at 300% elongation (M300) and hardness increased. These results were because RHP enhanced brittleness of NR composites and reduced flexibility of rubber chain.

Ismail, Ragunathan and Hussin, (2011) studied tensile and morphological properties of RHP/PP/recycled acrylonitrile butadiene rubber (NBRr) composites. PP was mixed with NBRr and RHP of various contents, *e.g.*, 10, 15, 20 and 30 phr. With increasing RHP content, tensile strength and elongation at break of RHP/PP/NBRr composites decreased while tensile modulus increased. This may be attributed to the weak filler-matrix interaction and the brittleness nature of the composites. The improvement of tensile modulus of the composites was because the rigid structure of RHP reduced flexibility of the composites. SEM micrographs of RHP/PP/NBRr composites showed numerous of voids and agglomeration of RHP implying the poor dispersion of RHP in PP/NBRr matrix.

Attharangsarn, Ismail, Bakar and Ismail, (2012) studied effect of RHP content on cure characteristics, mechanical properties and morphological properties of RHP/NR and RHP/epoxidized natural rubber (ENR) composites. NR and ENR 50

were mixed with RHP at various contents, *i.e.*, 10, 20, 30 and 40 phr. Scorch time and cure time of both of rubber composites decreased with increasing RHP content. They ascribes that the metal oxides in RHP accelerated vulcanization process in the rubber composites. Scorch time and cure time of RHP/ENR composites were shorter than those of RHP/NR composites due to the activation of an adjacent double bound by the epoxide groups in ENR. Tensile strength and elongation at break of both systems decreased with increasing RHP content while modulus at 100% elongation (M100) and modulus at 300% elongation (M300) of the rubber composites increased. However, tensile strength and elongation at break, M100 and M300 of RHP/ENR composites were lower than that of RHP/NR composites because the polarity of ENR was insufficient to enhance interfacial adhesion between RHP and rubber matrix. SEM micrographs of rubber composites showed numerous holes after RHP was pulled out from NR matrix suggesting the weak interfacial adhesion between RHP and rubber matrix.

2.4 Compatibility improvement between RH and polymer matrices

From above research studies, it is found that RH is widely used as reinforcing filler for thermoplastic and rubber composites. Nevertheless, one problem of utilization of RH as a filler for polymer composites is the incompatibility between RH and polymer matrix leading to poor mechanical properties of RH/polymer composites. In order to solve the problem, RH surface modification, addition of compatibilizer and matrix modification are used to enhance compatibility between RH and polymer.

2.4.1 RH surface modification

Surface modifications such as steam treatment, plasma treatment, electron beam (EB) irradiation, alkali treatment, acid treatment and silane treatment, were used to decrease the hydrophilic nature of RH and to enhance the compatibility between RH and polymer. Several research works attempted to find methods for RH surface modification.

2.4.1.1 Physical method

Ndazi, Karlsson, Tesha and Nyahumwa, (2007) modified RH surface with steam treatment and studied chemical functional groups and thermal properties of treated RH. RH was boiled in a boiler heat steam between 100 and 140°C at 2-2.4 bar for 1 h. They found that the increment of temperature of steam treatment did not affect on the components in RH since steam treated RH still showed three decomposition stages, *i.e.*, hemicellulose, cellulose and lignin decompositions, when was similar to untreated RH.

Adel, El-Wahab, Ibrahim and Al-Shemy, (2010) modified RH with water treatment in an autoclave at 120°C for 90 min. They found that water treated RH showed the three decomposition stages, *i.e.*, water evaporation (50-56°C), hemicellulose decomposition (200-333°C) and cellulose and lignin decomposition (372-476°C).

Kim, Kim and Kim (2006) studied effect of electron-beam (EB) irradiation on interfacial adhesion of rice husk flour (RHF)/polypropylene (PP) composites. RHF was treated with various EB irradiation doses, *i.e.*, 10, 20, 30, 40 and 50 Mrad, in the presence of oxygen and at room temperature. Non irradiated or irradiated RHF content was fixed at 30 wt%. At low radiation doses, *i.e.*, 1, 2, 5 and

10 Mrad, EB-irradiated RHF/PP composites showed higher tensile strength than nonirradiated RHF/PP composites. This was because rough surface of RHF from EB irradiation enhanced interfacial adhesion between RHF and PP matrix. Tensile strength of EB irradiated RHF/PP composites slightly decreased with increasing irradiation dose because of the degradation of RHF at the high radiation dose. SEM micrographs of tensile fracture surfaces of EB irradiated RHF/PP composites were in agreement with the mechanical properties of the composites. Irradiated RHF/PP composites revealed the good dispersion of RHF in matrix and good interfacial adhesion between RHF and PP.

Lane, Ahmad, Dahlan and Aubullah (2010) studied effects of liquid natural rubber (LNR) and EB irradiation on mechanical properties of rice husk powder (RHP)/high density polyethylene (HDPE)/natural rubber (NR) composites. RHP was soaked in 5 wt% sodium hydroxide (NaOH) for 1 h at room temperature before immersing in LNR solution for 30 min and exposing to EB irradiation at different irradiation doses, *e.g.*, 10, 20, 30, 40 and 50 kGy. HDPE was mixed with NR and RHP at 10 wt% to prepare HDPE/NR composites. RHP/HDPE/NR composites showed the maximum tensile strength and impact strength at 20 kGy irradiation dosage and exhibited the maximum tensile modulus at 30 kGy irradiation dosage. As irradiation dose increased, tensile strength, tensile modulus and impact strength of the composites decreased because the chain degradation of LNR at higher irradiation dose caused the agglomeration of RHP in matrix and weak filler-matrix adhesion.

Nguyen, Kim, Ha and Song, (2011) studied effect of plasma treatment on mechanical properties of rice husk (RH)/polypropylene (PP) composites. RH content was 50 wt%. The plasma treated RH/PP composites had higher tensile

strength, tensile modulus and elongation at break than untreated RH/PP composites. The increment of mechanical properties of treated RH/PP composites was because plasma treatment improved compatibility between RH and PP matrix.

Ahmad, Lane, Mohd and Abdullah, (2012) studied effect of EB irradiation on mechanical and morphological properties of rice husk powder (RHP)/high density polyethylene (HDPE)/natural rubber (NR) composites. RHP was pretreated with 5 wt% of sodium hydroxide (NaOH) before coating with liquid natural rubber (LNR) and exposing to EB irradiation at various irradiation doses, *e.g.*, 10, 20, 30, 40 and 50 kGy, in air. HDPE/NR blend was mixed with various RHP contents, *i.e.*, 10, 20 and 30 wt%. Tensile strength and impact strength of EB irradiated RHP/HDPE/NR composites showed the maximum values at 20 kGy radiation dosage whereas tensile modulus of the composites showed the highest value at 30 kGy radiation dosage. With increasing radiation dosage, tensile strength, impact strength and tensile modulus of RHP/HDPE/NR composites decreased. This was because the chain scission of LNR at higher radiation dosage reduced the interfacial adhesion between RHP and HDPE/NR matrix. Tensile strength and impact strength of RHP/HDPE/NR composites decreased with increasing RHP content while tensile modulus of the composites increased. The result was because of the agglomeration of RHP in HDPE/NR matrix. SEM micrograph of the composites with 20 kGy dosage irradiated RHP revealed homogeneous filler dispersion and good filler–rubber adhesion.

2.4.1.2 Chemical method

Park *et al.*, (2004) treated RH surface with maleated polypropylene (MAPP) and γ -aminopropyltrimethoxysilane (γ -APS, A-1100). Functional groups of RH were investigated using FTIR. Untreated RH showed the absorption band at 1730 cm^{-1} attributing to the ester bonds in hemicellulose and lignin in RH. The intensity of this band also increased after treating RH with MAPP. They suggested that the anhydride group of MAPP reacted with hydroxyl group of RH resulting in the increase in the intensity of this band. For silane treated RH, the additional absorption band can be observed at 1100 cm^{-1} . This was attributed to the vibration of Si-O-Si linkage. FTIR confirmed the presence of chemical linkage of MAPP treated RH and silane treated RH.

Ndazi, Karlsson, Tesha and Nyahumwa, (2007) treated RH with various sodium hydroxide (NaOH) concentrations, *i.e.*, 2, 4, 6 and 8% wt/v for 24 h. Chemical functional groups and thermal properties of treated RH were studied using FTIR and TGA, respectively. They found that for RH treated with NaOH, the FTIR absorption band at 1738 and 1217 cm^{-1} disappeared. This result indicated the removal of hemicelluloses and lignin during alkali treatment. All samples of alkali treated RH had lower thermal stability than untreated RH. Moreover, TGA thermograms showed that hemicellulose decomposition stage disappeared in alkali treated RH. This was attributed to the elimination of hemicellulose during alkali treatment. They also found that cellulose decomposition temperature shifted from 354°C to 324°C in alkali treated RH. The result indicated the reduction of thermal stability of RH due to alkali treatment.

Ndazi, Nyahumwa and Tesha, (2007) modified RH with various NaOH concentrations, *i.e.*, 2 %, 4%, 6% and 8% wt/v at 27°C for 24 h. Chemical compositions and thermal stability of alkali treated RH were investigated. Hemicellulose and lignin contents in RH decreased with increasing NaOH concentration from 4% to 8% whereas cellulose content in RH increased. This was because hemicellulose and lignin were removed more easily by alkali treatment than cellulose. In addition, ash content in RH slightly decreased with increasing NaOH concentration. The reduction of ash content in RH was because the silica on RH surface reacted with NaOH to form sodium silicate. Moreover, alkali treatment reduced thermal stability of RH due to the elimination of hemicellulose, lignin and silica in RH during alkali treatment.

Markovska *et al.*, (2010) studied thermal stability of alkali treated RH using TGA under nitrogen and air atmosphere. RH was treated with various NaOH concentrations, *e.g.*, 2N, 4N, 6N and 9N at 100°C for 1 and 3 h. Both raw RH and alkali treated RH showed two decomposition stages in nitrogen and three decomposition stages in air medium. The first stage began from room temperature to 160°C due to the elimination of adsorbed water in RH. The second stage occurred between 200-400°C involving the hemicellulose and cellulose decomposition. The third stage can be observed around 400-650°C in air medium due to the combustion of the product from the secondary stage. However, alkali treated RH showed higher weight loss and lower residue than raw RH. Alkali treated RH with 2N NaOH for 3 h exhibited fully thermal decomposition in air while the treated RH remained 6% residue when the experiment was done under nitrogen atmosphere. This was because silica component in RH was completely removed during 2 h of alkali treatment.

Rangel-Vázquez and Leal-García, (2010) treated RH surface with three different silanes, *i.e.*, 3-(triethoxysilyl) propylmethacrylate (TMS), dichlorodimethylsilane (DDS) and trichlorovinylsilane (TVS). They pretreated RH with 0.5N NaOH at room temperature for 2 h and then treated with 2 wt% silane solutions for 30 min. All silane treated RH showed the adsorption band at 1152 and 1154 cm^{-1} attributing to the C-O-Si stretching. This band confirmed the chemical linkage between RH and silanol groups of silane via condensation reaction.

Johar, Ahmad and Durfresne, (2012) used alkali and bleaching treatments to modify RH surface. RH was pretreated with 4 wt% NaOH for 2 h before treating with acetic acid solution, aqueous chlorite (1.7 wt%) and distilled water at 100-130°C for 4 h. Chemical compositions and thermal properties of RH were studied. When RH was pretreated with alkali treatment, hemicellulose content in RH reduced from 33 wt% to 12 wt% while silica in RH was not measured. This was because hemicellulose and silica in RH were eliminated during alkali treatment. In contrast, bleaching treated RH contained pure cellulose compositions due to the complete elimination of hemicellulose and lignin by bleaching treatment. In addition, thermal stability of bleaching treated RH was higher than those of untreated and alkali treated RH. This was because of the elimination of non cellulosic components, *i.e.*, hemicellulose and pectin by alkali treatment. Untreated RH showed higher amount of residue than alkali treated RH due to the presence of ash and lignin in RH.

Rozman, Lee, Kumar, Abusamah and Ishak, (2000) treated rice husk (RH) with glycidyl methacrylate (GMA). RH was soaked in GMA/dimethylformamide (DMF) solution at 90°C for several hours. Then, polystyrene (PS) was mixed with 40 wt% and 60 wt% RH and 5 wt% benzoyl peroxide (BPO) to

prepare RH/PS composites. Mechanical properties and water absorption of RH/PS composites were studied. Tensile, flexural and impact properties of RH/PS composites were improved by GMA treatment because of the increase in interfacial adhesion between GMA treated RH and PS. GMA treated RH/PS composites with 40 wt% RH content showed higher flexural strength, tensile strength and impact strength but lower flexural modulus and tensile modulus than the composites with 60 wt% RH content. In addition, GMA treated RH/PS composites exhibited lower water absorption as compared to untreated RH/PS composites. This was because the hydrophilic hydroxyl groups of RH were replaced by the methacrylic groups of GMA for the GMA treated RH leading to the increase in hydrophobicity of RH.

Zurina, Ismail and Bakar, (2004) studied effects of esterification and acetylation treatments on mechanical properties of rice husk powder (RHP)/polystyrene (PS)/styrene butadiene rubber (SBR) composites. RHP were treated with either 2% maleic anhydride (MAH) in xylene at 65°C for 18 h (MAH treated RHP) or 50% acetic acid aqueous solutions for 1 h (acetylated treated RHP). Then, PS was mixed with SBR and treated RHP of various contents, *i.e.*, 15, 30, 45 and 60 phr. PS/SBR composites containing MAH treated RHP or acetylated treated RHP showed lower tensile strength, elongation at break and Young's modulus than PS/SBR composites containing untreated RH. This was because the elimination of wax substances in RHP during chemical treatment reduced adhesion between RHP and matrix.

Rozman, Musa and Abubakar (2005) treated RH surface with maleic anhydride (MAH), glycidyl methacrylate (GMA) and succinic anhydride (SAH) in *N,N*-dimethylformamide solution at 90°C for a certain reaction time. To

prepare the composites, GMA treated RH, MAH treated RH or SAH treated RH (at the content of 57 wt%) were mixed with polyester. Mechanical properties of RH/polyester composites were investigated. GMA treated RH/polyester and MAH treated RH/polyester composites showed higher tensile properties and flexural properties than SAH treated RH/polyester composites because the C=C groups of GMA and MAH formed copolymerization reaction with the C=C groups of polyester chain leading to the long bridging linking between RH and polyester chain. The chemical bond between GMA and MAH treated RH with polymer matrix led to the improvement of mechanical properties of both types of the composites. However, the low mechanical properties of SAH treated RH/polyester composites was due to the absence of C=C groups on the surface RH resulting in the lack of ability of SAH to crosslink with polyester matrix.

Ahmad, Bakar, Mokhtilas and Raml (2007) studied effect of alkali treatment on mechanical properties and water absorption of rice husk (RH)/unsaturated polyester (UPS) composites. RH was treated with 5 wt% sodium hydroxide (NaOH) solution at 30°C for 1 h. UPS was fabricated with 10-40 wt% RH using a hand lay-up technique. Alkali treated RH/UPS composites had higher tensile strength, tensile modulus, elongation at break and impact strength than untreated RH/UPS composites. The result revealed that alkali treatment enhanced the interfacial adhesion between filler and matrix by an increase in sites of mechanical interlocking on RH surface. Moreover, SEM micrographs of tensile fracture surface of alkali treated RH/UPS composites showed good filler-matrix adhesion without crack propagation at filler-matrix interface. The enhancement of mechanical properties agreed with morphologies of alkali treated RHP/UPS composites.

Bera and Kale (2008) modified RH with various chemical solutions, *i.e.*, 10 wt% hydrochloric acid (HCl), 2 wt% sodium hydroxide (NaOH), 10 wt% HCl and 2 wt% NaOH or 10 wt% HCl and dimethyl sulfoxide (DMSO) using various treatment times. RH/polypropylene (PP) composites were prepared at 10 wt% RH. Mechanical and morphological properties of the composites were investigated. Tensile and flexural properties of acid treated RH/PP composites were higher than those of alkali treated RH/PP composites. This was because acid treatment enhanced the relative percentage of α -cellulose, silica and lignin in RHP leading to the improvement of properties of the composites. Mechanical properties of alkali treated RH/PP, acid/alkali treated RH/PP and acid/DMSO treated RH/PP composites were insignificantly changed because these chemical treatments removed the part of silica and lignin in RHP. SEM micrographs of acid treated RH/PP composites supported the mechanical properties results by showing the uniform filler dispersion in PP matrix.

Favaro, Lopes, Neto, Santana and Radovanovic (2010) studied effect of acetylation treatment on mechanical and morphological properties of RH/post-consumer high-density polyethylene (PE) composites. RH was soaked in pure acetic before immersing in acetic anhydride acidified with 0.1% sulfuric acid acetylated RH. Post-consumer PE was mixed with 5 wt% and 10 wt% RH to prepare post-consumer PE composites. The incorporation of treated RH in the matrix improved tensile, flexural properties and notch Izod impact strength of RH/post-consumer PE composites and all properties tended to increase with increasing acetylated RH content. From SEM micrographs of tensile fracture surface of acetylated RH/post-consumer PE composites, RH was embedded in PE matrix

indicating the good interfacial adhesion between acetylated RH and PE matrix. This led to the improvement of mechanical properties of the composites.

Syafri, Ahmad and Abdullah, (2011) pretreated RH with 5 wt%/v NaOH at room temperature for 3 h before treating with 5, 10 and 20 wt% liquid epoxidized natural rubber (LENR) solution in toluene for 1 h. HDPE and NR were mixed with 10 wt% treated RH to prepare the composites. Effect of LENR on mechanical properties of RH/HDPE/NR composites was studied. RH/HDPE/NR composites with 10 wt% LENR revealed the optimum tensile strength, tensile modulus and impact strength as compared with alkali treated RH and LENR treated RH/HDPE/NR composites. This was because LENR improved interfacial adhesion between RH and HDPE/NR matrix. With increasing LENR content, tensile properties and impact strength of the composites decreased. This was because the higher rubber coating on RH surface led to the more filler agglomeration in the composites. SEM micrographs of RH/HDPE/NR composites with 10 wt% LENR presented the wetting of polymer matrix onto RH surface supporting the improvement of mechanical properties of the composites.

Maziad, EL-Nashar and Sadek (2009) studied effect of 3-aminopropyl triethoxy silane (3-APE) on properties of rice husk (RH) filled maleic anhydride (MAPP) compatibilized low density polyethylene (LDPE)/natural rubber (NR) composites. RH was treated with 3-APE solution (1 wt% of filler content) at room temperature for 30 min. LDPE was blended with NR, untreated RH or silane treated RH at different RH contents, *i.e.*, 10, 20, 30, 40, 50 and 60 phr, on a two-roll mill. Silane treated RH/LDPE/NR composites showed higher tensile strength, Young's modulus, impact strength than untreated RH/LDPE/NR composites but lower

elongation at break. This was ascribed that 3-APE improved the interfacial adhesion between treated RH and LDPE/NR matrix.

Nordin, Said and Ismail, (2006) studied the effect of bis (triethoxysilylpropyl) tetrasulfide (Si69) on cure characteristics and mechanical properties of rice husk powder (RHP)/NR composites. NR was compounded with RHP at various contents, *e.g.*, 10, 20, 30 and 50 phr and Si69 content of 2.5 phr. The RHP/NR composites with Si69 showed shorter scorch time and cure time than the RHP/NR composites without Si69 due to improvement of filler dispersion by silane coupling agent. Tensile strength, tensile modulus and hardness of RHP/NR composites were improved by the incorporation of Si69. This was because Si69 enhanced RHP dispersion and filler–rubber interaction in NR composites. The mechanical properties results of RHP/NR composites with Si69 were confirmed by SEM micrographs. The micrographs revealed that the RHP/NR composites with Si69 had the less filler pull-out from rubber matrix and better adhered RHP in NR as compared with the RHP/NR composites without Si69.

2.4.2 Addition of compatibilizer

One of the most common methods to improve compatibility between RH and polymer matrix is the addition of compatibilizer. Several kinds of compatibilizers, *i.e.*, maleic anhydride grafted polypropylene (MAPP), maleic anhydride grafted high density polyethylene (MAHDPE), maleic grafted linear low density polyethylene (MALLDPE) and maleic anhydride grafted styrene-ethylene-butadiene-styrene triblock copolymer (MA-SEBS), are added into RH/polymer composites. Several studies reported that MAPP can effectively improve compatibility between rice husk (RH) and polypropylene (PP). Mustapa, Hassan and

Rahmant, (2005) studied effect of maleic anhydride grafted polypropylene (MAPP) on mechanical properties of rice husk flour (RHF)/polypropylene (PP) composites. PP was melt-mixed with RHF at contents of 30 to 40 wt% and MAPP content of 4 wt%. The addition of MAPP improved flexural strength and flexural modulus but reduced impact strength of RH/PP composites. This was because MAPP improved interfacial adhesion between RH and PP matrix.

Razavi-Nouri, Jafarzadeh-Dogouri, Oromiehie and Langroudi (2006) investigated effect of MAPP on mechanical properties of RH/PP composites. PP was mixed with RH at various contents from 0 to 40 parts per hundred of polymers (php) and 3 php MAPP using a twin screw extruder. With the addition of MAPP, tensile modulus, flexural strength and flexural modulus of the composites increased while their impact strength insignificantly decreased. The result was because MAPP enhanced the interfacial interaction between RH and PP matrix. In addition, SEM micrographs of fracture surface of RH/PP composites with MAPP revealed the good dispersion of RHP in PP matrix and the good interfacial adhesion between these two components.

Kim, Lee, Choi, Kim and Kim (2007) studied effect of MAPP types on interfacial adhesion properties of rice husk flour (RHF) filled polypropylene (PP) composites. Five types of MAPP, *i.e.*, Epolene G-3003, Epolene E-43, Polybond 3150, Polybond 3200 and Bondyram 1004, were used as compatibilizers in PP composites. The differences among those MAPP were molecular weight (M_w), *i.e.*, high M_w (Bondyram 1004, G-3003), medium M_w (Polybond 3150, Polybond 3200) and low M_w (E-43) and MA grafted (%), *i.e.*, high MA grafted (%) (G-3003, E-43), medium MA grafted (%) (Polybond 3200) and low MA grafted (%) (Bondyram 1400,

Polybond 3150). The RHF and MAPP contents were fixed at 30 wt% and 3 wt%, respectively. RHF/PP composites with G-3003 showed the highest tensile, impact and flexural strength values. This result was because G-3003 had adequate molecular weight and MA grafted (%) of MAPP which led to the easy diffusion into PP matrix and the good interfacial interaction between RHF and PP matrix. Polybond 3150 and E-43 gave the lowest mechanical properties of RHF/PP composites due to the low molecular weight of E-43 and low amount of MA graft of Polybond 3150. SEM micrographs of tensile fracture surfaces of RHF/PP composites containing G-3003 exhibited the good interfacial adhesion between RHF and matrix and slight RHF pull out which confirmed the obtained mechanical property results.

Yang, Kim, Park, Lee and Hwang (2007) investigated effect of MAPP on mechanical properties of RHF reinforced polypropylene (PP) composites. Two types of MAPP were used, *i.e.*, Epolene E-43TM containing molecular weight (M_w) of 9100 and acid number of 45 and G-3003TM containing M_w of 103,500 and acid number of 8. RHF content was 30 wt% and MAPP content was varied from 1 to 5 wt%. Tensile strength, tensile modulus and impact strength of RHF/PP composites were improved by the addition of MAPP. With increasing compatibilizer content, tensile properties of RHF/PP composites increased while impact strength of the composites slightly decreased. This was because MAPP improved the interfacial bonding between RH and PP matrix resulting in the improvement of mechanical properties of RHF/PP composites.

Kim, Kim, Kim and Yang (2006) investigated effect of compatibilizer types, *i.e.*, maleic anhydride (MA) grafted polypropylene (MAPP), MA grafted high density polyethylene (MAHDPE) and MA grafted linear low density polyethylene

(MALLDPE), on thermal properties of rice husk flour (RHF)/PP and RHF/low density polyethylene (LLDPE) composites. PP or LLDPE was mixed with 30 wt% RHF and 1, 3 and 5 wt% compatibilizers. The degradation temperatures and thermal stability of the composites containing MAPP or MAHDPE were higher than that of the composites without the compatibilizer and slightly increased with increasing compatibilizer content. The result was because of the improvement of interfacial adhesion between RHF and polymer matrix resulting from the esterification reaction between hydroxyl groups of RHF and the anhydride functional group of MAPP and MAHDPE. The addition of 5wt% MAPP or MAHDPE in polymer gave the highest thermal stability. On the other hand, degradation temperatures and thermal stability of the composites with MAHDPE or MALLDPE insignificantly changed.

Martí-Ferrer *et al.*, (2005) used different compatibilizer types *i.e.*, maleic anhydride grafted polypropylene (MAPP), maleic anhydride grafted styrene-ethylene-butadiene-styrene triblock copolymer (MA-SEBS), 3-triaminopropyltrimethoxysilane (Ameo-T) and titanate with linear low density polyethylene (Ti-LLDPE), to improve compatibility between RHF and polypropylene block copolymer (PPB). PPB was mixed with 37 wt% RHF and compatibilizer at various contents, *i.e.*, 1, 3, 5, and 7 wt%. Dynamic mechanical properties of RHF/PPB composites were investigated. The incorporation of MAPP and Ameo-T into the composites enhanced storage modulus (E') and decreased the peak of the $\tan \delta$ of RHF/PPB composites. On the contrary, the addition of MASEBS into the composites decreased the storage modulus and increased the loss tangent of the composites. The composites containing MAPP revealed the maximum storage modulus and the minimum loss tangent because MAPP had the strong interfacial bonding between

RHF and PPB. RHF/PPB composites containing Ameo-T showed an increase in storage modulus and impact properties due to the good performance of Ameo-T for the composites. MASEBS improved only impact strength of the composites whereas Ti-LLDPE did not improve both storage modulus and loss tangent of the composites.

Pires de Carvalho, Felisberti, Oviedo, Vargas, Farah and Ferreira, (2011) added different compatibilizers, *i.e.*, maleic anhydride (MA) grafted polypropylene (MAPP), MA grafted high density polyethylene (MAPE), acid comonomer grafted PP (CAPP) or acid comonomer grafted high density polyethylene (CAPE) into RH/poly (propylene-*co*-ethylene) (PPc) composites. RH and compatibilizer contents were fixed at 50 wt% and 10 wt%, respectively. Mechanical and morphological properties of RH/PPc composites were examined. RH/PPc composites with MAPP or CAPP exhibited higher tensile strength, elongation at break, Young's modulus and impact strength than RH/PPc composites with MAPE or CAPE. The result involved the better compatibility between PP based compatibilizers and PPc matrix, as compared to that between PE based compatibilizers and PPc matrix, leading to the stronger interfacial adhesion between filler and polymer matrix. The good interfacial adhesion between RH and PPc matrix was confirmed by SEM observations. The fewer holes after filler pull-out and the decrease in gap size was found.

El-Sayed *et al.*, (2012) investigated effect of MAPP on mechanical properties of rice husk flour (RHF)/polypropylene (PP) composites. They prepared maleic anhydride grafted PP (MAPP) in xylene solution under nitrogen atmosphere. To prepare PP composites, PP was mixed with RHF at various contents, *e.g.*, 10, 20, 30, 40, 50, 60 and 70 wt% and 3 wt% MAPP. The incorporation of MAPP enhanced

tensile strength, Young's modulus and hardness of RHF/PP composites because MAPP improved interfacial bonding between RHF and PP. However, elongation at break of RHF/PP composites was not improved by the addition of MAPP because MAPP increased the stiffness of the composites.

Yang, Wolcott, Kim, Kim and Kim (2007) used MAPP and maleic anhydride grafted polyethylene (MAPE) as compatibilizers for RHF/low density polyethylene (LDPE) and RHF/high density polyethylene (HDPE) composites. LDPE or HDPE was mixed with RHF at various contents (10, 20, 30, 40 and 60 wt %) and 3 wt% MAPP or MAPE. Tensile strength of both LDPE and HDPE composites was improved by the addition of MAPP or MAPE because MAPP and MAPE enhanced the interfacial adhesion between RHF and PE matrix. However, the composites with MAPP exhibited lower mechanical properties than the composites with MAPE due to the incompatibility between MAPP and PE matrix. Impact strength of LDPE and HDPE composites with MAPE was higher as compared to the composites with MAPP. This suggested that MAPE had good compatibility and good wetting to the PE matrix.

Panthapulakkal, Sain and Law (2005) added two types of compatibilizer based on ethylene-(acrylic ester)-(maleic anhydride) terpolymer (EBMA1, EBMA2) or ethylene-(acrylic ester)-(glycidyl methacrylate) terpolymer (EGMA1, EGMA2) into rice husk flour (RHF)/HDPE composites. The RHF content was 65 wt% and EBMA or EGMA content was 2.5 wt%. Mechanical properties of RHF/HDPE composites were increased by adding EBMA or EGMA. The anhydride or glycidyl methacrylate pendent groups of compatibilizer reacted with RH and entangled with polymer matrix leading to the enhancement of compatibility between

RHF and HDPE matrix. However, the composites containing EGMA1 showed the highest mechanical properties due to the flexibility of methyl acrylate pendant groups on polymer backbones of EGMA1. For EBMA1 and EBMA2 containing acrylate pendent groups, the flexibility of polymer chains of the coupling agents was decreased leading to the reduction of flexibility interface between the filler and the matrix. Similarly, EGMA2 with the high methyl acrylate content led to the brittleness of the polymer main chains and the brittle interface between RHF and HDPE matrix resulting in the decrease in mechanical properties of the composite. In addition, Panthapulakkal *et al.*, (2005) also studied effect EGMA content on mechanical properties of RHF/HDPE composites. EGMA contents were varied from 0.75 to 5 wt%. The addition of EGMA into HDPE matrix improved tensile, flexural and impact strength of the RHF/HDPE composites. The result suggested that the EGMA enhanced the interaction between RHF and HDPE matrix. The composites containing 2.5 wt% EGMA illustrated the maximum tensile, flexural and impact strength values. However, tensile and flexural modulus of the composites did not improve by the addition of EGMA.

Jamil, Ahmad and Aubdullah (2006) used liquid natural rubber (LNR) as a compatibilizer for rice husk (RH)/high density polyethylene (HDPE)/NR composites. HDPE was blended with NR and mixed with RH at various contents (0 to 10 wt%) and LNR at various contents (0 to 10 wt%). Mechanical and morphological properties of RH/HDPE/NR composites were studied. Tensile strength and impact strength of both RH/HDPE/NR/LNR and RH/HDPE/NR composites decreased with increasing RH content while tensile modulus and hardness of both composites increased. However, RH/HDPE/NR/LNR composites showed higher tensile strength,

Young's modulus and impact strength than RH/HDPE/NR composites. The result was because LNR decreased surface tension between RH and polymer matrix leading to the enhancement of filler-matrix interaction and filler dispersion. However, hardness of RH/HDPE/NR/LNR composites was lower than that of RH/HDPE/NR composites. This was because LNR enhanced flexibility of NR in the composites leading to the decrease in stiffness of the composites. SEM micrographs of tensile fracture surface of RH/HDPE/NR/LNR supported the mechanical properties results of the composites by revealing the good RH dispersion in HDPE/NR matrix.

Nordin *et al.*, (2007) prepared rice husk powder (RHP) filled natural rubber (NR) composites using epoxidized natural rubber (ENR) as a compatibilizer. RHP contents were 10, 20, 30 and 50 phr and ENR content was fixed at 10 phr. Cure characteristics and mechanical properties of RHP/NR composites were determined. Scorch time and cure time of NR composites with ENR were shorter than those of NR composites without ENR. This was because the epoxide groups and amine groups from the ring opening of sulfur accelerated vulcanization process of NR composites. Tensile strength, elongation at break, modulus at 100% elongation (M100), modulus at 300% elongation (M300) and hardness of NR composites with ENR were better than those of NR composites without ENR. This suggested that ENR improved filler dispersion and adhesion between filler and matrix leading to the improvement of mechanical properties of the composites.

2.4.3 Matrix modification

Favaro *et al.*, (2010) studied mechanical properties of rice husk (RH)/post-consumer HDPE composites. Post-consumer HDPE pellet was soaked in 0.25 M of potassium permanganate (KMnO_4) solution in 0.5 M of hydrochloric acid (HCl) acidic medium for 8 h at 25°C. RH at various contents of 5 and 10 wt% was compounded with oxidized HDPE matrix in a single screw extruder. FTIR spectra of oxidized HDPE showed the vibration of C=O and C-O groups resulting from the modification by KMnO_4/HCl solution. This indicated the formation of unsaturated vinyl group of oxidized HDPE. Tensile modulus, flexural strength, flexural modulus and impact strength of unmodified and modified HDPE composites were increased with the addition of RH while tensile strength of both composites decreased. In addition, all properties of both composites except tensile strength slightly increased with increasing RH content. The modified HDPE composites showed higher mechanical properties than the unmodified HDPE composites. The enhancement of properties of the composites resulted from the high hydrophilicity of polymer matrix after matrix modification leading to good compatibility with hydrophilic RH.

CHAPTER III

EXPERIMENTAL

3.1 Materials

Natural rubber (STR 5L) was purchased from Thai Hua Rubber Public Co., Ltd. Rice husk (RH) was purchased from a local rice mill in Nakhon Ratchasima, Thailand. Hydrochloric acid (HCl, 37 %v/v) and sodium hydroxide (NaOH) were purchased from Italma Co., Ltd. Bis (triethoxysilylpropyl) tetrasulfide (Si69) was obtained from Louis T. Leonowens (Thailand) Co., Ltd. N-cyclohexyl-2-benzothiazole-2-sulphenamide (CBS), stearic acid, zinc oxide (ZnO), and sulfur (S) were supplied by Channel Chemicals Co., Ltd. The chemical structures of Si69 and CBS are shown in Figure 3.1.

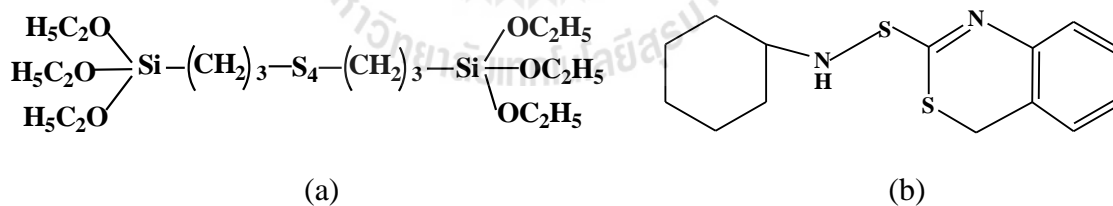


Figure 3.1 Chemical structures of (a) Bis (triethoxysilylpropyl) tetrasulfide (Si69) and (b) N-cyclohexyl-2-benzothiazole-2-sulphenamide (CBS).

3.2 Experimental

3.2.1 Preparation of RHF

Rice husk was washed thoroughly with tap water to remove the adhered soil and dust, and then dried in open air. The dried rice husk was ground using a grinding machine (RETSCH/ZM200). Then, RHF was sieved with a sieve shaker (RETSCH/AS200). RHF retained in sieve size ranging between 150-300 μm was used. Then, RHF was dried in an air oven at 80°C overnight to discharge the moisture before compounding.

3.2.2 Surface treatment of RHF

3.2.2.1 Acid treatment

RHF was immersed in 1 M HCl solution at room temperature and at a RHF to solution ratio of 1:25 (w/v). The treatment time was varied, *i.e.*, 1, 2, 6, 12 and 24 h. After that, RHF was filtered, rinsed with water several times to eliminate the residual acid and dried at 80°C for 24 h. The HCl treated RHF were called according to the treatment time as 1ACT, 2ACT, 6ACT, 12ACT and 24ACT.

3.2.2.2 Alkali treatment

RHF was immersed in 1 M NaOH solution at room temperature and at a RHF to solution ratio of 1:25 (w/v). The treatment time was varied, *i.e.*, 1, 2, 6, 12 and 24 h. After that, RHF was filtered, rinsed with water several times to eliminate the residual sodium hydroxide and dried at 80°C for 24 h. The NaOH treated RHF were called according to the treatment time as 1ALT, 2ALT, 6ALT, 12ALT and 24ALT.

3.2.2.3 Silane treatment

RHF was pretreated with NaOH at certain treatment time prior to do silane treatment. The silane coupling agent, bis (triethoxysilylpropyl) tetrasulfide (Si69), was dissolved in ethanol. Pretreated RHF was immersed in the ethanol solution at a RHF to solution ratio of 1:15 (w/v) for 3 h. Then, RHF was filtered and dried at 80°C for 24 h. The silane concentration was varied, *i.e.*, 2, 5 and 10 wt% based on content of RHF. The silane treated RHF were called according to the silane concentration as 2ST, 5ST and 10ST.

3.2.3 Characterization of untreated and surface treated RHF

3.2.3.1 Thermal properties

Thermal decomposition patterns and char residues of untreated and surface treated RHF were characterized by a thermogravimetric analyzer (TGA) (TA INSTRUMENT/SDT2960). TGA and DTGA curves of untreated and surface treated RHF were obtained by heating a sample from 25 to 800°C at a heating rate of 10°C/min under a nitrogen atmosphere.

3.2.3.2 Functional group analysis

Functional groups of untreated and surface treated RHF were characterized by a Fourier transform infrared spectrometer (FTIR) (BRUKER/VERTEX 70) using MIRacle-single reflection attenuated total reflectance (ATR) equipped with platinum diamond crystal (TYPE A225/QL). Their spectra were recorded in a wavenumber range from 4000 to 400 cm^{-1} with a resolution of 4 cm^{-1} and a number of scans of 64.

3.2.3.3 Morphological properties

Fiber surface of untreated and surface treated RHF was observed by a scanning electron microscope (SEM) (JEOL/JCM-5000) at 10 kV. The samples were coated with gold before analysis.

3.2.3.4 Fiber dimension

Fiber length and diameter of untreated and surface treated RHF were measured based on 100 samples by an optical microscope (OM) (NIKON/ELIPSE E600 POL).

3.2.4 Preparation of RHF/NR composites

RHF was dried in an air oven at 80°C overnight to discharge the moisture before compounding. RHF was mixed with NR on a two-roll mill (CHAICHAREON) at room temperature for 20 min to prepare NR composites. Firstly, NR was masticated for 5 min to reduce its viscosity. Then, stearic acid, zinc oxide, CBS and RHF were added, respectively. Lastly, sulfur was added. Formulations of RHF/NR composites are given in Table 3.1.

Table 3.1 Formulation of RHF/NR composites.

Materials	Contents (phr)				
Natural rubber	100	100	100	100	100
Stearic acid	1.5	1.5	1.5	1.5	1.5
Zinc oxide	5	5	5	5	5
CBS ^a	0.5	0.5	0.5	0.5	0.5
Untreated RHF	-	x	-	-	-
Acid treated RHF	-	-	y	-	-
Alkali treated RHF	-	-	-	y	-
Silane treated RHF	-	-	-	-	y
Sulfur	2.5	2.5	2.5	2.5	2.5

x: 10, 20, 30, 40, 50 phr

y: optimum RHF content from the first experimental step

^aN-cyclohexyl-2-benzothiazole-2-sulphenamide

Experimental steps were as follows:

- (i) Untreated RHF at various contents, *i.e.*, 10, 20, 30, 40 and 50 phr, were used to prepare NR composites. Effect of RHF content on cure characteristics, mechanical properties and morphologies of RHF/NR composites was investigated. Based on the mechanical properties of the obtained NR composites, the optimum RHF content was chosen and used to prepare composites in the following experimental steps; (ii) and (iii).
- (ii) Acid treated RHF or alkali treated RHF at various treatment times, *i.e.* 1, 2, 6, 12 and 24 h, were used to prepare NR composites. The

content of fiber was fixed. Effects of acid and alkali treatment on cure characteristics, mechanical properties and morphologies of RHF/NR composites were investigated. Based on the mechanical properties of the obtained NR composites, the treatment method and the treatment time were chosen and used to pretreat RHF before treating with a silane coupling agent.

- (iii) Silane treated RHF at various concentrations of silane, *i.e.*, 2, 5 and 10 wt% based on RHF content, were used to prepare NR composites. The content of fiber was fixed. Effect of silane concentration on cure characteristics, mechanical properties and morphologies of RHF/NR composites was investigated.

3.2.5 Characterization of RHF/NR composites

3.2.5.1 Cure characteristics

Cure characteristics of gum NR and RHF/NR composites were determined using a moving die rheometer (MDR) (GOTECH/GT-M200F) at a temperature of 150°C. Scroch time (T_s), cure time (T_{90}), maximum torque (S_{max}) and minimum torque (S_{min}) of the RHF/NR composites were determined.

3.2.5.2 Mechanical properties

Gum NR and RHF/NR composites were vulcanized using a compression molding machine (LAB TECH/L320) at 150°C. The vulcanized time was based on the cure time obtained from MDR. The composite sheet was cut into dumbell specimens and tear specimens, respectively, with die cutters (Type C).

Tensile properties of RHF/NR composites were determined according to ASTM D 412–06a while tear properties were determined following ASTM D 624. The specimens were examined using a universal testing machine (UTM) (INSTRON/5569) with a load cell of 5 kN and a crosshead speed of 500 mm/min.

3.2.5.3 Morphological properties

Dispersion of RHF in RHF/NR composites and surface morphologies of tensile fracture surfaces of the composites were characterized using a SEM (JEOL/JCM-5000). The sample preparation was shown in the section of characterization of RHF.

3.2.5.4 Crosslink density

Crosslink density (V_e) of RHF/NR composites was measured according to ASTM D 6814. The vulcanized NR composites were swollen in toluene at 27°C for 72 h until equilibrium swelling stage. Crosslink density of sample was calculated by the Flory-Rhener equation as follows (Flory, 1953).

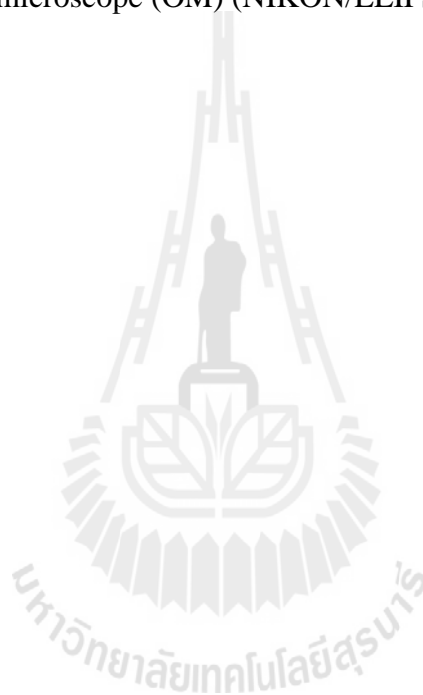
$$V_e = \frac{-[\ln(1-V_r) + V_r + \chi_1 V_r^2]}{V_1 [V_r^{1/3} - (V_r/2)]} \quad (3.1)$$

Where V_e is effective number of chains in a real network per unit volume. χ_1 is polymer-solvent interaction parameter (χ_1 is 0.391 for toluene). V_1 is molecular volume of solvent (V_1 is 106.2 in toluene). V_r is volume fraction of polymer in swollen network in equilibrium with pure solvent and calculated as follows (Ahmed, Nizami, Raza and Mahmood, 2012):

$$V_r = \frac{\text{Weight of dry rubber/density of dry rubber}}{\frac{\text{Weight of dry rubber}}{\text{Density of dry rubber}} + \frac{\text{Weight of solvent absorbed by sample}}{\text{Density of solvent}}} \quad (3.2)$$

3.2.5.5 Fiber length and diameter

RHF was removed by dissolution of 1 g of uncured RHF/NR composites in toluene. The length and diameter of RHF were measured based on 100 samples by an optical microscope (OM) (NIKON/ELIPSE E600 POL).



CHAPTER IV

RESULTS AND DISCUSSION

4.1 Effect of rice husk fiber (RHF) content on physical properties of RHF/NR composites

4.1.1 Cure characteristics

Cure characteristics, *i.e.*, scorch time (T_s), cure time (T_{90}), maximum torque (S_{max}), minimum torque (S_{min}) and torque difference ($S_{max} - S_{min}$) of gum NR and NR composites containing various RHF contents are shown in Figure 4.1 - 4.3 and summarized in Table 4.1.

As shown in Figure 4.1, NR composites containing RHF showed shorter scorch time and cure time as compared with gum NR. Several research works had been reported the similar cure characteristics results in systems of NR composites containing coir fiber (Geethamma, Mathew, Lakshminarayanan and Thomas, 1995), oil palm (Ismail, Rozman, Jaffri and Ishak, 1997), short sisal/oil palm (Jacob, Thomas and Varughese, 2004) or rice husk powder (RHP) (Attharangsana, Ismail, Barkar and Ismail, 2012). They found that the addition of the natural fibers into NR decreased both scorch time and cure time of NR composites. Wang, Wu, Wang and Zhang, (2011) gave the explanation that the reduction in scorch time and cure time of the NR composites was attributed to the longer mixing time of NR composites. When RHF was added into NR, the time of incorporation increased. This generated the high heat buildup during compounding resulting in the formation of premature crosslinking

in the NR composites.

In this study, with increasing RHF content, scorch time and cure time of NR composites insignificantly changed. This may be due to the compromization between the adsorption of accelerator by hydroxyl groups on RHF surface and the premature crosslinking in NR composites leading to the insignificant change of scorch time and cure time of the composites. The main composition of RHF was cellulose which had many hydroxyl groups and these groups adsorbed the rubber accelerator resulting in the delay of scorch time and cure time of NR composites (Sae-oui, Sirisinha, Thepsuwan and Hatthapanit, 2004). On the other hand, the premature crosslinking in NR composites may reduce scorch time and cure time of NR composites.

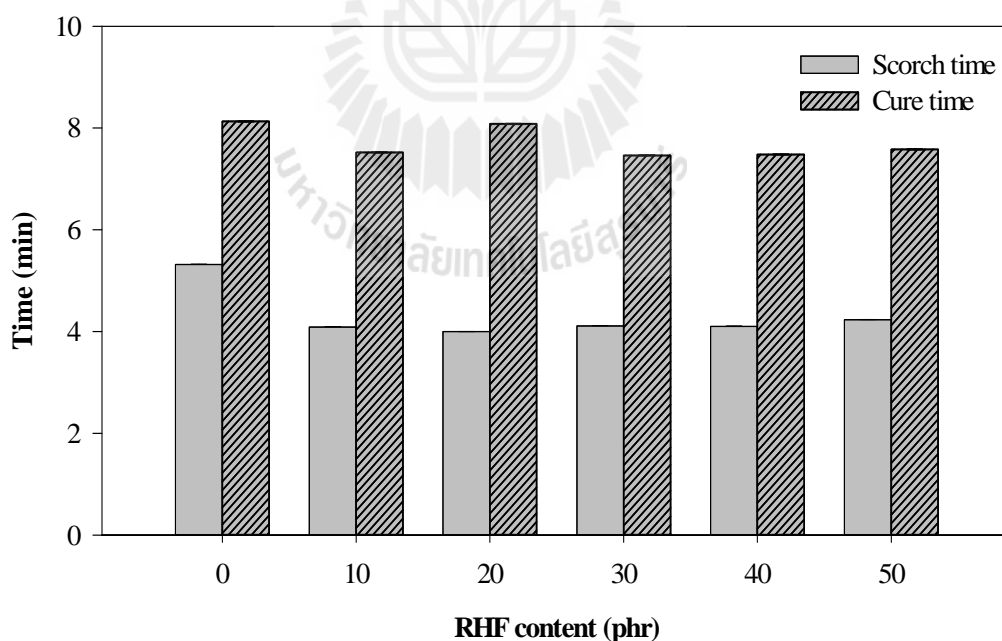


Figure 4.1 Scorch time and cure time of gum NR and NR composites at various RHF contents.

Minimum and maximum torques of gum NR and NR composites at various RHF contents are shown in Figure 4.2. Minimum torque (S_{\min}) is related to the viscosity of rubber compound while maximum torque (S_{\max}) is related to stiffness of fully vulcanized elastomer. When compared with gum NR, minimum and maximum torques of NR composites containing RHF slightly changed. This was because the incorporation of RHF into NR increased the viscosity of rubber compound and restricted the mobility of rubber chains leading to the increase in stiffness of NR composites (De, De and Adhikari, 2004). With increasing RHF content, minimum and maximum torque of NR composites increased. The similar trend was observed by Ismail, Othman and Komethi, (2012), Ismail, Rozman, Jaffri and Ishak, (1997), and Lopattananon, Panawarangkul, Sahakaro and Ellis, (2006).

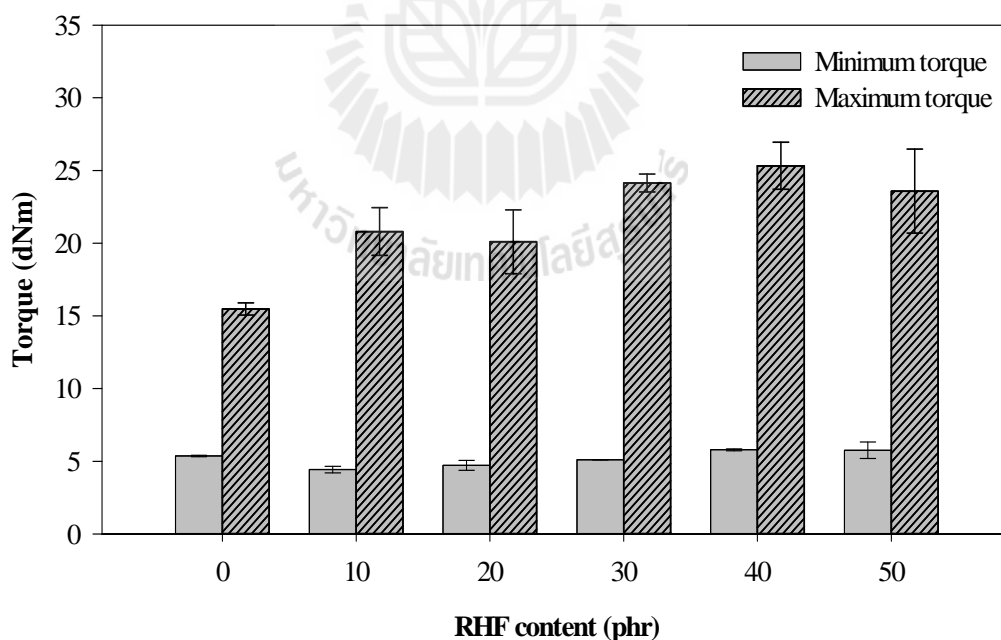
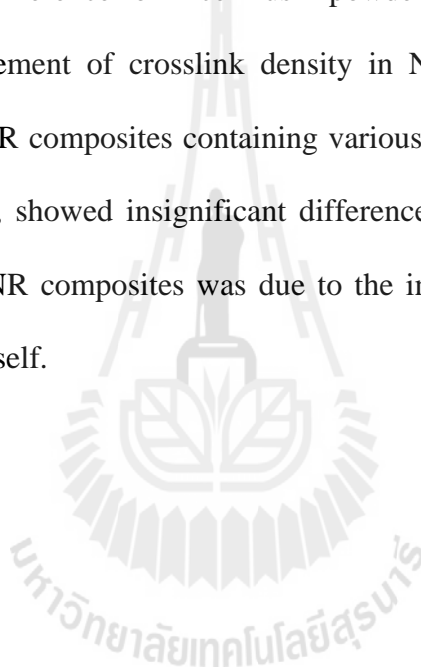


Figure 4.2 Minimum and maximum torques of gum NR and NR composites at various RHF contents.

Torque difference of gum NR and NR composites at various RHF contents is shown in Figure 4.3. The torque difference, the difference between maximum torque and minimum torque ($S_{\max} - S_{\min}$), is indirectly related to the extent of crosslink density of rubber composites (Ismail and Chia, 1998). As compared with gum NR, RHF/NR composites revealed the slight enhancement of torque difference with increasing RHF content. Nordin, Said and Ismail, (2006) reported that the increase in torque difference of rice husk powder (RHP)/NR composites was attributed to the increment of crosslink density in NR composites. However, the crosslink density of NR composites containing various RHF contents, as observed in this work (Table 4.2), showed insignificant difference. Therefore, the increment of torque difference of NR composites was due to the increased filler content and the stiffness of the filler itself.



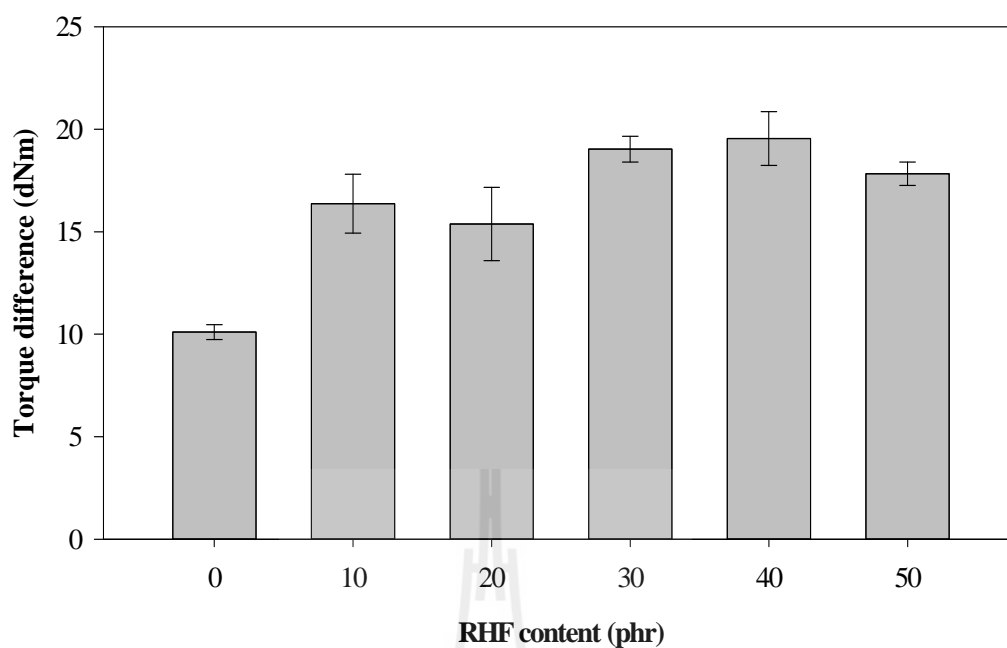


Figure 4.3 Torque difference of gum NR and NR composites at various RHF contents.

Table 4.1 Cure characteristics of gum NR and NR composites at various RHF contents.

Designation	Scorch time (min)	Cure time (min)	S_{max} (dNm)	S_{min} (dNm)	$S_{max}-S_{min}$ (dNm)
NR	5.32	8.13	15.47	5.37	10.10
10RHF/NR	4.10	7.52	20.80	4.43	16.37
20RHF/NR	4.00	8.08	20.09	4.71	15.38
30RHF/NR	4.12	7.46	24.13	5.11	19.02
40RHF/NR	4.10	7.48	25.33	5.79	19.54
50RHF/NR	4.23	7.58	23.58	5.75	17.83

4.1.2 Mechanical properties and crosslink density

Stress-strain curve, modulus at 100% strain (M100), modulus at 300% strain (M300), elongation at break, tensile strength, tear strength and crosslink density of gum NR and NR composites at various RHF contents are shown in Figure 4.4 - 4.10 and summarized in Table 4.2.

4.1.2.1 Tensile properties

As shown in Figure 4.4, it can be seen that stress of gum NR continuously increased with strain. Gum NR exhibited higher tensile strength (Ultimate tensile strength) than NR composites. The high tensile strength of gum NR was because of strain-induced crystallization of NR (Jacob, Thomas and Varughese, 2004). When RHF was incorporated into NR, RHF interrupted the arrangement of NR chain resulting in the reduction of strain induce crystallization ability of NR. This reason led to the decrement of tensile strength of NR composites as RHF content increased. Similar results were reported by Jacob *et al.*, (2004) and Joseph, Joseph and Thomas, (2006) in sisal/oil palm/NR and oil palm/NR composites.

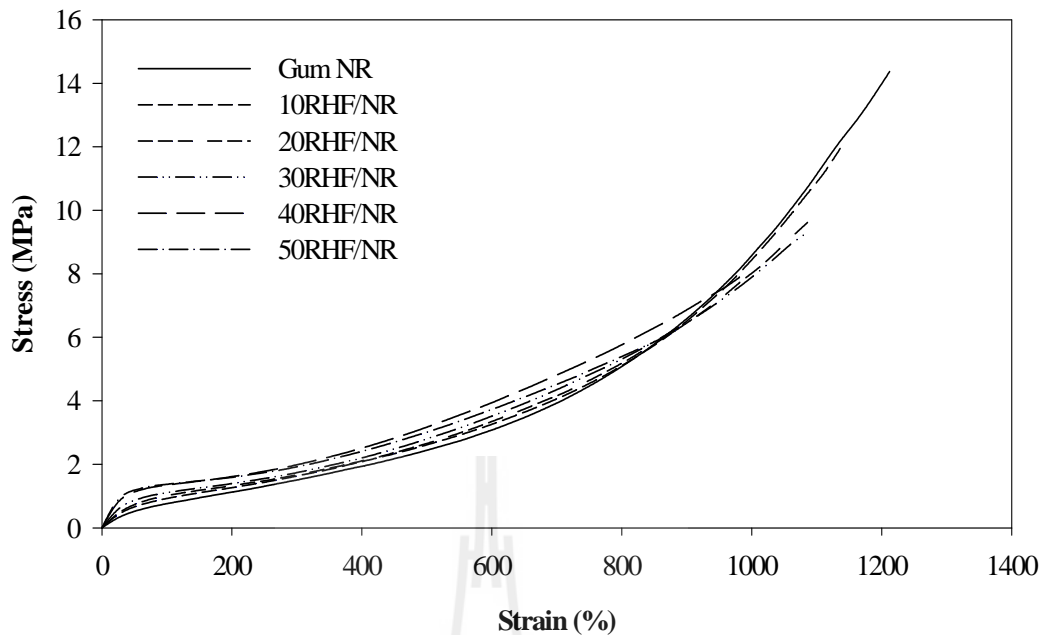


Figure 4.4 Stress-strain curve of gum NR and NR composites at various RHF contents.

Modulus at 100% strain (M100) and 300% strain (M300) of gum NR and NR composites are shown in Figure 4.5 - 4.6. M100 and M300 of NR composites were higher than those of gum NR. This was because the incorporation of RHF into NR matrix reduced elasticity while improved stiffness of NR composites. With increasing RHF content, M100 and M300 of NR composites increased. Similar results were found by De, De and Adhikari, (2004), Ismail, Othman and Komethi, (2012) and Wang, Wu, Wang and Zhang, (2011). They reported that modulus of rubber composites, *i.e.*, bamboo fiber/NR, grass fiber/NR, rattan powder/NR and hemp hurd powder/styrene butadiene rubber (SBR) composites, increased when fiber contents in the rubber composites were increased. Zao, Bi and Zao, (2010) suggested the change in modulus of NR composites involved the change of crosslink density of

the composites. However, crosslink density of NR composites in this study insignificantly changed with increasing RHF content. Therefore, the improvement of modulus of NR composites was because the effect of RHF content.

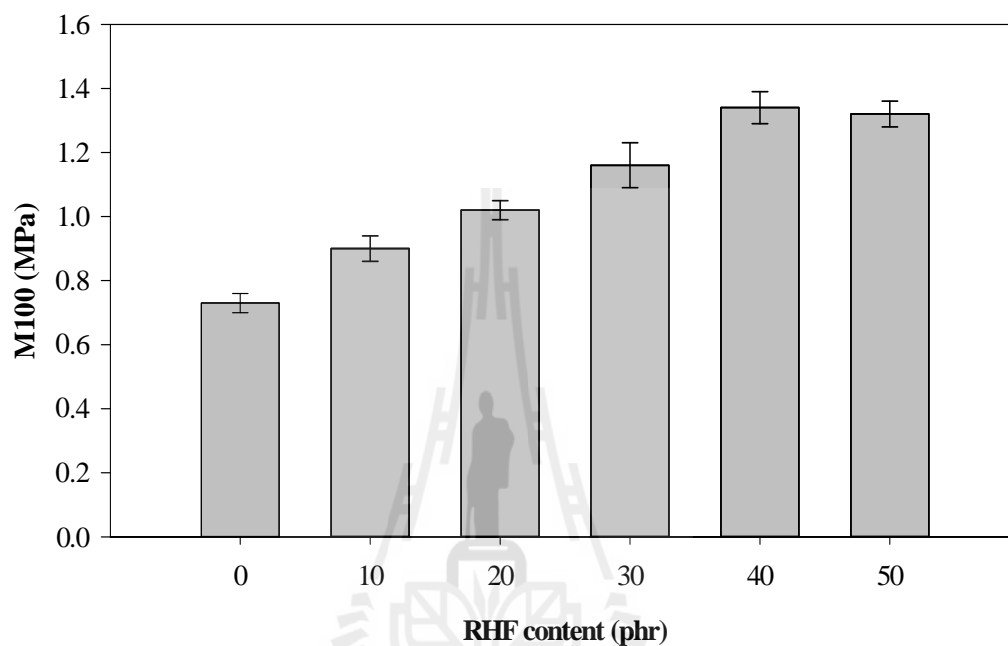


Figure 4.5 Modulus at 100% strain (M100) of gum NR and NR composites at various RHF contents.

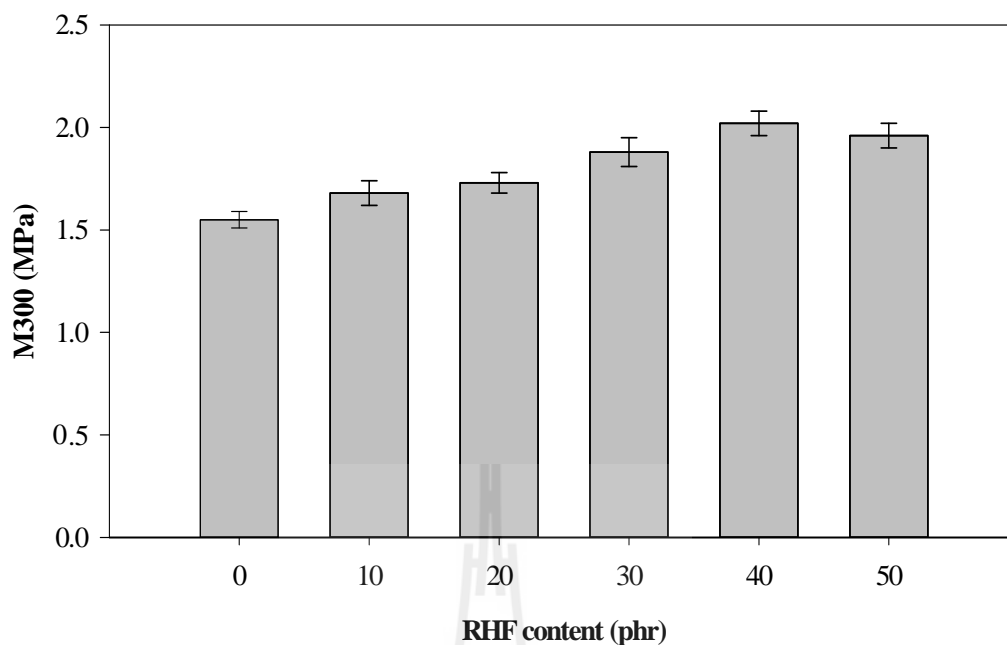


Figure 4.6 Modulus at 300% strain (M300) of gum NR and NR composites at various RHF contents.

Elongation at break of NR was higher than that of RHF/NR composites, as shown in Figure 4.7. The elongation at break of NR composites decreased with increasing RHF content. This suggested that the addition of RHF into NR enhanced stiffness of NR composites.

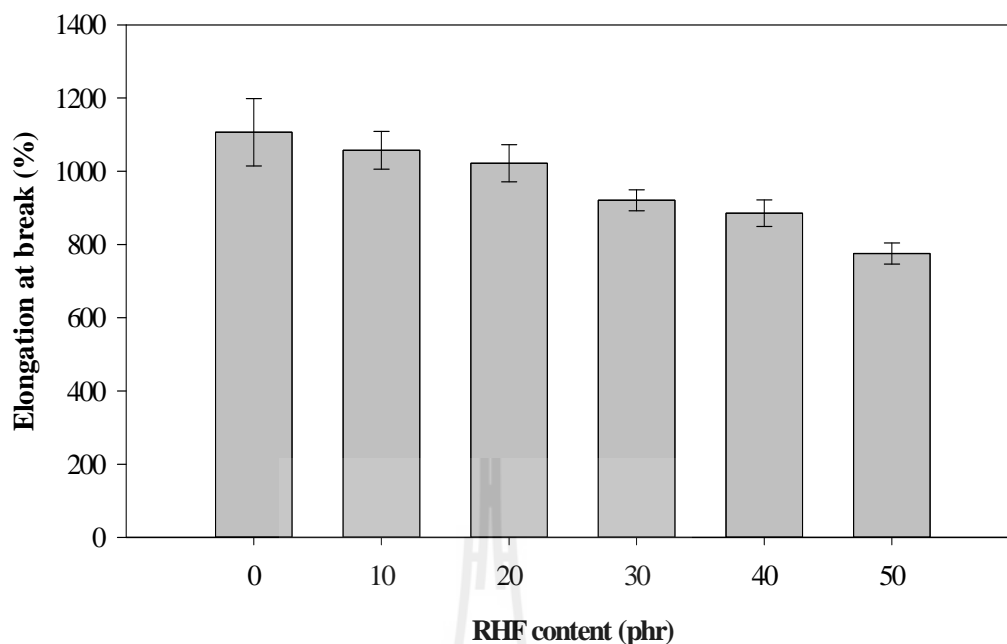


Figure 4.7 Elongation at break of gum NR and NR composites at various RHF contents.

Tensile strength of gum NR and NR composites at various RHF contents is shown in Figure 4.8. Tensile strength of gum NR showed the highest value. This was because of the combination between strain-induced crystallization and high crosslink density of NR. When the fibers were added into NR, the fibers inhibited the arrangement of NR chain leading to the interruption of the strain-induced crystallization behavior of NR. In addition, the reduction of tensile strength of NR composites may be due to the adsorption of accelerator by hydroxyl groups on RHF leading to the decrease in crosslink density of the composites (Wolff, 1996). Thus, this resulted in decreased tensile strength of RHF/NR composites with increasing RHF content. Moreover, the decrement of tensile strength of NR composites was also attributed to the incompatibility between RHF and NR as observed by SEM

micrograph in Figure 4.11. Similar trends were reported by Jacob *et al.*, (2004) and Mathew and Joseph, (2007) in sisal/oil palm/NR and short isora fiber/NR composites, respectively.

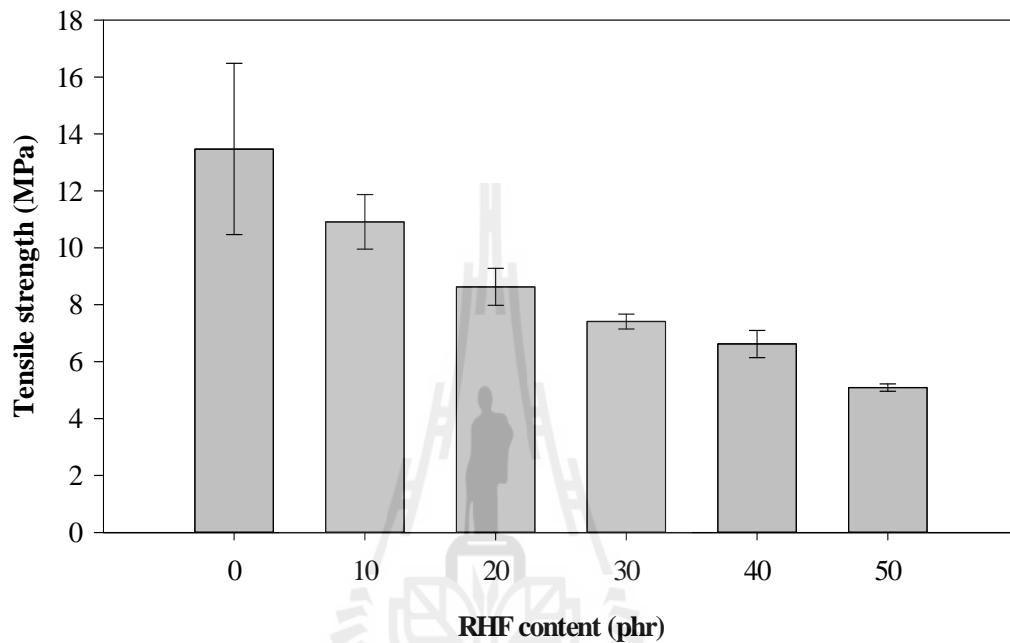


Figure 4.8 Tensile strength of gum NR and NR composites at various RHF contents.

4.1.2.2 Tear properties

Figure 4.9 shows tear strength of gum NR and NR composites at various RHF contents. NR showed the maximum tear strength. Tear strength of NR composites slightly decreased with increasing RHF content. The reduction of tear strength may be due to the packed fibers in rubber matrix. When tearing force was applied, the fiber in NR matrix was closely packed resulting in the enlarged tearing and the reduced tear strength of rubber composites (Ismail, Rosnah and Rozman, 1997). In addition, the decrement of tear strength of NR composites was due to the incompatibility between RHF and NR matrix. Sarkawi *et al.*, (2003) also suggested

that the decrement of tear strength of rice husk powder (RHP)/NR composites involved filler dispersion in rubber matrix. The similar trend was reported by Jacob, *et al.*, (2004) and Sareena, Ramesan and Purushothaman, (2012) in systems of sisal/oil palm/NR and peanut shell powder/NR composites, respectively.

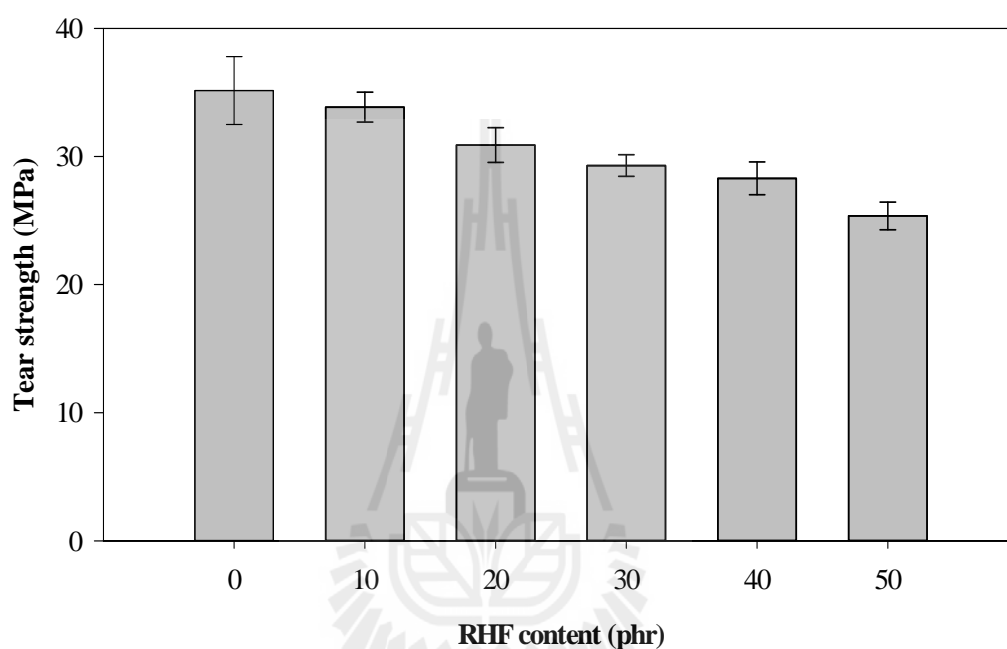


Figure 4.9 Tear strength of gum NR and NR composites at various RHF contents.

4.1.2.3 Crosslink density

It is well known that crosslink density has directly affected mechanical properties, *i.e.*, tensile strength, elongation at break, tensile modulus and tear strength of rubber vulcanizates (Zhao *et al.*, 2011). Crosslink density of gum NR and NR composites at various RHF contents is shown in Figure 4.10. Crosslink density of NR composites was slightly lower than that of NR. The similar observations were reported by Zeng *et al.*, (2009) and Hong, He, Jia and Zhang, (2011) in the systems of cotton fiber/NR and wood flour/NR composites. They

suggested that the incorporation of fiber obstructed vulcanization of rubber chains resulting in the reduction of crosslink density in NR composites. In addition, Wolff, (1996) also found that the decrement of crosslink density in the rubber composites was attributed to the adsorption of accelerator by hydroxyl groups on fiber surface. However, in this study, with increasing RHF content, crosslink density of NR composites was insignificantly different as shown in Table 4.2. This indicated that the change in mechanical properties of NR composites containing various RHF contents in this study was not influenced by crosslink density of the systems.

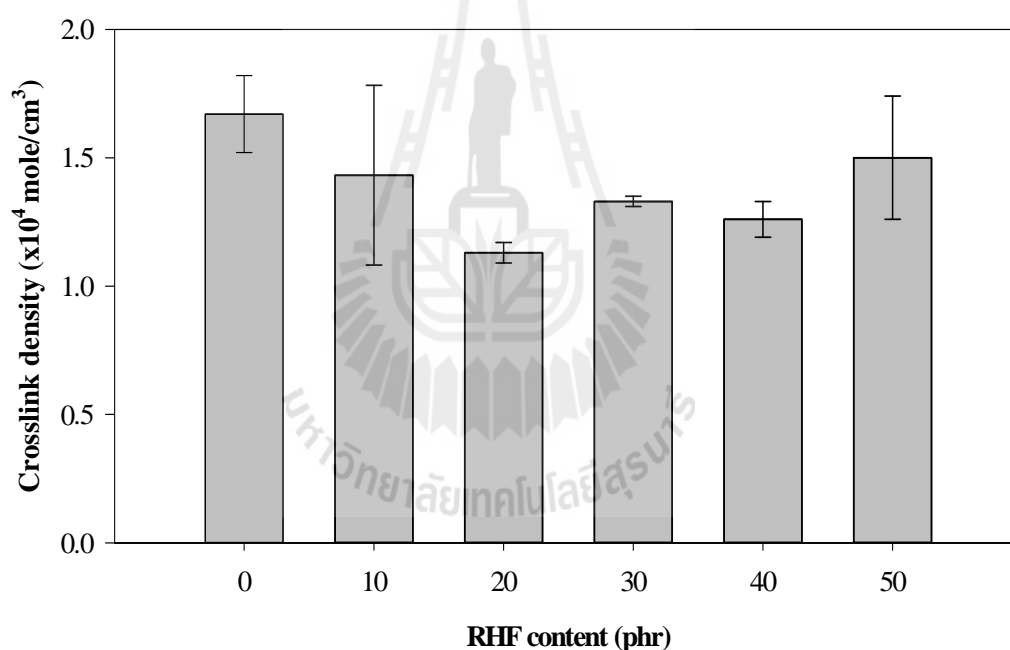


Figure 4.10 Crosslink density of gum NR and NR composites at various RHF contents.

Table 4.2 Mechanical properties and crosslink density of gum NR and NR composites at various RHF contents.

Designation	M100 (MPa)	M300 (MPa)	Elongation at break (%)	Tensile strength (MPa)	Tear strength (kN/m)	Crosslink density ($\times 10^4$ mol/cm³)
Gum NR	0.73 \pm 0.03	1.55 \pm 0.03	1106.54 \pm 92.18	13.47 \pm 3.01	35.15 \pm 2.65	1.67 \pm 0.15
10RHF/NR	0.90 \pm 0.04	1.68 \pm 0.06	1057.37 \pm 51.66	10.91 \pm 0.96	33.85 \pm 1.17	1.43 \pm 0.35
20RHF/NR	1.02 \pm 0.03	1.73 \pm 0.05	1022.12 \pm 50.71	8.63 \pm 0.65	30.89 \pm 1.35	1.13 \pm 0.04
30RHF/NR	1.16 \pm 0.07	1.88 \pm 0.06	920.79 \pm 28.72	7.41 \pm 0.26	29.29 \pm 0.83	1.33 \pm 0.02
40RHF/NR	1.38 \pm 0.05	2.02 \pm 0.06	885.55 \pm 36.20	6.62 \pm 0.48	28.29 \pm 1.28	1.26 \pm 0.07
50RHF/NR	1.32 \pm 0.04	1.96 \pm 0.05	775.40 \pm 28.72	5.09 \pm 0.13	25.36 \pm 1.08	1.50 \pm 0.24

4.1.3 Morphological properties

SEM micrographs of tensile fracture surfaces of gum NR and NR composites at various RHF contents are shown in Figure 4.11 (a-f). The surface of gum NR in Figure 4.11 (a) was smooth. When RHF was added into NR (Figure 4.11 (b-f)), NR composites exhibited rough surfaces. With increasing RHF content, the RHF agglomeration in the NR matrix became more distinguishable. In addition, all composites showed many holes indicating that RHF was pulled out from NR matrix. These implied the poor interfacial adhesion between RHF and NR matrix. The SEM micrographs of NR composites were in good agreement with the reduction in tensile properties of NR composites.

From the previous result section, RHF content affected mechanical properties of NR composites. As the RHF content increased, tensile strength, elongation at break and tear strength of NR composites decreased whereas M100 and M300 increased. The objective of this study was to obtain NR composites with acceptable mechanical properties and low cost. Therefore, a RHF content of 40 phr was chosen to prepare NR composites in the next experiment steps.

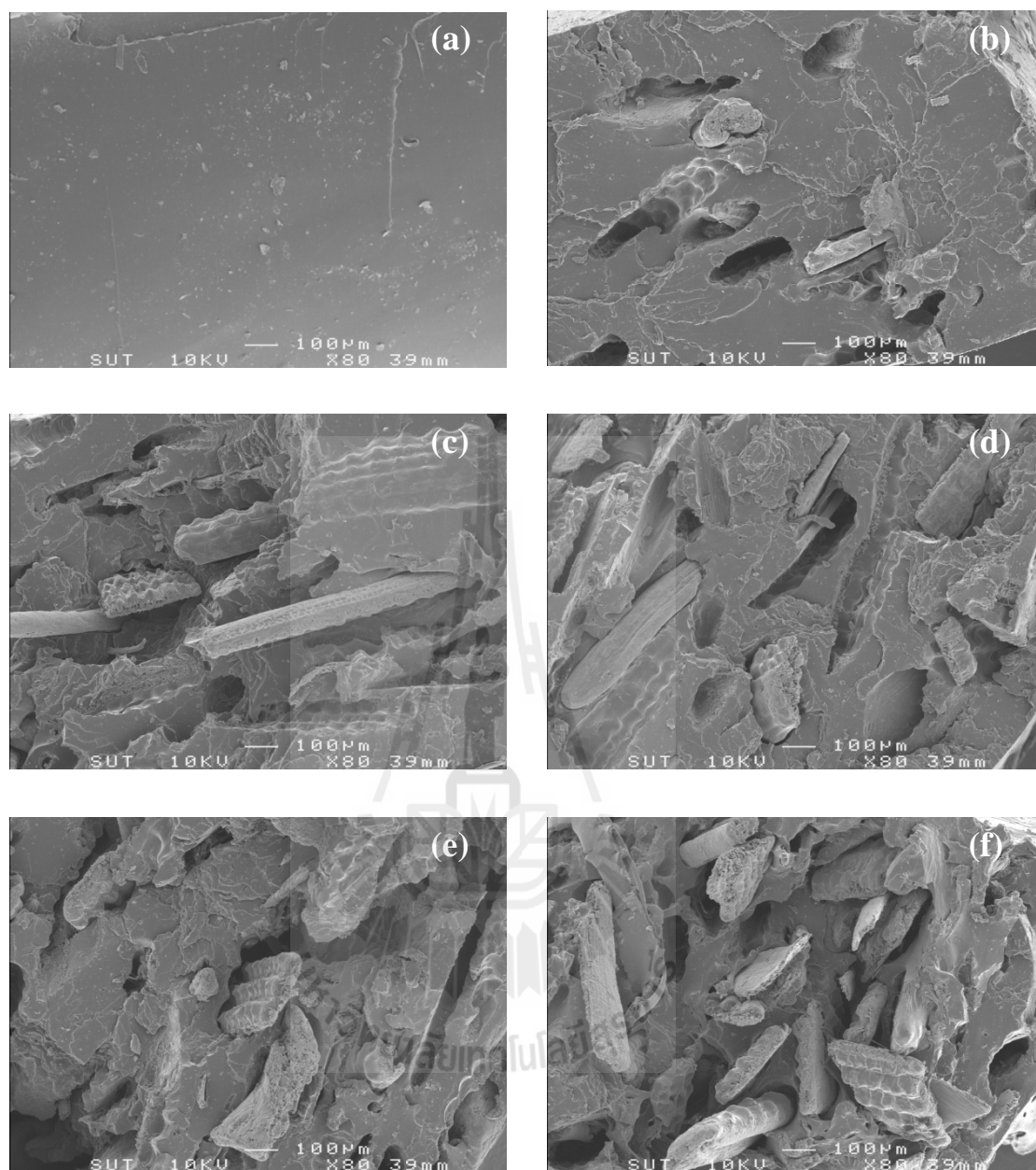


Figure 4.11 SEM micrographs of (a) gum NR, (b) 10RHF/NR, (c) 20RHF/NR, (d) 30RHF/NR, (e) 40RHF/NR and (f) 50RHF/NR composites.

4.2 Effect of acid and alkali treatments on physical properties of RHF and RHF/NR composites

From the previous section, RHF at content of 40 phr was selected to prepare NR composites. However, RHF and NR were incompatible due to the hydrophilicity of RHF and the hydrophobicity of NR. The incompatibility between RHF and NR led to the poor mechanical properties of RHF/NR composites. Therefore, this section aimed to improve the compatibility between RHF and NR by treating RHF surface with acid or alkali solutions.

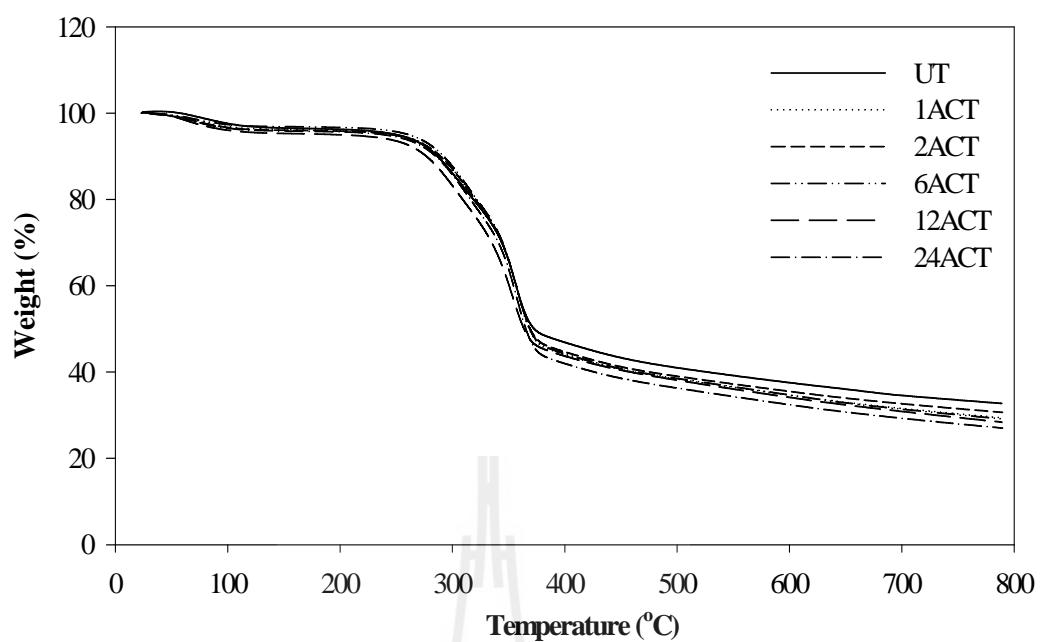
4.2.1 Fiber characterization

4.2.1.1 Thermal properties

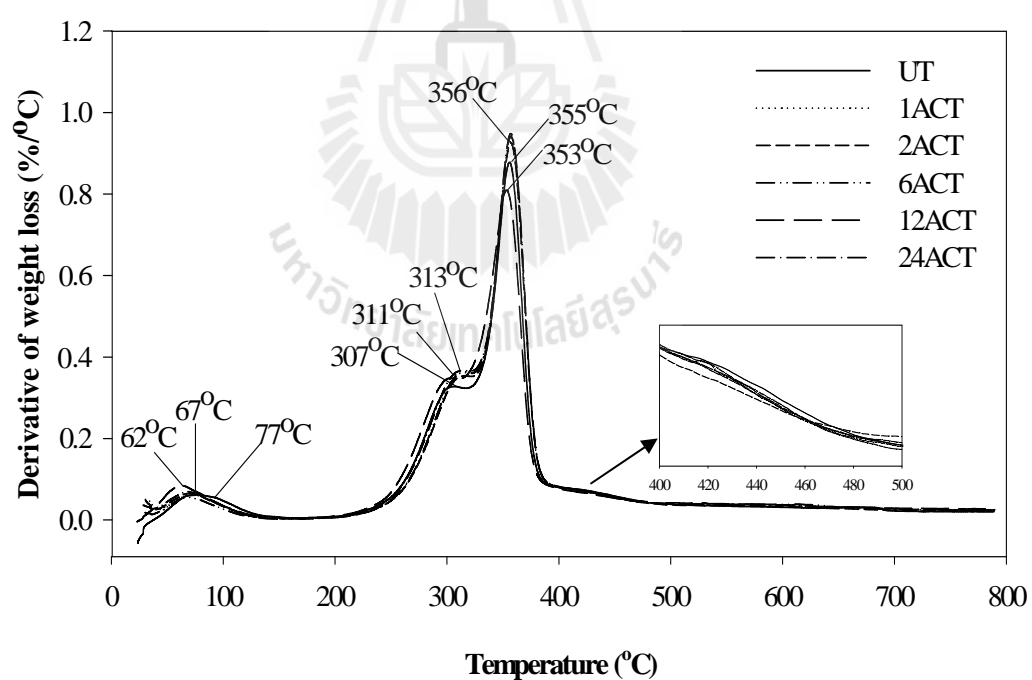
Thermogravimetric analysis (TGA) and their derivative (DTGA) thermograms of untreated RHF (UT), acid treated RHF (ACT) and alkali treated RHF (ALT) at various treatment times are shown in Figure 4.12 - 4.13 and the data are summarized in Table 4.3. From Figure 4.12, UT, ACT and ALT showed initial weight loss below 100°C attributing to the evaporation of adsorbed water on the RHF surface. The first decomposition step of UT was the shoulder peak at around 307°C involving hemicellulose decomposition. The second decomposition peak of UT was observed at 355°C which associated with cellulose decomposition. The third decomposition step of UT revealed as a small shoulder around 426°C corresponding to lignin decomposition. At 800°C, UT showed the residue amount of 32 wt% which composed of silica and carbonaceous products. Similar result was reported by many researchers. Rice husk showed three decomposition stages according to the decompositions of hemicellulose (150-300°C), cellulose (300-350°C) and lignin (400-

500°C) (Ciannamea , Stefan and Ruseckaite, 2010; Luduena, Vazquez and Alvarez, 2010; Mansaray and Ghaly, 1998).

For the treated RHF, *i.e.*, ACT and ALT, their thermal decomposition behaviors depended on treatment methods and treatment times. All samples of ACT had three decomposition steps similar to UT. The acid treated RHF showed decomposition of hemicellulose, cellulose and lignin at around 303-313, 353-356 and 424-429°C, respectively. The hemicellulose decomposition peak was still observed even with increasing acid treatment time. This indicated that hemicellulose could not be removed by treating RHF surface with HCl. Mishra, Mohanty, Drzal, Misra and Hinrichsen, (2004) suggested that hemicellulose and cellulose were slowly hydrolyzed in acid condition at low temperature. The amounts of residues at 800°C of acid treated RHF were slightly lower than that of untreated RHF. With increasing treatment time, the residue amount at 800°C was insignificant difference. This implied that treatment time had no effect on the residue weight of ACT.



(a)

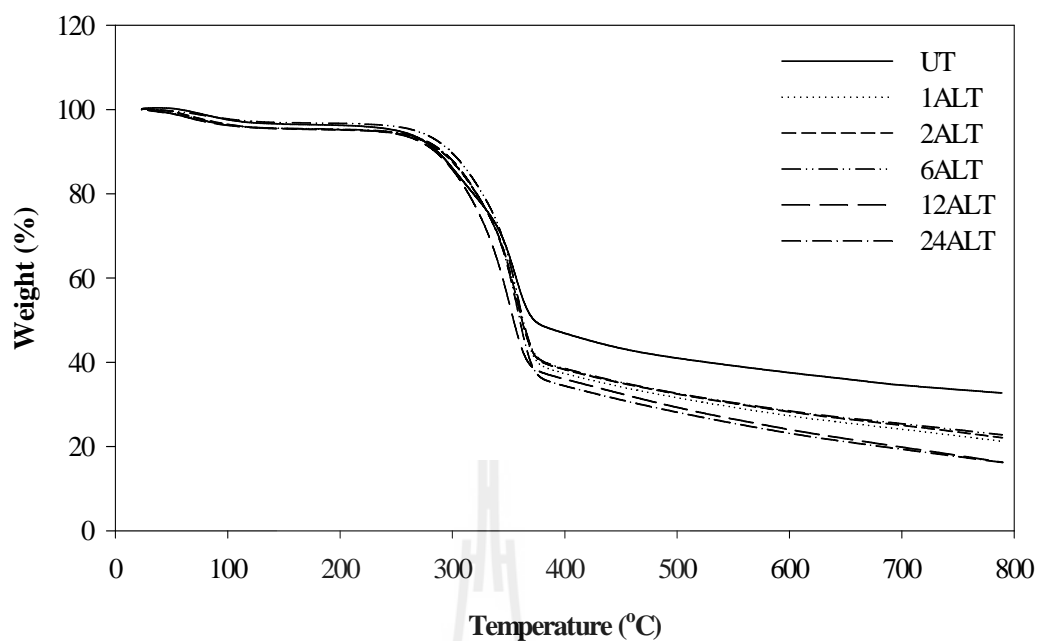


(b)

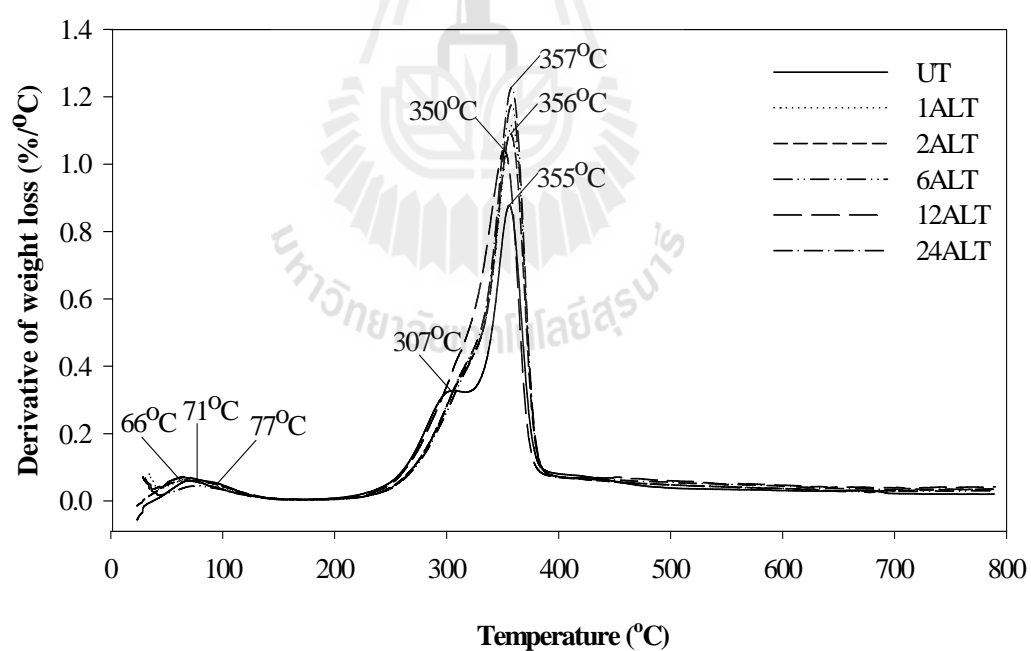
Figure 4.12 TGA (a) and DTGA (b) thermograms of UT and ACT at various treatment times.

For all ALT samples, hemicellulose and lignin peaks disappeared. This result confirmed the removal of hemicellulose and lignin in RHF during alkali treatment. ALT showed only one decomposition step at around 350-357°C corresponding to cellulose decomposition compared with UT and ACT. Moreover, the residues remaining after heating ALT at 800°C were lower than that of UT and ACT. The reduction of ALT residue was because of the removal of silica during alkali treatment (Ndazi, Nyahumwa and Tesha, 2007). The amount of residues of alkali treated RHF decreased more drastically with increasing treatment time.





(a)



(b)

Figure 4.13 TGA (a) and DTGA (b) thermograms of UT and ALT at various treatment times.

Table 4.3 Thermal decomposition temperatures of UT, ACT and ALT at various treatment times.

Treatment conditions	Water evaporation			Thermal decomposition temperature (°C)			Residue (wt%)
	Onset (°C)	Peak (°C)	Weight loss (%)	1 st step	2 nd step	3 rd step	
UT	57	77	3	307	355	426	32
1ACT	34	72	4	311	356	428	29
2ACT	30	71	4	313	356	429	30
6ACT	30	67	3	313	356	429	29
12ACT	30	62	4	303	353	424	28
24ACT	30	67	4	313	356	429	27
1ALT	34	71	4	-	357	-	22
2ALT	36	66	4	-	356	-	22
6ALT	36	77	3	-	356	-	22
12ALT	30	65	4	-	350	-	16
24ALT	28	65	4	-	357	-	16

4.2.1.2 Functional group analysis

FTIR spectra of UT, ACT and ALT at various treatment times are shown in Figure 4.14 - 4.15 and the assignment of absorption bands are presented in Table 4.4. According to FTIR results, the absorption bands observed in FTIR spectra of untreated and treated RHF were attributed to their chemical compositions, *i.e.*, hemicellulose, cellulose and lignin (Genieva, Turmanova, Dimitrova and Vlaev, 2008; Luduena, Fasce, Alvarez and Stefani, 2011; Markovska and Lyubchev, 2007). UT showed absorption bands at 3339 and 2923 cm^{-1} relating to the stretching vibrations of -O-H and -C-H stretching of hemicellulose, cellulose and lignin. The band observed at 1727 cm^{-1} was attributed to $\text{C}=\text{O}$ stretching of the ester groups in hemicellulose or the carboxylic acid groups in lignin. The absorbance bands appeared at 1603 and 1511 cm^{-1} relating to vibration $\text{C}=\text{C}$ stretching vibration of aromatic rings of lignin. In addition, the bands of -CH₂ bending and -CH stretching of hemicellulose, cellulose and lignin in RHF were observed at 1450, 1424, 1369 and 1321 cm^{-1} . Moreover, the absorption bands observed at 1032 and 795 cm^{-1} were attributed to the C-O stretching of cellulose and Si-O-Si bonds of silica in RHF. After acid treatment, the spectra of ACT at various treatment times were similar to that of UT. This result indicated that hemicellulose, cellulose, lignin and silica components were not removed during the acid treatment. The FTIR results well agreed with the TGA results shown in Figure 4.12.

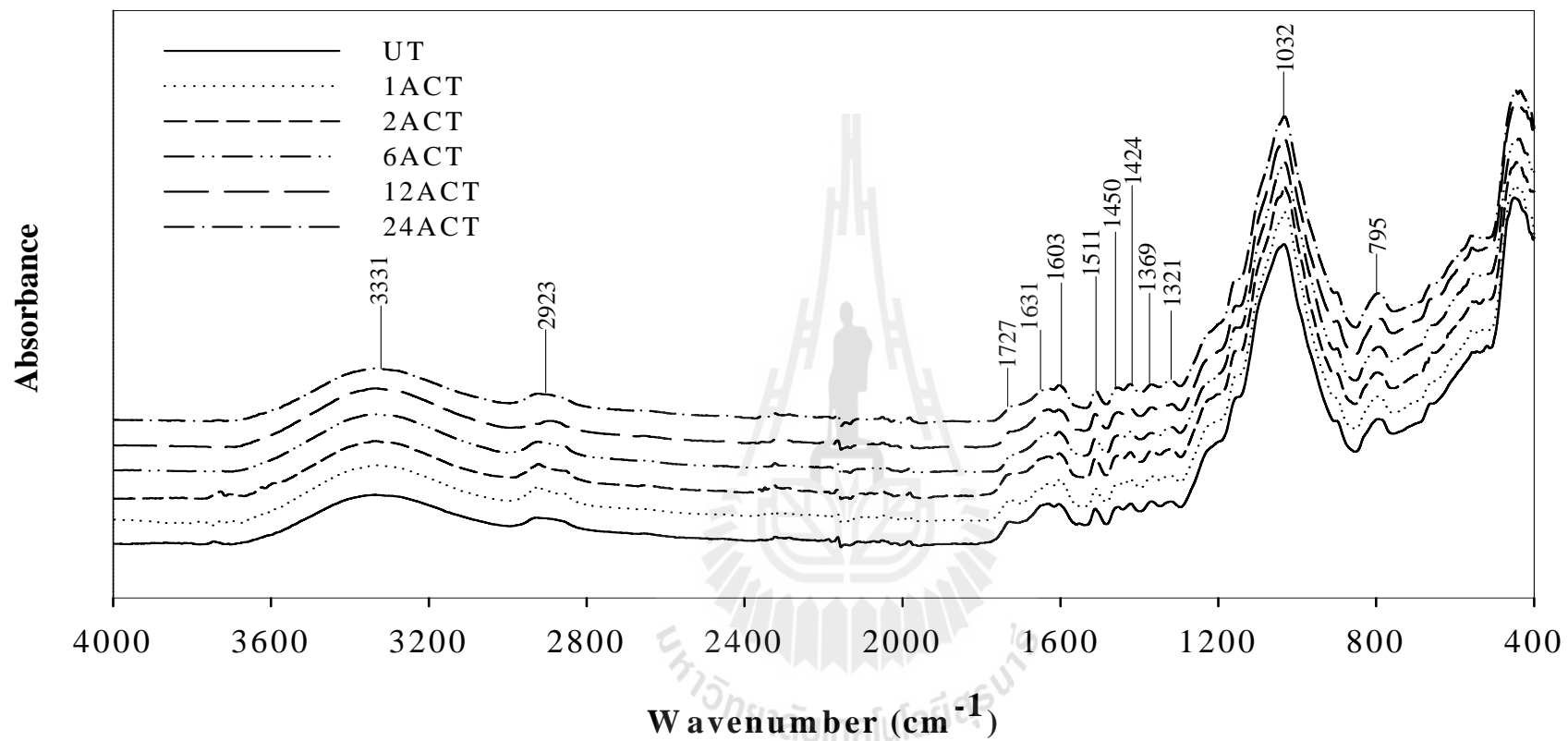


Figure 4.14 FTIR spectra of UT and ACT at various treatment times.

After alkali treatment, FTIR spectra of ALT were almost similar to the UT except the disappearance of the absorption band at 1727 cm^{-1} . This indicated the removal of hemicellulose and lignin in RHF during the alkali treatment. In addition, the appearance of bands between $793\text{-}783\text{ cm}^{-1}$ in ALT indicated the partial remaining of silica in ALT. As the treatment time increased, absorption bands of ALT had insignificant difference.



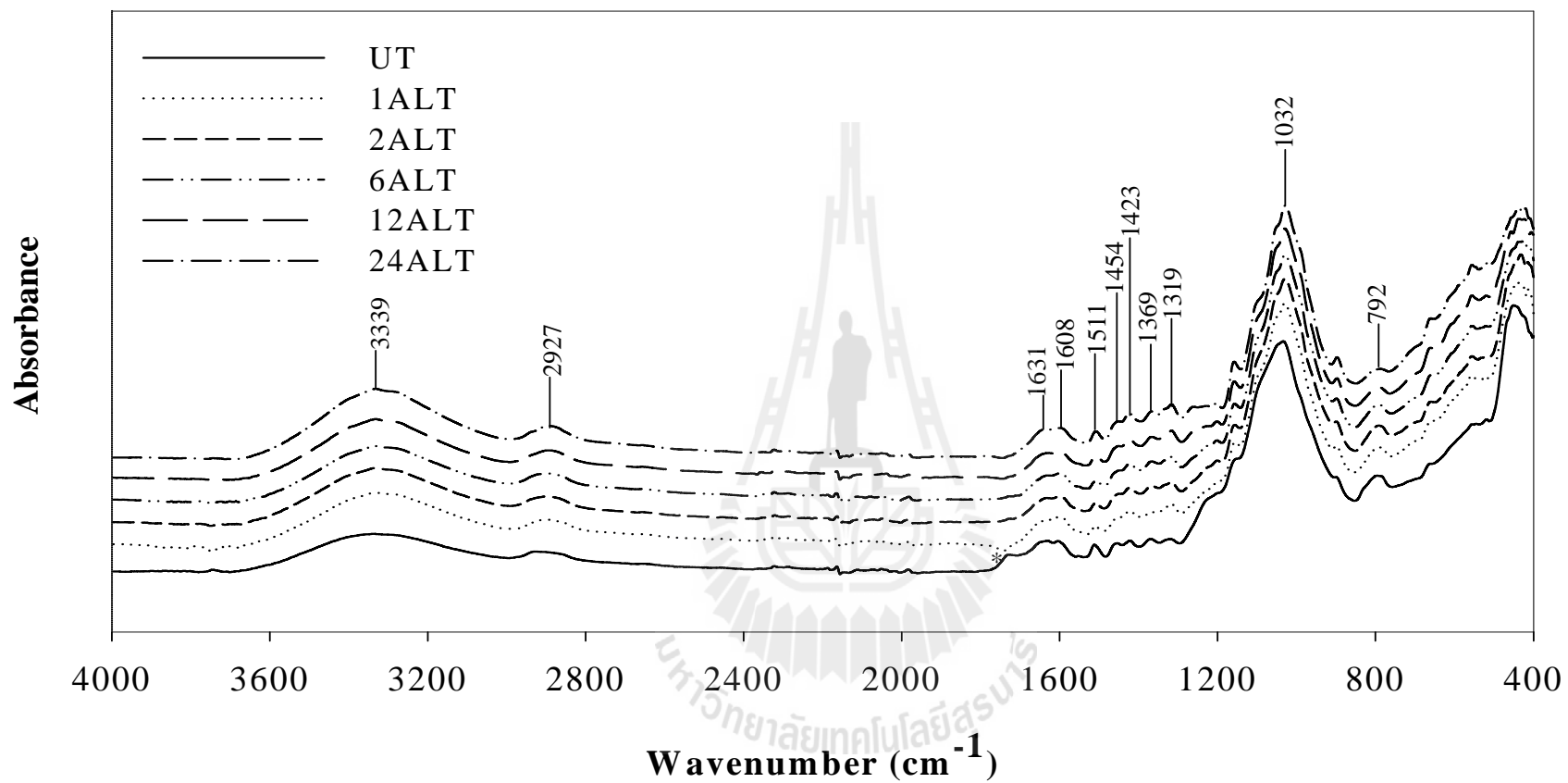


Figure 4.15 FTIR spectra of UT and ALT at various treatment times.

Table 4.4 FTIR peak positions of UT, ACT and ALT at various treatment times (Genieva *et al.*, 2008; Luduena *et al.*, 2011; Markovska *et al.*, 2007).

Wavenumber (cm ⁻¹)			Vibration	Source
UT	ACT	ALT		
3339	3339-3329	3334-3331	OH stretching	hemicellulose, cellulose, lignin, water
2927	2939-2921	2899-2893	C-H stretching	hemicellulose, cellulose, lignin
1729	1727	-	C=O stretching	lignin
1631	1631-1630	1633-1630	OH stretching	adsorbed water
1604	1604-1603	1601-1598	C=C stretching	lignin
1512	1512-1511	1512-1508	C=C stretching	aromatic ring
1454-1424	1453-1423	1448-1423	CH ₂ strain	hemicellulose, cellulose, lignin
1369-1320	1368-1318	1361-1316	CH bending	hemicellulose, cellulose, lignin
1034	1032-1030	1030-1029	C-O stretching	cellulose
795	797-790	793-789	Si-O-Si stretching	silica

4.2.1.3 Morphological properties

SEM micrographs of UT, ACT and ALT at various treatment times are illustrated in Figure 4.16 - 4.19. The micrographs of the outer surfaces of UT and ACT are shown in Figure 4.16 (a-f) while the micrographs of the inner surfaces of UT and ACT at various treatment times are shown in Figure 4.17 (a-f). According to Figure 4.16 (a), the outer surface of UT revealed the ridged and furrow structures. The ridged structures were separated with dome shape protrusions. Some research work ascribed that at high silica content, silica concentrated in this region corresponding to dome-shape protrusion and adjoining sloping area (Park *et al.*, 2003). In addition, impurities, *i.e.*, wax and dust, were observed on the outer surface of UT. After acid treatment (Figure 4.16 (b-f)), ACT showed clean outer surface. This implied that acid treatment eliminated wax and dust on RHF surface. However, with increasing treatment time, the outer surface of ACT was not changed. The similar trend was found in the inner surface of RHF. The inner surface of UT showed the smooth surface (Figure 4.17 (a)). After treating RHF with acid solution at various treatment time (Figure 4.17 (b-f)), the inner surface of ACT was not dramatically changed. This result corresponded to TGA and FTIR results of ACT.

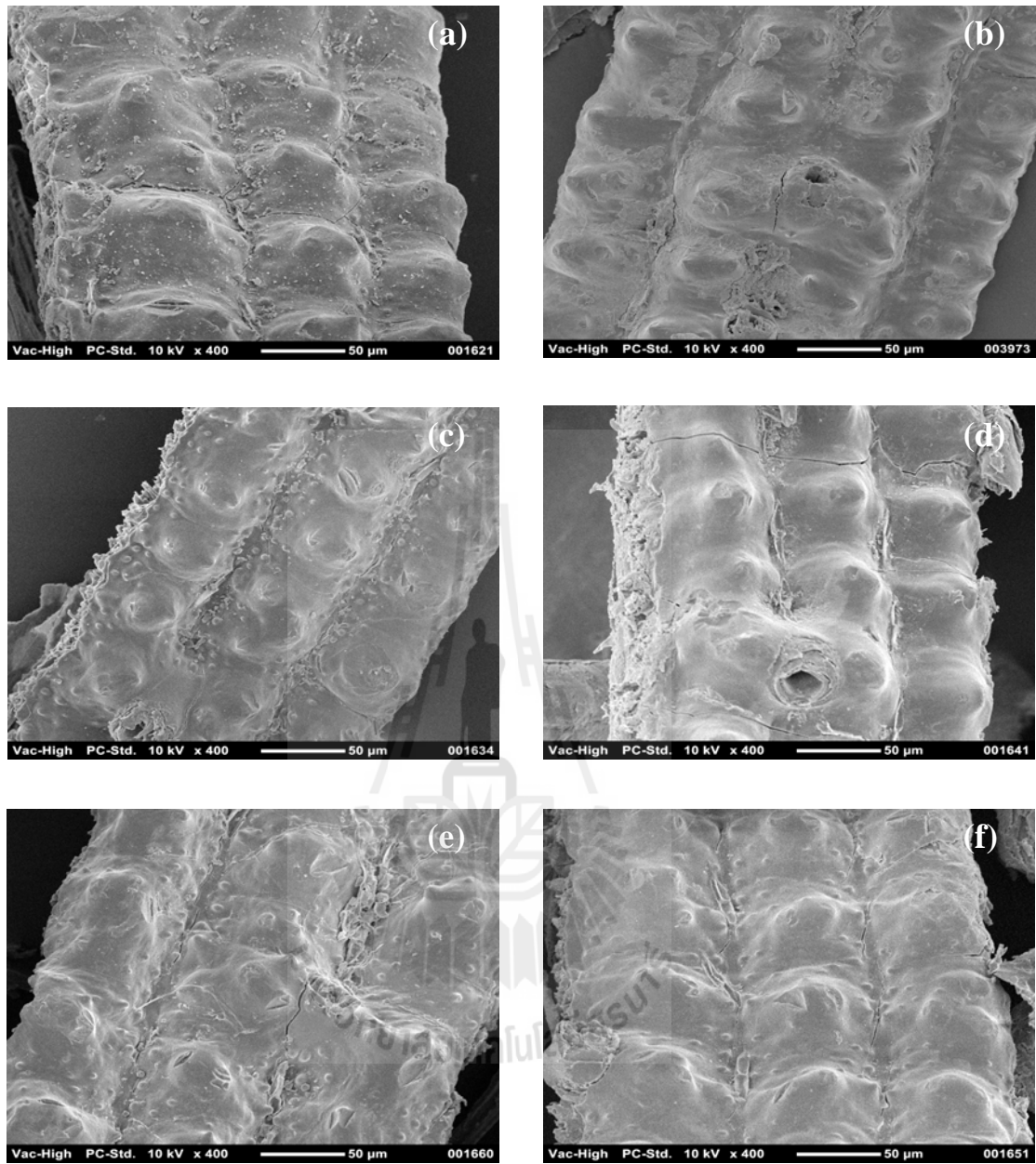


Figure 4.16 SEM micrographs of outer surfaces of (a) UT, (b) 1ACT, (c) 2ACT, (d) 6ACT, (e) 12ACT and (f) 24ACT.

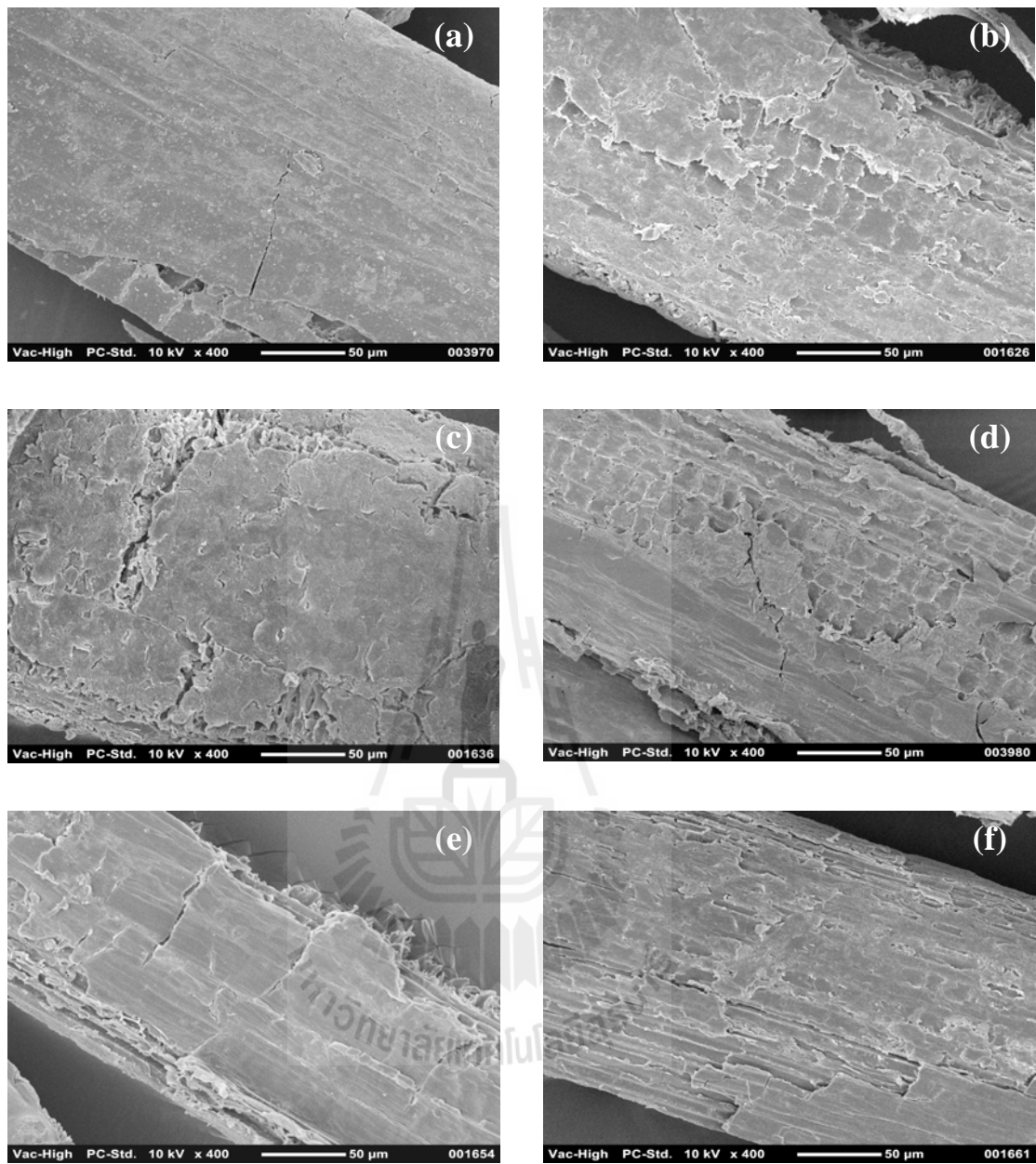
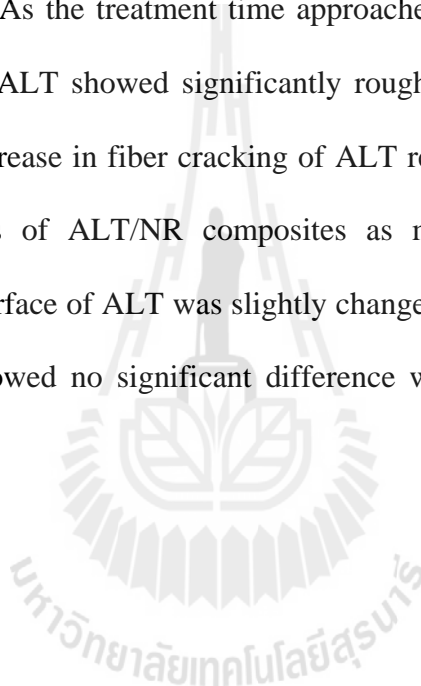


Figure 4.17 SEM micrographs of inner surfaces of (a) UT, (b) 1ACT, (c) 2ACT, (d) 6ACT, (e) 12ACT and (f) 24ACT.

The micrographs of the outer surfaces of UT and ALT are presented in Figure 4.18 (a-f) and the inner surfaces of UT and ALT are shown in Figure 4.19 (a-f). After alkali treatment (Figure 4.18 (b-f)), it can be seen that the outer surfaces of ALT were cleaner and rougher than that of UT. This was due to the removal of hemicellulose, lignin and wax on RHF surface during alkalization. The increase in surface roughness of ALT may enhance mechanical interlocking between RHF and NR matrix. As the treatment time approached 12-24 h (Figure 4.18 (e-f)), the outer surfaces of ALT showed significantly rougher surface, fiber splitting and fiber cracking. An increase in fiber cracking of ALT resulted in an adverse effect on mechanical properties of ALT/NR composites as mentioned in section 4.2.2.2. However, the inner surface of ALT was slightly changed as compared to those of UT. The inner surface showed no significant difference with increasing treatment time (Figure 4.19 (b-f)).



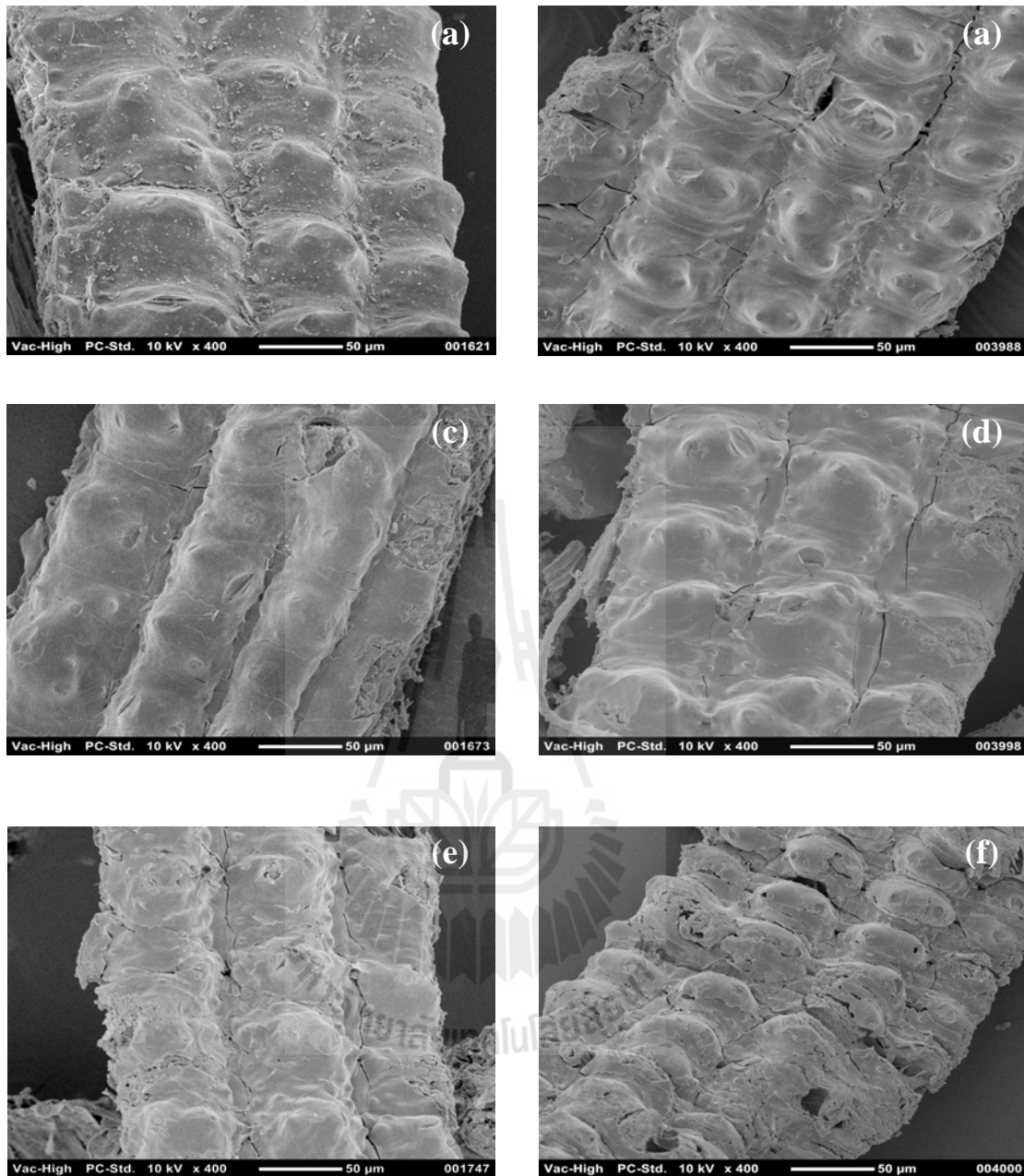


Figure 4.18 SEM micrographs of the outer surfaces of (a) UT, (b) 1ALT, (c) 2ALT, (d) 6ALT, (e) 12ALT and (f) 24ALT.

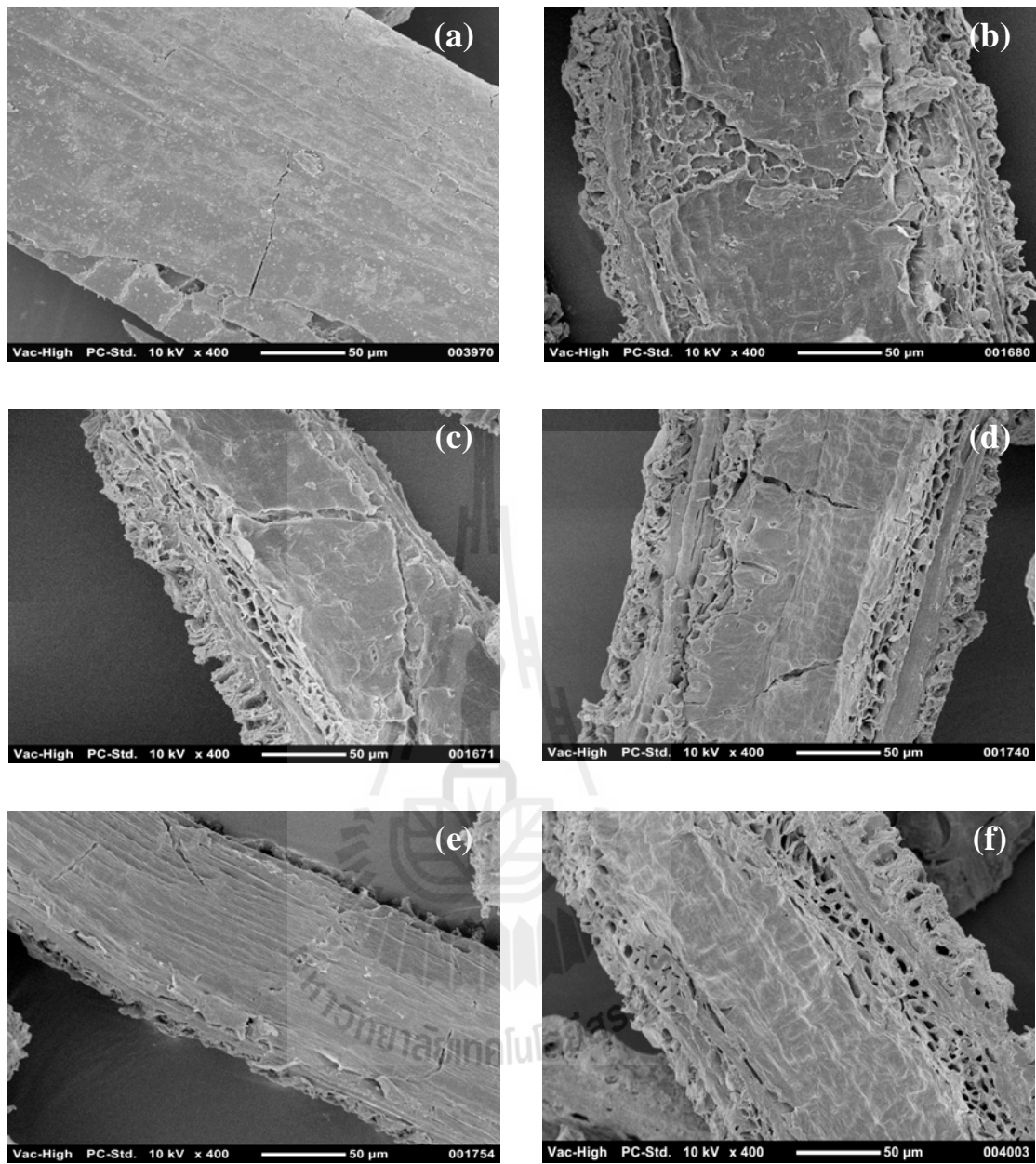


Figure 4.19 SEM micrographs of inner surfaces of (a) UT, (b) 1ALT, (c) 2ALT, (d) 6ALT, (e) 12ALT and (f) 24 ALT.

4.2.1.4 Length/diameter (L/D) ratio

L/D ratio of fiber was calculated from dividing length (L) by its diameter. The L/D ratio of UT, ACT and ALT at various treatment times are shown in Table 4.5. As compared with UT, L/D ratio of ACT showed insignificant change with increasing treatment times due to the existence of cement component, *i.e.*, hemicellulose and lignin, in RHF. Hemicellulose and lignin performed as a binder in fiber to prevent the bundle from acid treatment (Johar, Ahmad and Durfresne, 2012).

L/D ratio of ALT significantly increased as compared with that of UT. This was because alkali treatment removed hemicellulose and lignin in fiber resulting in fiber splitting and cracking (Hornsby, Hinrichsen and Tarverdi, 1997). The fiber splitting and cracking made the reduction of diameter of RHF leading to an increase in L/D ratio of ALT. L/D ratio of ALT slightly increased as treatment time increased. The increase in L/D ratio of ALT may enhance mechanical properties of ALT/NR composites. However, at treatment time of 24 h, L/D ratio of ALT slightly decreased. This was due to an increase in fiber cracking leading to a reduction of ALT length. The fiber cracking of rice husk (RH) after alkali treatment was also reported by Ndazi, Karlsson, Tesha and Nyahumwa (2007). They found that fiber cracking occurred in horizontal axis and was observed at high alkali concentration (8 wt%).

Table 4.5 L/D ratio of UT, ACT and ALT at various treatment times.

Designation	L/D
UT	4.48±1.43
1ACT	4.17±1.95
2ACT	3.79±1.46
6ACT	4.42±1.30
12ACT	4.47±1.12
24ACT	5.13±2.58
1ALT	4.88±3.10
2ALT	6.58±3.36
6ALT	7.54±2.29
12ALT	8.52±2.79
24ALT	6.87±2.80

4.2.2 Composite characterization

4.2.2.1 Cure characteristics

Cure characteristics, *i.e.*, scorch time (T_s), cure time (T_{90}), maximum torque (S_{max}), minimum torque (S_{min}) and torque difference ($S_{max} - S_{min}$), of untreated RHF (UT)/NR, acid treated RHF (ACT)/NR and alkali treated RHF (ALT)/NR composites are presented in Figure 4.20 - 4.24 and summarized in Table 4.6.

From Figure 4.20, it can be seen that scorch times of ACT/NR and ALT/NR composites slightly changed as compared with those of UT/NR composites. Scorch time of ACT/NR and ALT/NR composites was insignificant difference as compared between the fiber treatment time of 1 and 2 h. With increasing treatment time from 2 to 24 h, scorch times of ALT/NR composites were longer than those of ACT/NR composites. Generally, cure characteristics of rubber composites depend on filler properties, *i.e.*, surface area, surface reactivity, particle size, moisture content and metal oxide content (Ichazo, Herná'ndez, Albano and Gonza'lez, 2006; Ismail, Rozman, Jaffri and Ishak, 1997). The delay of scorch time of ALT/NR composite may be attributed to the enhancement of RHF surface area by alkali treatment. When RHF was treated with alkali solution, hemicellulose and lignin on RHF surface were removed resulting in enhanced surface area of RHF. The higher surface areas of ALT prolonged scorch time of NR composites. Cure times of UT/NR, ACT/NR and ALT/NR composites showed different trends from scorch times of NR composites as shown in Figure 4.21. Cure times of all composites was not changed with changing treatment methods and treatment times. De, *et al.*, (2004) studied the effect of alkali and water treatments on cure characteristics of grass fiber/NR

composites. They suggested that NR composite containing water treated grass fiber (pH=5.1) had longer scorch time and cure time than NR composites containing alkali treated grass fiber (pH=8.1). This was ascribed to acidity and alkalinity of the treated grass fiber surface. The acidity of water treated grass fiber prolonged vulcanization process of NR composites but the alkalinity of alkali treated grass fiber accelerated vulcanization process of the composites. In this work, RHF was treated with acid and alkali solutions and washed with distilled water until the water became neutral. Consequently, cure time of NR composites was not affected by treatment methods and treatment times.



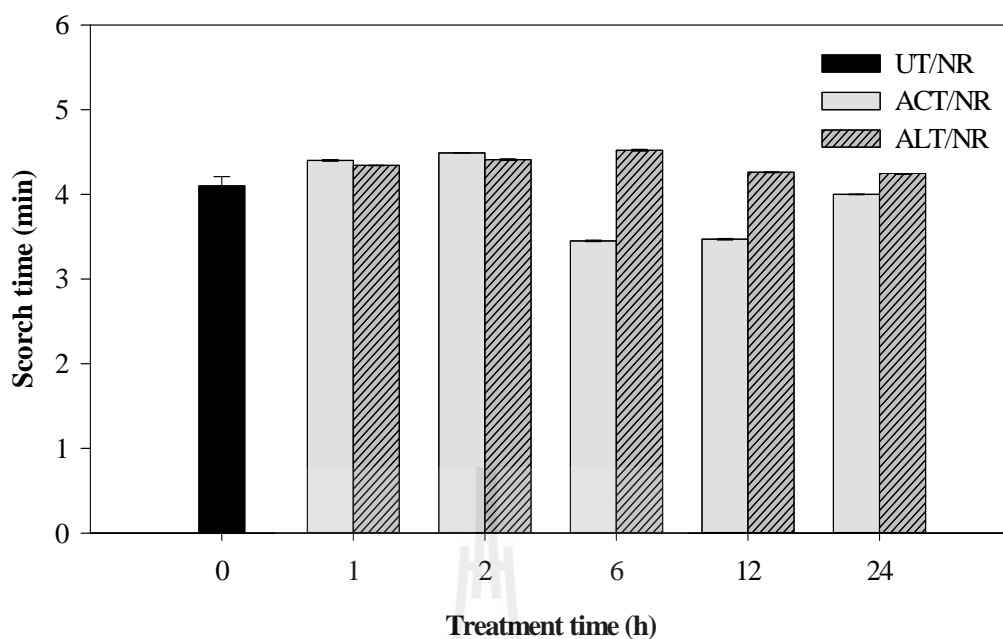


Figure 4.20 Scorch time of UT/NR, ACT/NR and ALT/NR composites at various treatment times.

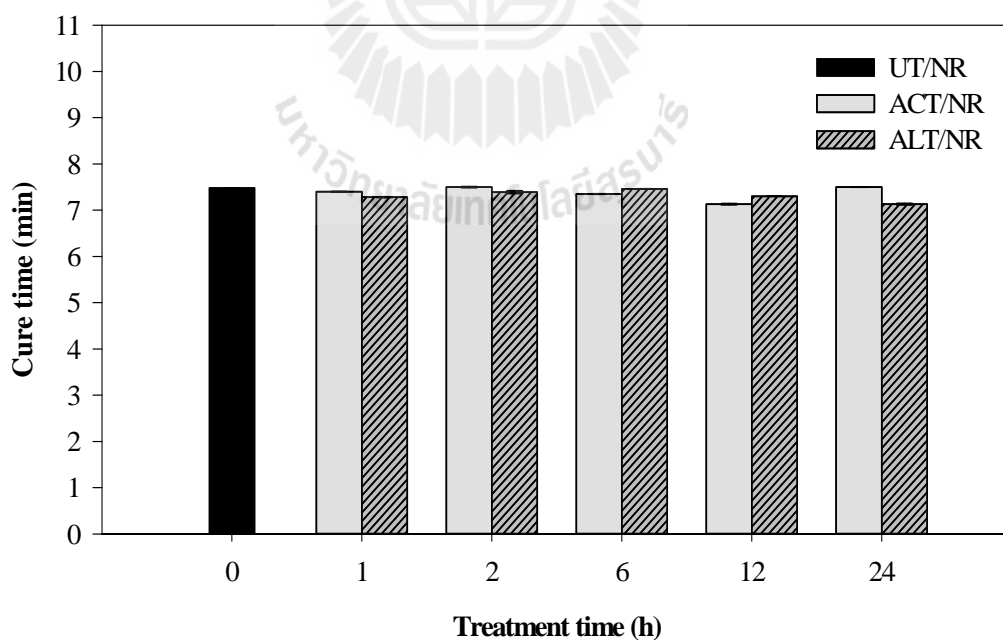


Figure 4.21 Cure time of UT/NR, ACT/NR and ALT/NR composites at various treatment times.

Minimum torque and maximum torque of UT/NR, ACT/NR and ALT/NR composites at various treatment times are shown in Figure 4.22 - 4.23. Minimum torque of both ACT/NR and ALT/NR composites showed the highest values at treatment time of 6 h and tended to decrease with increasing treatment time. It is well known the minimum torque of rubber composites indicates the softening of rubber before vulcanization corresponding to viscosity of the rubber composites. The viscosity of rubber composites was controlled by mixing time, filler type, molecular weight and entanglement of molecular chain (Saramolee, Lertsuriwat, Hunyek and Sirisathitkul, 2010). In this study, the mixing time of all composites was constant. Thus, the change of the minimum torque of NR composites was attributed to properties of RHF. In case of acid treatment, the remaining of cement materials, *i.e.*, hemicellulose and lignin, in RHF led to the high stiffness of ACT. The stiffness of ACT restricted the movement of rubber molecules resulting in the increment of viscosity of NR composites. On the contrary, the enhancement of minimum torque of ALT/NR composites in this study involved the better dispersibility of treated RHF in NR matrix. Similar result was found by Hussain, Abdel-Kader and Ibrahim, (2010) in linen fiber waste/NR composites. Similar trend was found in the maximum torque value. Maximum torque of ACT/NR composites showed the maximum value at treatment time of 6 h while the maximum torque of ALT/NR composites exhibited the highest value at treatment time of 12 h. The increase in maximum torque in ACT/NR composites was due to the stiffness of ACT sample. In contrast, the enhancement of maximum torque of ALT/NR composites was because the surface roughness of RHF after alkali treatment enhanced rubber-filler interaction by the mechanical interlocking. Similar observations have been reported by Mathew and Joseph, (2007),

Sareena, *et al.*, (2012) and Wongsorat, (2009). They found that the maximum torques of natural fibers based NR composites were improved by alkalization. The results may be due to the better interfacial adhesion between fiber and NR matrix.

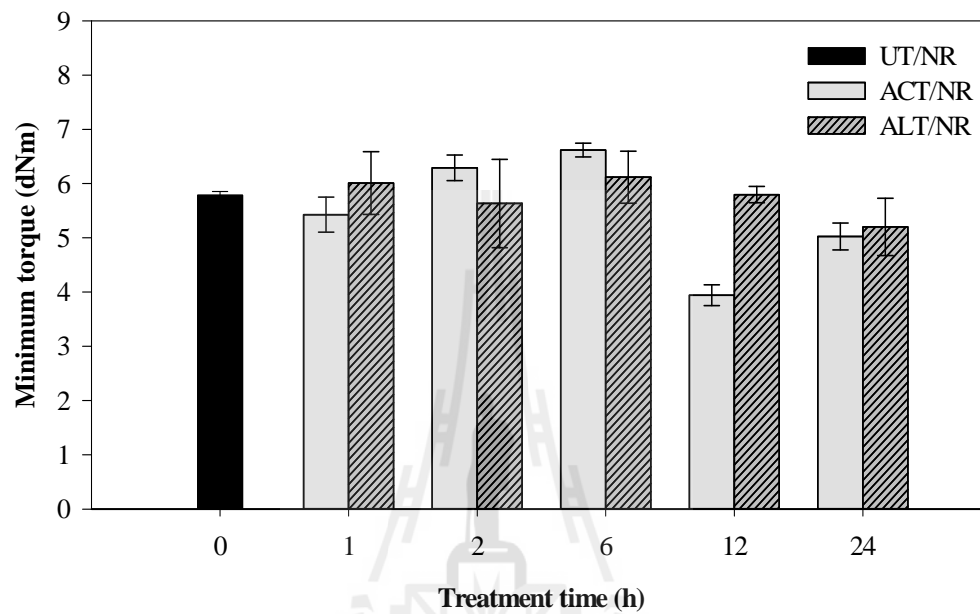


Figure 4.22 Minimum torque of UT/NR, ACT/NR and ALT/NR composites at various treatment times.

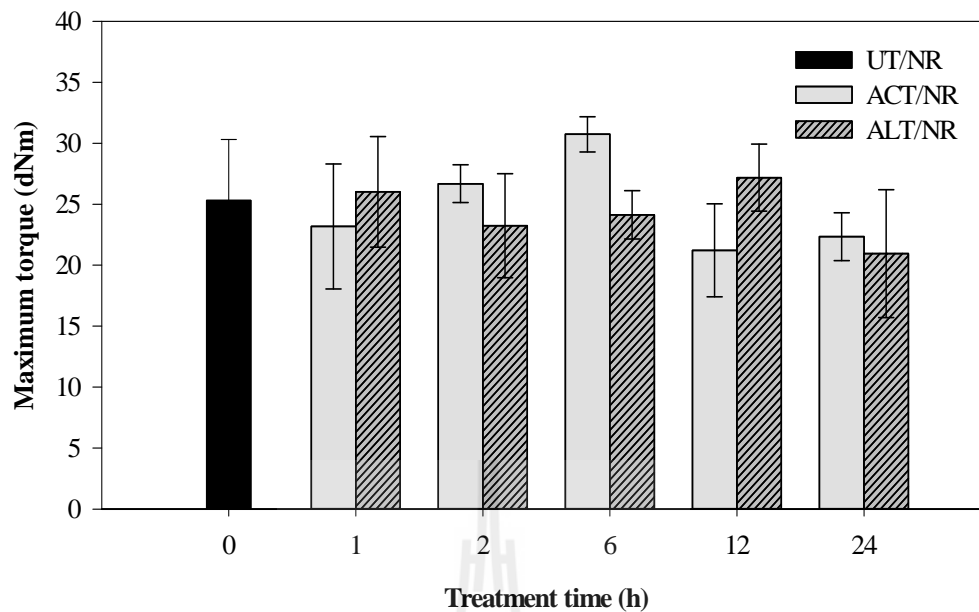


Figure 4.23 Maximum torque of UT/NR, ACT/NR and ALT/NR composites at various treatment times.

Torque differences of UT/NR, ACT/NR and ALT/NR composites at various treatment times are shown in Figure 4.24. It can be seen that the torque differences of ACT/NR composites presented the maximum value at treatment time of 6 h whereas ALT/NR composites revealed the maximum torque difference at treatment time of 12 h. This trend was similar to the observed maximum torque of NR composites. However, the crosslink density of UT/NR, ACT/NR and ALT/NR composites was insignificantly different. Therefore, the increase in torque difference of ACT/NR and ALT/NR composites was attributed to the fiber properties after acid and alkali treatments. After acid treatment, wax on RHF surface was removed while the other chemical components, *i.e.*, hemicellulose, cellulose, lignin, and silica were restrained. The remaining of cement materials in ACT may probably cause its higher stiffness leading to higher torque difference of ACT/NR composites. In contrast,

alkali treatment effectively removed hemicellulose, lignin and wax on RHF surface resulting in rough surface and low stiffness of the obtained ALT. This resulted in the insignificant change torque difference of ALT/NR composites.

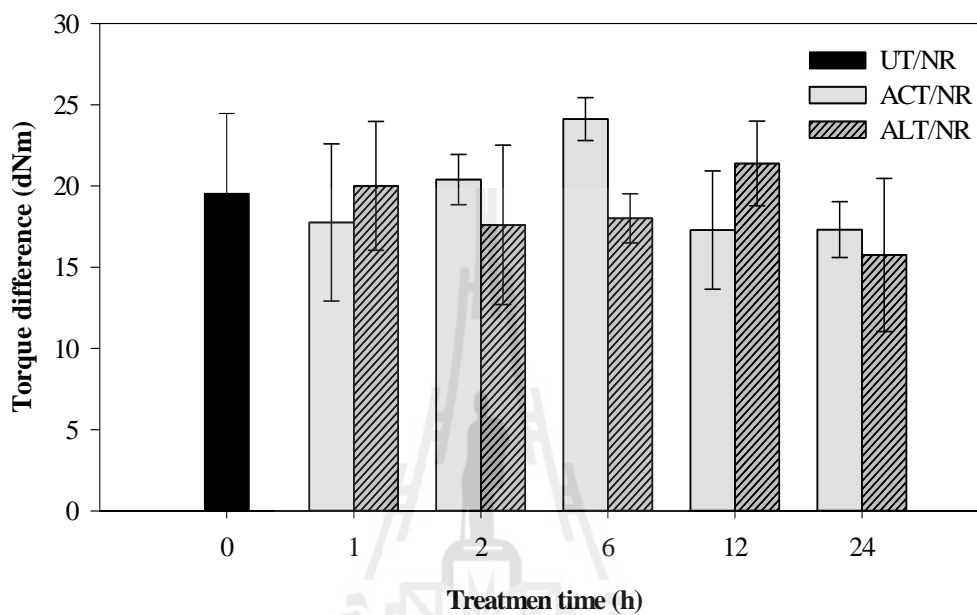


Figure 4.24 Torque difference of UT/NR, ACT/NR and ALT/NR composites at various treatment times.

Table 4.6 Cure characteristics of UT/NR, ACT/NR and ALT/NR composites at various treatment times.

Designation	Scorch time (min)	Cure time (min)	S _{max} (dNm)	S _{min} (dNm)	S _{max} -S _{min} (dNm)
UT/NR	4.10	7.48	25.33	5.79	19.54
1ACT/NR	4.40	7.40	23.18	5.43	17.75
2ACT/NR	4.49	7.44	24.19	5.64	18.55
6ACT/NR	3.45	7.35	30.74	6.62	24.12
12ACT/NR	3.47	7.13	21.22	3.94	17.28
24ACT/NR	4.00	7.50	22.34	5.02	17.32
1ALT/NR	4.34	7.28	24.08	5.71	18.37
2ALT/NR	4.41	7.39	23.24	5.53	17.71
6ALT/NR	4.52	7.46	24.13	6.12	18.01
12ALT/NR	4.26	7.30	27.18	5.79	21.39
24ALT/NR	4.25	7.13	20.95	5.2	15.75

4.2.2.2 Mechanical properties and crosslink density

Modulus at 100% strain (M100), modulus at 300% strain (M300), elongation at break, tensile strength, tear strength and crosslink density of UT/NR, ACT/NR and ALT/NR composites at various treatment times are illustrated in Figure 4.25 - 4.30 and summarized in Table 4.7.

4.2.2.2.1 Tensile properties

Modulus at 100% strain (M100) and modulus at 300% strain of UT/NR, ACT/NR and ALT/NR composites at various treatment times are shown in Figure 4.25 - 4.26. Both M100 and M300 of ACT/NR and ALT/NR composites insignificantly increased as compared with those of UT/NR composites. Moreover, treatment methods and treatment times exhibited no remarkable effect on M100 and M300 of NR composites. Nonetheless, Ismail, Norjulia and Ahmad, (2010) and Sareena, *et al.*, (2012) found that the NR composites filled with alkali treated kenaf fiber and alkali treated peanut shell powder (PSP) had higher modulus than NR composites filled with untreated fiber. In general, modulus of rubber composites is controlled by filler content, filler-matrix interaction, filler dispersion, filler surface reactivity and crosslink density (Radovanovic', Markovic' and Radovanovic, 2008; Sareena, *et al.*, 2012). In addition, the insignificant change in modulus of ACT/NR and ALT/NR composites was due to the insignificant difference of crosslink density of NR composites. From this study, it can be suggested that the effect of RHF content was more dominant than the performance of RHF surface treatment on modulus of NR composites.

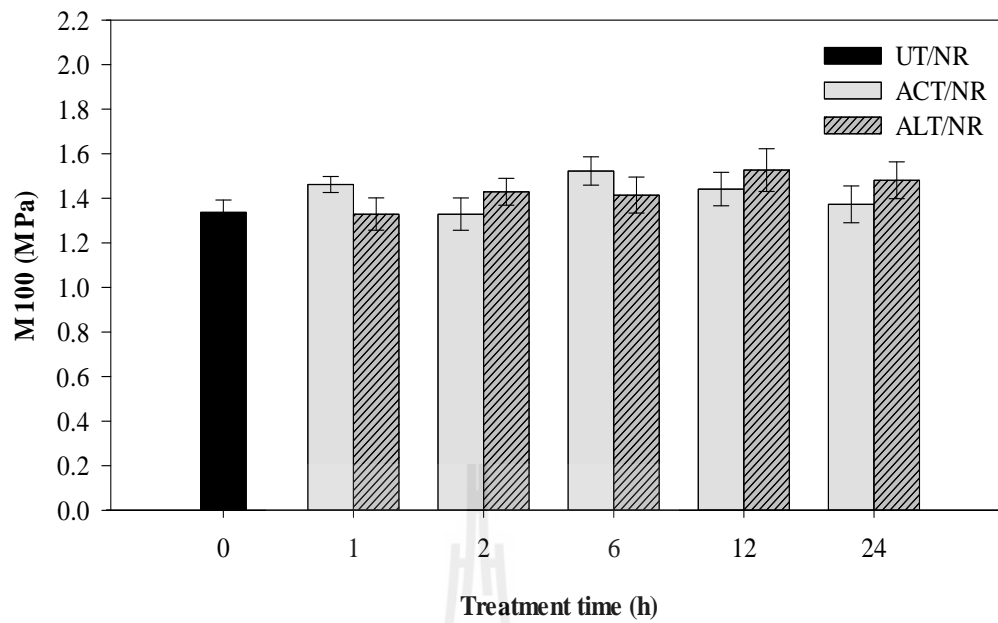


Figure 4.25 Modulus at 100% strain (M100) of UT/NR, ACT/NR and ALT/NR composites at various treatment times.

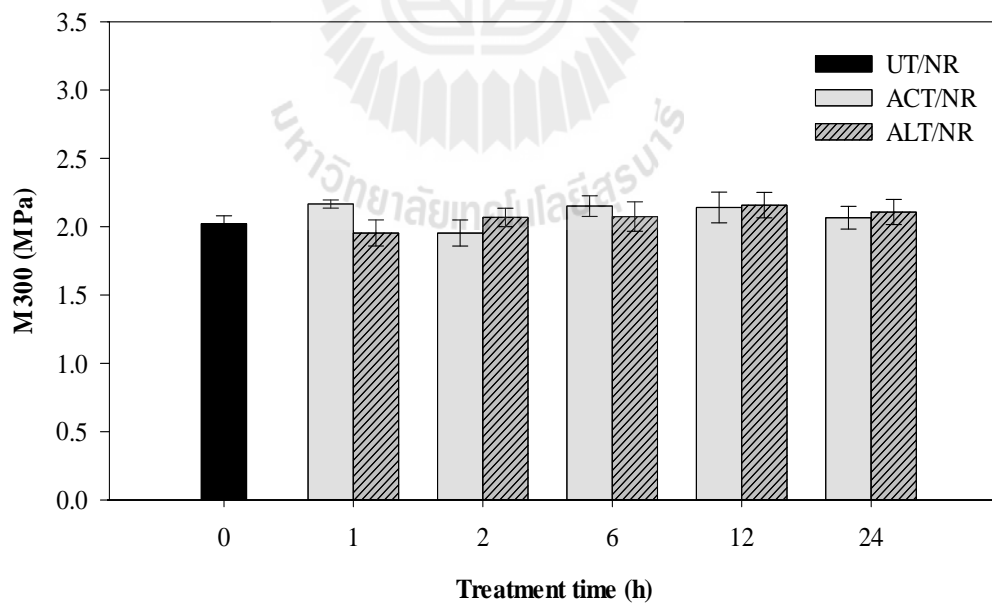


Figure 4.26 Modulus at 300% strain (M300) of UT/NR, ACT/NR and ALT/NR composites at various treatment times.

Elongation at break of UT/NR, ACT/NR and ALT/NR composites is illustrated in Figure 4.27. Elongation at break of ACT/NR composites insignificantly changed as compared with that of UT/NR composites while elongation at break of ALT/NR composites slightly increased. Similar observation was found in NR composites filled with alkali treated pine apple fiber (PALF) by Lopattananon, Panawarangkul, Sahakaro and Ellis, (2006). They reported that the elimination of hemicellulose in PALF by alkali treatment resulted in the improvement of interfacial adhesion between the fiber and NR. Elongation at break of ALT/NR composites was higher than those of ACT/NR composites. This was because the increase in surface area and roughness of ALT led to the enhancement of interfacial adhesion between RHF and NR matrix via mechanical interlocking. The elongation at break of NR composites exhibited the maximum value at treatment time of 2 h for ALT/NR composites and at treatment time of 1 h for ACT/NR composites. As treatment time increased, the elongation at break of both ACT/NR and ALT/NR composites slightly decreased. The reduction of elongation at break of ACT/NR and ALT/NR composites was attributed to the stiffness of ACT and fiber cracking of ALT.

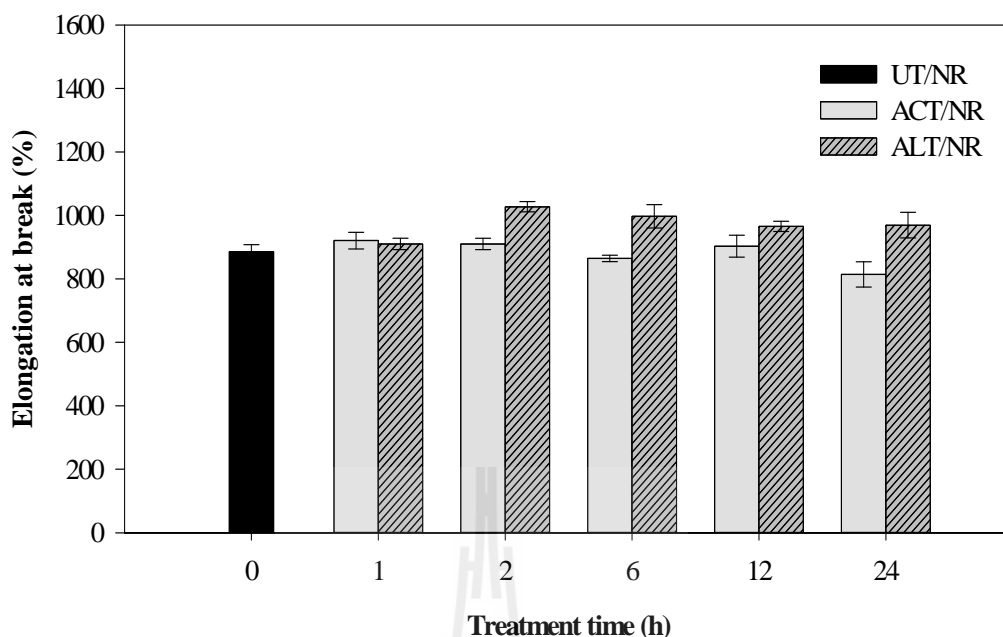


Figure 4.27 Elongation at break of UT/NR, ACT/NR and ALT/NR composites at various treatment times.

Tensile strength of UT/NR, ACT/NR and ALT/NR composites at various treatment times is presented in Figure 4.28. It can be seen that tensile strength of ACT/NR composites insignificantly changed while that of ALT/NR composites slightly increased as compared to UT/NR composites. In addition, tensile strength of ALT/NR composites was higher than those of ACT/NR composites. This was probably because the alkali treatment effectively removed hemicellulose, lignin and wax on RHF surfaces when compared to the acid treatment leading to the increased surface roughness and the mechanical interlocking between treated RHF and NR. The tensile property results corresponded to the TGA and FTIR results of ACT and ALT shown in Figure 4.12 – 4.13 and Figure 4.14 – 4.15. Additionally, the improvement of mechanical properties of ALT/NR composites was due to the increase in L/D ratio of ALT shown in Table 4.5. The similar results were reported by

Ismail, *et al.*, (2010) and Mathew and Joseph, (2007) in kenaf/NR and short isora fiber/NR systems. Tensile strength of ALT/NR composites showed the maximum value at treatment time of 2 h whereas tensile strength ACT/NR composites had the maximum value at treatment time of 1 h. Tensile strength of both ACT/NR and ALT/NR composites tended to decrease with increasing treatment time. The change in tensile strength of ACT/NR and ALR/NR composites was due to the change of L/D ratio of ACT and ALT after fiber surface treatment.

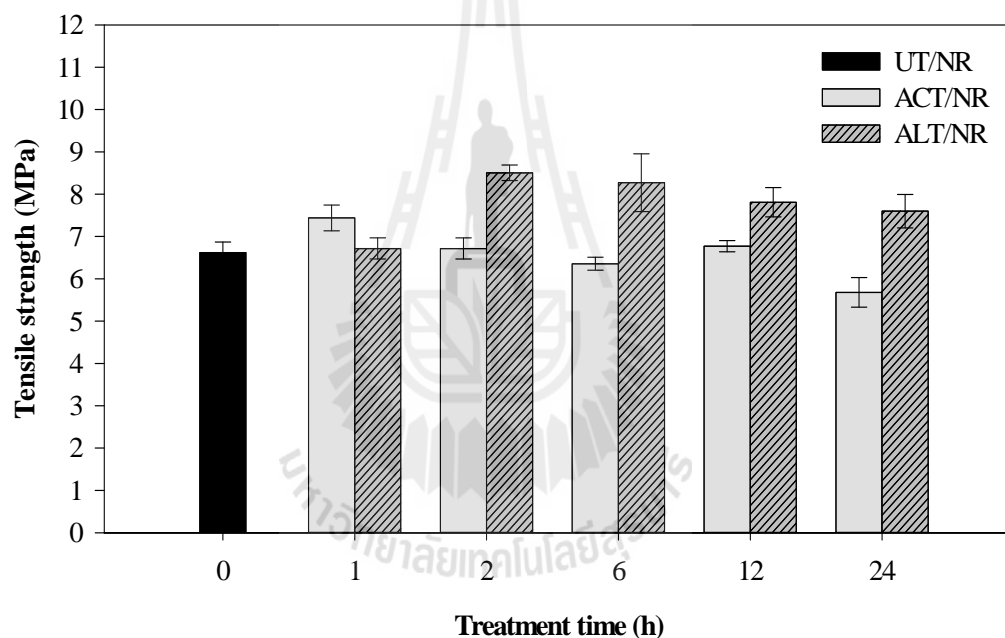


Figure 4.28 Tensile strength of UT/NR, ACT/NR and ALT/NR composites at various treatment times.

4.2.2.2.2 Tear properties

Tear strength of UT/NR, ACT/NR and ALT/NR composites at various treatment times is shown in Figure 4.29. There was no significant difference among tear strength of UT/NR, ACT/NR and ALT/NR composites. In addition, tear strength of ACT/NR and ALT/NR composites insignificantly changed with increasing treatment time. This result indicated that surface treatment methods and treatment times had no effect on tear properties of NR composites.

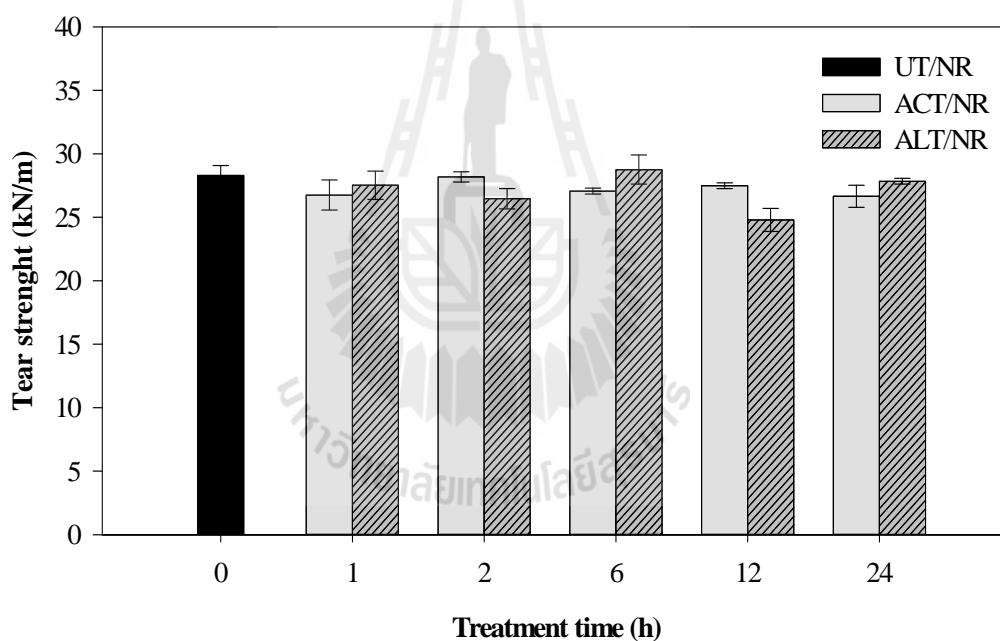


Figure 4.29 Tear strength of UT/NR, ACT/NR and ALT/NR composites at various treatment times.

4.2.2.2.3 Crosslink density

Crosslink density of UT/NR, ACT/NR and ALT/NR at various treatment times are shown in Figure 4.30. It can be observed that crosslink density of ACT/NR and ALT/NR composites was similar to that of UT/NR composite. With increasing treatment time, crosslink density of ACT/NR and ALT/NR composites had no significant difference. This implied that acid and alkali treatment showed no effect on crosslink density of NR composites. Therefore, the change in mechanical properties of NR composites was because of the enhancement of interfacial adhesion between treated RHF and NR matrix.

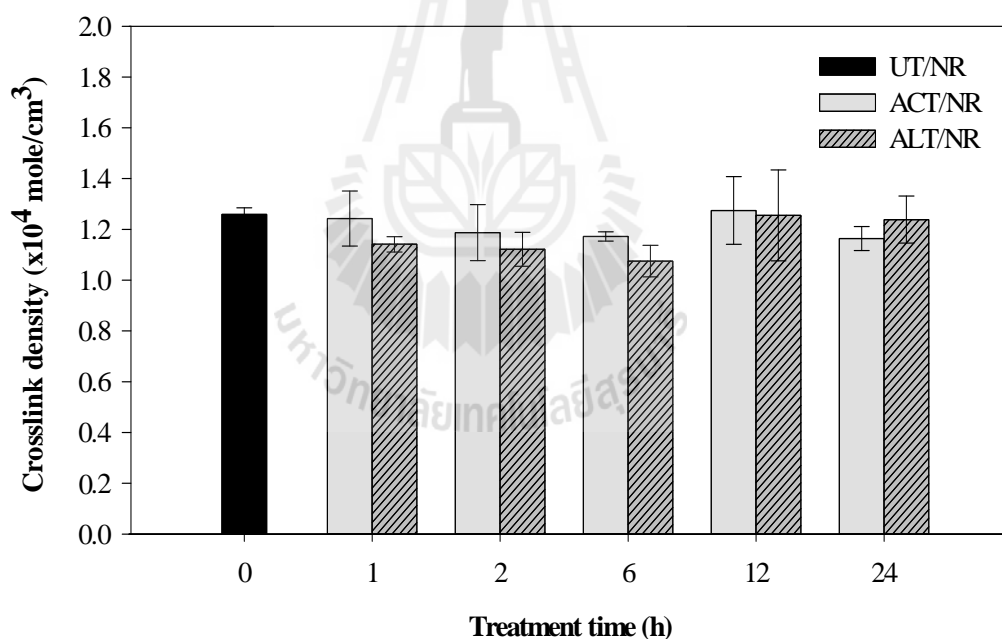


Figure 4.30 Crosslink density of UT/NR, ACT/NR and ALT/NR composites at various treatment times.

Table 4.7 Mechanical properties and crosslink density of UT/NR, ACT/NR and ALT/NR composites at various treatment times.

Designation	M100 (MPa)	M300 (MPa)	Elongation at break (%)	Tensile strength (MPa)	Tear strength (kN/m)	Crosslink density ($\times 10^4$ mol/cm³)
UT/NR	1.34 \pm 0.06	2.02 \pm 0.06	885.55 \pm 22.07	6.62 \pm 0.26	28.29 \pm 0.78	1.26 \pm 0.03
1ACT/NR	1.46 \pm 0.04	2.17 \pm 0.03	920.57 \pm 26.06	7.44 \pm 0.30	26.75 \pm 1.18	1.24 \pm 0.11
2ACT/NR	1.33 \pm 0.07	1.95 \pm 0.09	909.94 \pm 17.74	6.72 \pm 0.25	28.19 \pm 0.41	1.19 \pm 0.11
6ACT/NR	1.52 \pm 0.06	2.15 \pm 0.08	864.59 \pm 10.45	6.36 \pm 0.15	27.06 \pm 0.24	1.17 \pm 0.02
12ACT/NR	1.44 \pm 0.08	2.14 \pm 0.11	902.73 \pm 34.72	6.77 \pm 0.13	27.49 \pm 0.36	1.27 \pm 0.13
24ACT/NR	1.37 \pm 0.08	2.07 \pm 0.08	813.83 \pm 39.97	5.68 \pm 0.35	26.65 \pm 0.87	1.16 \pm 0.05
1ALT/NR	1.33 \pm 0.07	1.95 \pm 0.09	909.94 \pm 17.73	6.72 \pm 0.25	27.51 \pm 1.11	1.14 \pm 0.03
2ALT/NR	1.43 \pm 0.06	2.07 \pm 0.07	1027.24 \pm 16.11	8.50 \pm 0.18	26.461 \pm 0.79	1.12 \pm 0.07
6ALT/NR	1.41 \pm 0.08	2.07 \pm 0.10	997.28 \pm 36.93	8.27 \pm 0.68	28.76 \pm 1.14	1.08 \pm 0.06
12ALT/NR	1.53 \pm 0.09	2.16 \pm 0.09	965.38 \pm 16.18	7.81 \pm 0.345	24.78 \pm 0.91	1.26 \pm 0.18
24ALT/NR	1.48 \pm 0.08	2.11 \pm 0.09	969.16 \pm 40.347	7.59 \pm 0.39	27.83 \pm 0.22	1.24 \pm 0.09

4.2.2.3 Morphological properties

SEM micrographs of UT/NR, ACT/NR and ALT/NR composites at various treatment times are shown in Figure 4.31 - 4.32. The micrographs of UT/NR composites in Figure 4.31 (a) showed numerous holes of RHF which pulled out from NR matrix. In addition, the gap between RHF and NR matrix was observed. This indicated the poor adhesion between RHF and NR matrix due to the different polarity of RHF and NR. After acid treatment, numerous holes and gaps were still observed on ACT/NR composites surface (Figure 4.31). This implied that the adhesion between fiber and NR was not effectively improved by acid treatment. This result corresponded to SEM results in fiber characterization section (Figure 4.16). The morphologies of ACT fiber and the morphologies of ACT/NR composites confirmed that acid treatment only cleaned RHF surface by removal of wax and dust on RHF surface resulting in the insignificant change in mechanical properties of ACT/NR composites. With increasing treatment time (Figure 4.30 (b-f)), the fracture surfaces of ACT/NR composites were not different.

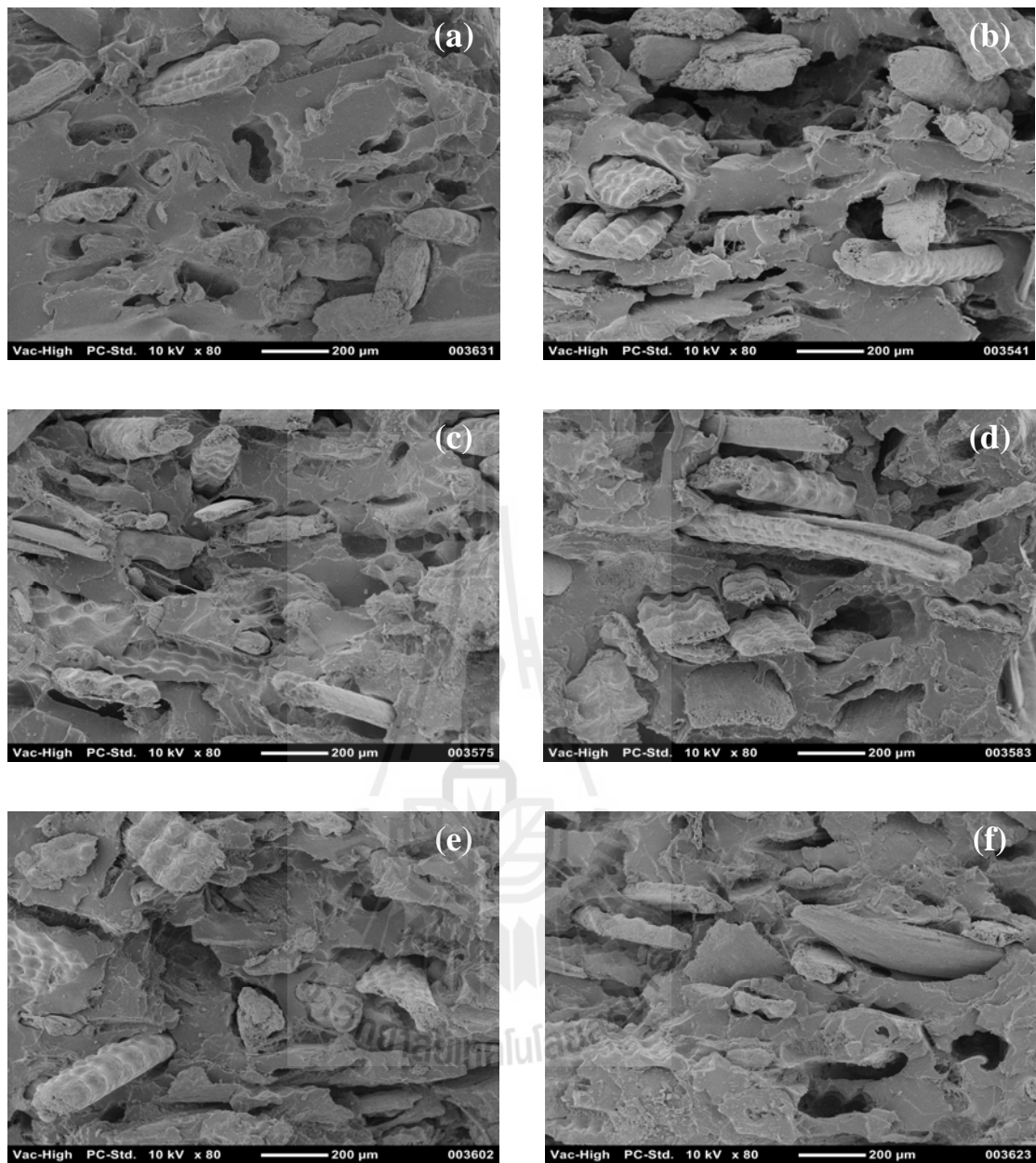


Figure 4.31 SEM micrographs of (a) UT/NR, (b) 1ACT/NR, (c) 2ACT/NR, (d) 6ACT/NR, (e) 12ACT/NR and (f) 24ACT/NR composites.

In Figure 4.32 (b-f), after alkali treatment, the numbers holes and gap size on the ALT/NR composites were less than those observed on the surface of the ACT/NR composites. This indicated the improvement of adhesion between treated RHF and NR matrix leading to the enhanced tensile properties of ALT/NR composites. However, with increasing fiber treatment time, the ALT/NR composites revealed the fiber splitting and fiber cracking in NR matrix. This resulted in the reduction in tensile properties of ALT/NR composites at higher fiber treatment time.

From this section, fiber surface treatment method and fiber treatment time affected properties of RHF and RHF/NR composites. Alkali treatment was more effective method than acid treatment in the removal of hemicellulose, lignin and wax on RHF as indicated by the increase in surface roughness and L/D ratio of ALT. However, alkali treatment removed partial silica on RHF surface. Based on mechanical properties, NR composites containing ALT at treatment time of 2 h showed the optimum mechanical properties due to the improvement of interfacial adhesion between RHF and NR and the increment of L/D ratio of ALT. This confirmed that surface roughness and L/D ratio of fiber after surface treatment were more dominant effect than silica content in RHF on mechanical properties of NR composites. Therefore, alkali treatment at treatment time of 2 h was selected to pretreat RHF before treating fiber surface with a silane coupling agent.

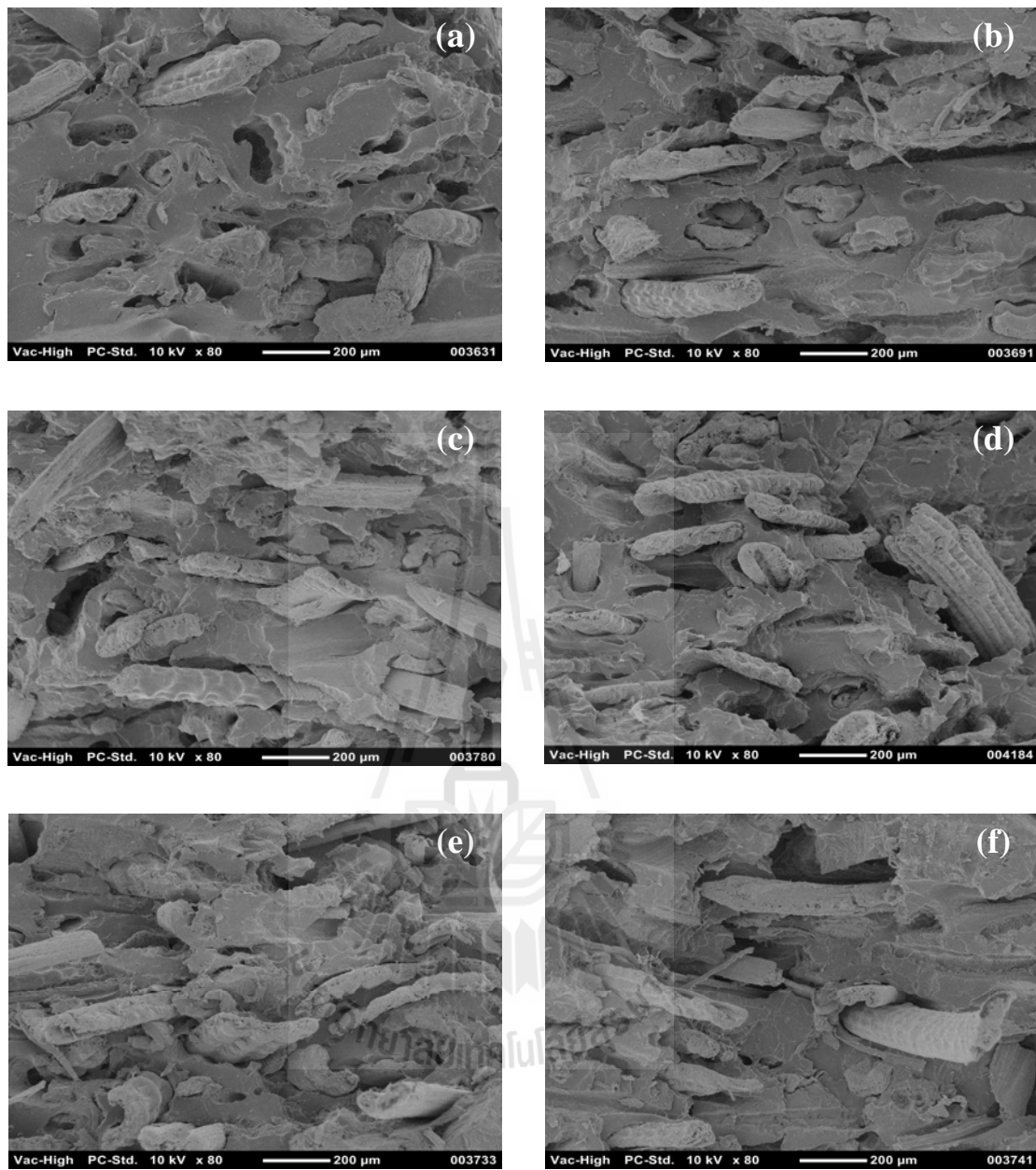


Figure 4.32 SEM micrographs of (a) UT/NR, (b) 1ALT/NR, (c) 2ALT/NR, (d) 6ALT/NR, (e) 12ALT/NR and (f) 24ALT/NR composites.

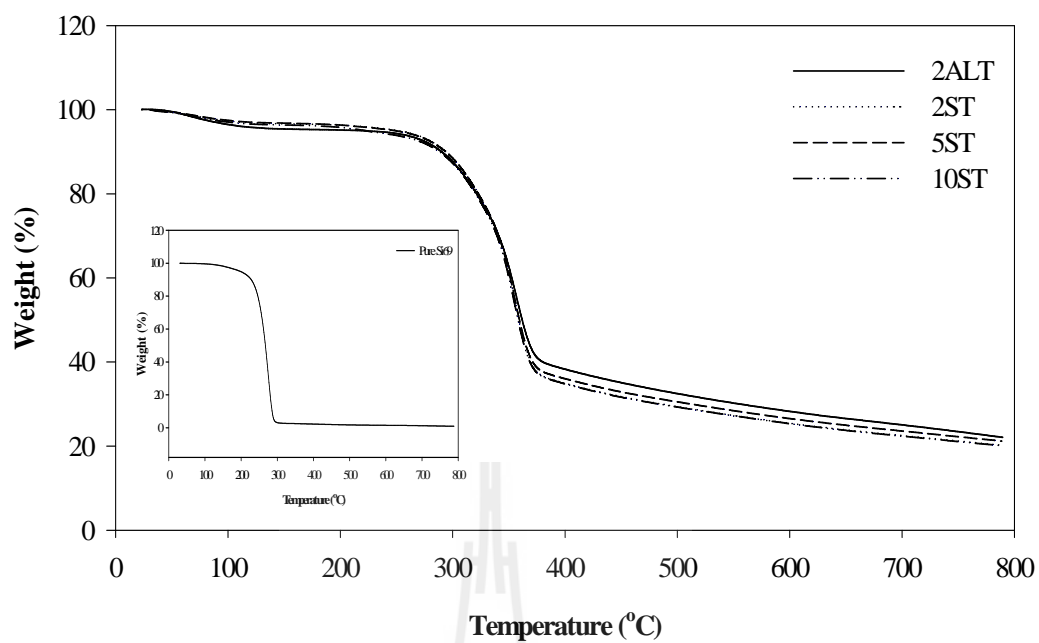
4.3 Effect of bis (triethoxysilylpropyl) tetrasulfide (Si69) content on physical properties of RHF and RHF/NR composites

In this section, alkali treatment at treatment time of 2 h was used to pretreat RHF surface before coating the RHF with a silane coupling agent, bis (trimethoxysilylpropyl) tetrasulfide (Si69).

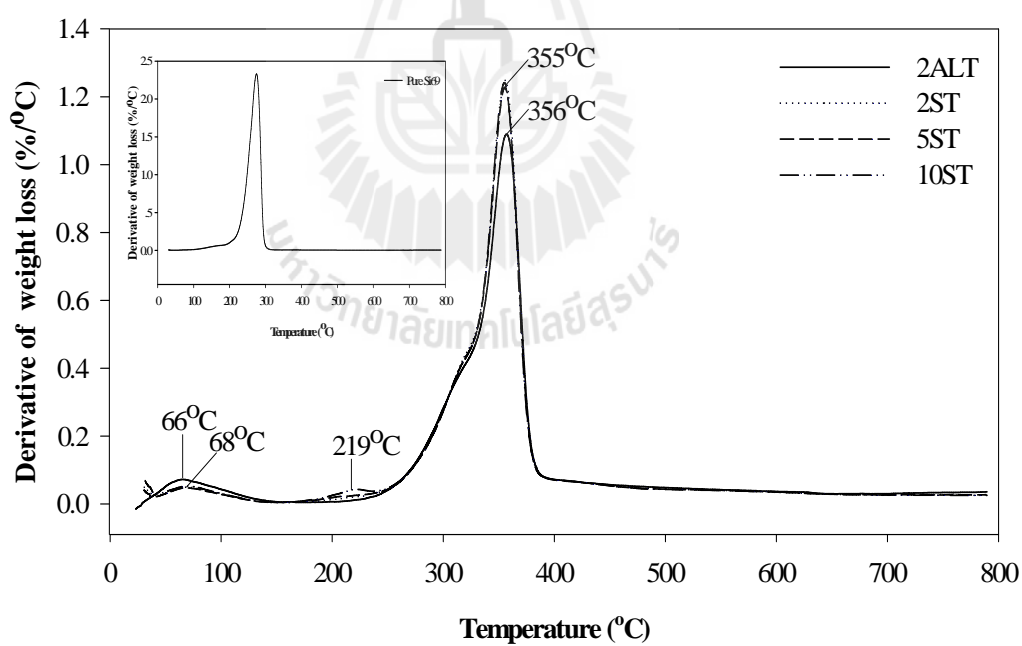
4.3.1 Fiber characterization

4.3.1.1 Thermal properties

TGA and DTGA thermograms of 2ALT and silane treated RHF (ST) at various Si69 contents are shown in Figure 4.33 and summarized in Table 4.8. Both ALT and ST showed the initial weight loss between 36 and 100°C relating to water evaporation. ST samples revealed less weight loss in this region than ALT sample implying the lower moisture adsorption on ST surface. This may be because the micropores appeared on ALT surface enhanced the silane penetration leading to the reduction of moisture adsorption of the RHF (Singha and Thakur, 2009). After this stage, the TGA thermograms of ST samples presented the small shoulder at 219°C which was not shown in that of ALT. This was attributed to the Si69 decomposition as confirmed by the TGA thermogram of pure Si69 shown in the left bottom of Figure 4.32. The Si69 thermogram showed one decomposition stage at 200-300°C which revealed the maximum decomposition peak at 270°C. Both ALT and ST showed the second decomposition stage at 355-356°C due to cellulose decomposition. The residue at 800°C of ALT and ST was 20-22 wt% which corresponded to the silica content in RHF. Si69 content applied on RHF surface was a small amount so the Si69 content had no effect on the remaining residue at 800°C of ST. As Si69 content increased, thermal decomposition behavior of ST was not changed.



(a)



(b)

Figure 4.33 TGA (a) and DTGA (b) thermograms of ALT and ST at various Si69 contents.

Table 4.8 Thermal decomposition temperatures of ALT and ST at various Si69 contents.

Treatment condition	Water evaporation			Thermal decomposition temperature (°C)			Residue (wt%)
	Onset (°C)	Peak (°C)	Weight loss (%)	1 st step	2 nd step	3 rd step	
2ALT	36	66	4	-	356	-	22
Pure Si69	30	-	-	274	-	-	0.9
2ST	31	69	1.4	219	356	-	20
5ST	31	68	1.2	219	355	-	21
10ST	31	68	1.5	219	355	-	20

4.3.1.2 Functional group analysis

FTIR spectra of 2ALT and ST at various Si69 contents are presented in Figure 4.34 and the assignment of absorption bands is summarized in Table 4.9. For ALT, the broad band at 3334 cm^{-1} related to -O-H stretching of hemicellulose, cellulose and water in RHF. The absorption band at 2898 cm^{-1} was due to -CH₂ stretching of hemicellulose and cellulose in RHF. The band at 1631 cm^{-1} assigned to -O-H stretching of the adsorbed water of ALT. The shoulder at 1602 and 1508 cm^{-1} related to C=C stretching of aromatic ring in lignin components. The bands at 1448, 1423, 1367 and 1317 cm^{-1} associated to -CH₂ bending and -CH stretching of hemicellulose, cellulose and lignin components. In addition, the bands at 1038 and 792 cm^{-1} were due to C-O stretching of cellulose and Si-O-Si stretching of the remaining silica in RHF after alkalization. When 2ALT was treated with Si69, the spectra of ST samples were similar to that of 2ALT. When compared with 2ALT, ST exhibited an additional small shoulder at 2972-2969 cm^{-1} indicating -CH₂ and -CH₃ groups of Si69 (Lopattananon, Jitkalong and Seadan, 2011). From this band, it confirmed the presence of Si69 on ALT surface. However, with increasing Si69 content, the absorption bands of ST did not change.

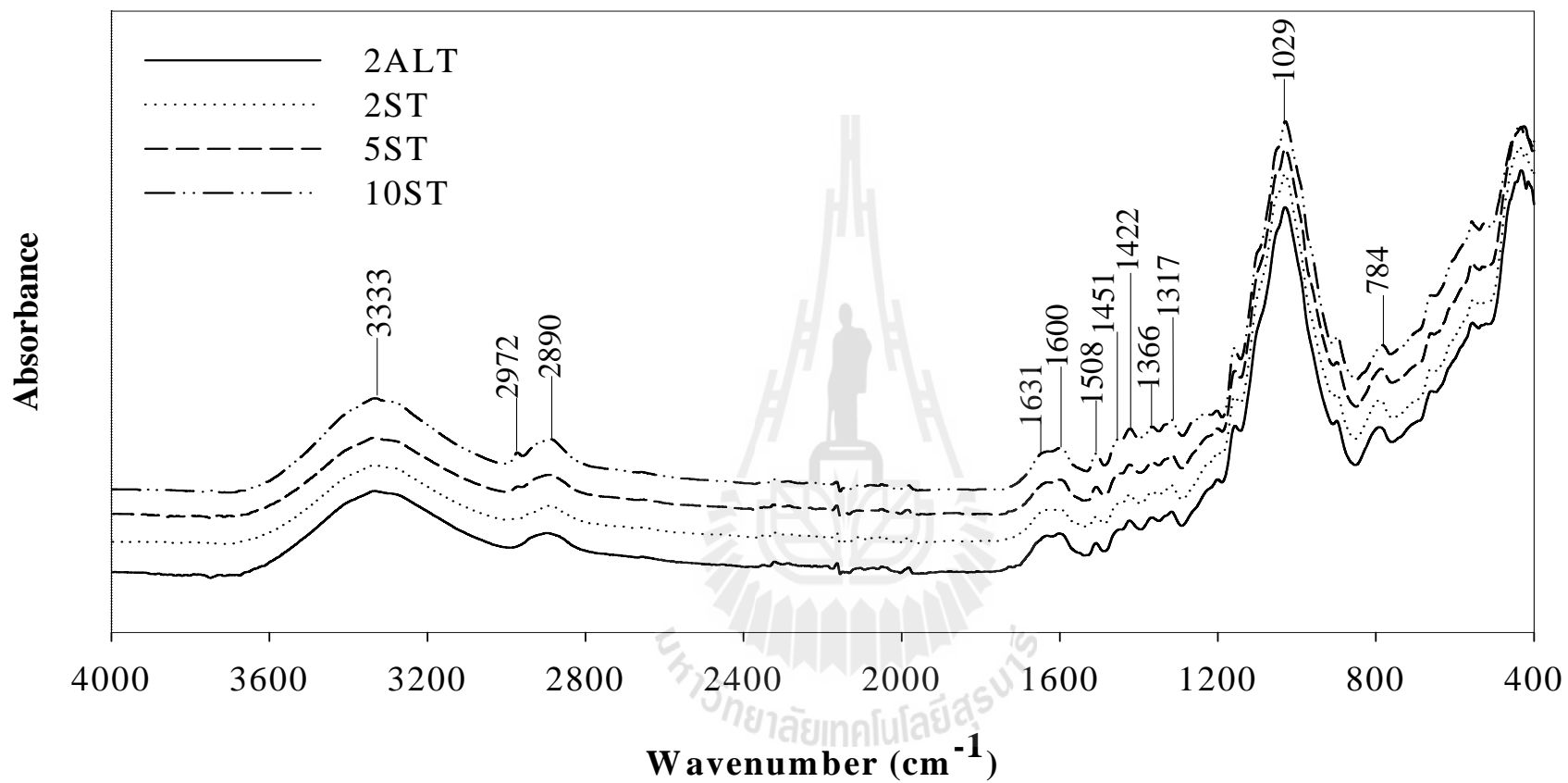


Figure 4.34 FTIR spectra of 2ALT and ST at various Si69 contents.

Table 4.9 FTIR peak positions of 2ALT and ST at various Si69 contents(Lopattananon *et al.*, 2011; Luduena, Fasce, Alverz and Stefani, 2011).

Wavenumber (cm ⁻¹)		Vibration	Source
ALT	ST		
3334	3334-3333	OH stretching	hemicellulose, cellulose, lignin, water
-	2972-2969	CH ₂ , CH ₃ stretching	Si69
2898	2891-2890	C-H stretching	hemicellulose, cellulose, lignin
1632	1631	OH stretching	adsorbed water
1602	1694-1600	C=C stretching	lignin
1508	1508-1506	C=C stretching	aromatic ring
1448-1423	1450-1422	CH ₂ strain	hemicellulose, cellulose, lignin
1367-1316	1367-1316	CH bending	hemicellulose, cellulose, lignin
1038	1030-1029	C-O stretching	cellulose
792	788-781	Si-O-Si stretching	silica

4.3.1.3 Morphological properties

SEM micrographs of outer surfaces and inner surfaces of 2ALT and ST at various Si69 contents are presented in Figure 4.35 (a-d) and Figure 4.36 (a-d), respectively. From Figure 4.35 (a), it was observed that the outer surface of 2ALT showed roughness and micropores due to the removal of hemicellulose, lignin and partial amount of silica from RHF surface (Ndazi, Nyahumwa and Tesha, 2007). After silane treatment (Figure 4.35 (b-d)), ST revealed similar outer surface to 2ALT. The insignificant difference between the surface of ST and 2ALT was because the applied Si69 penetrated into micropores on the RHF surface. Similar result was found in the inner surfaces of 2ALT and ST. It was seen in Figure 4.36 (a) that 2ALT showed the smooth inner surface. After coating with Si69 (Figure 4.36 (b-d)), the inner surface of ST was smooth and similar to 2ALT. Moreover, Si69 content exhibited no effect on the inner surface of ST.

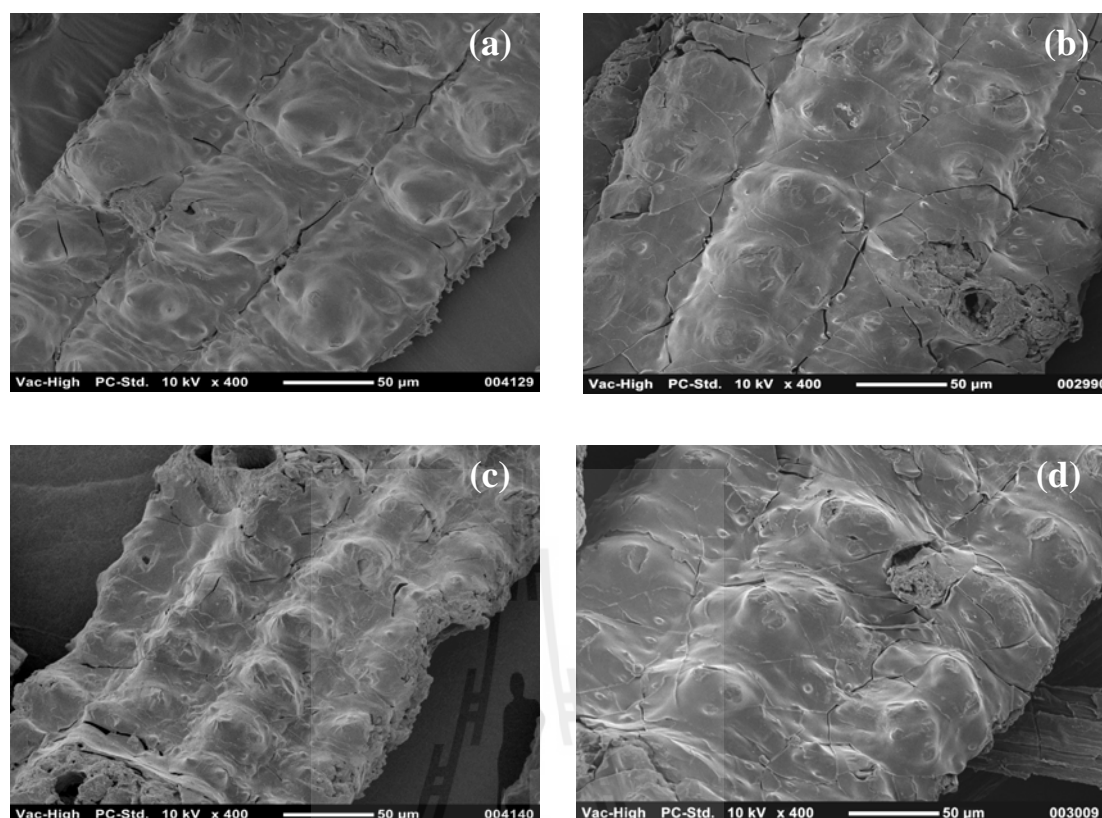


Figure 4.35 SEM micrographs of outer surfaces of (a) 2ALT, (b) 2ST, (c) 5ST and (d) 10ST.

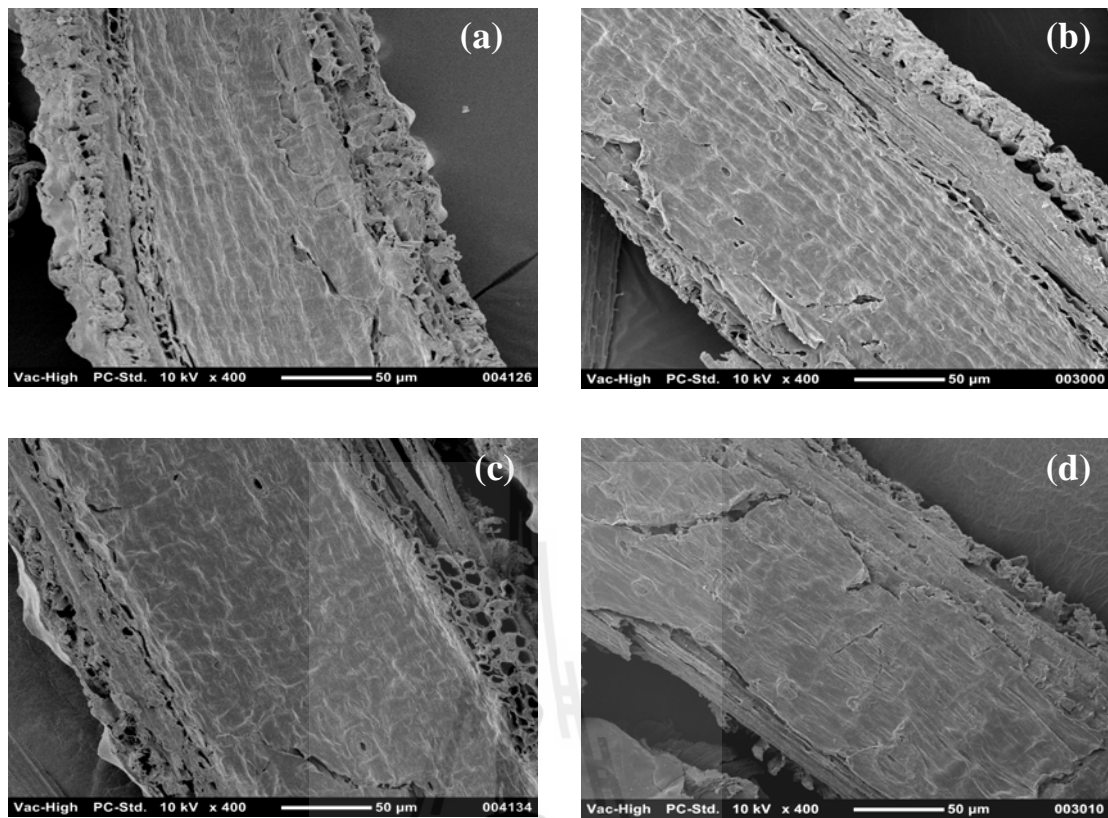


Figure 4.36 SEM micrographs of inner surfaces of (a) 2ALT, (b) 2ST, (c) 5ST and (d) 10ST.

4.3.2 Composite characterization

4.3.2.1 Cure characteristics

Cure characteristics, *i.e.*, scorch time (T_s), cure time (T_{90}), maximum torque (S_{max}), minimum torque (S_{min}) and torque difference ($S_{max} - S_{min}$), of alkali treated RHF (ALT)/NR and silane treated RHF (ST)/NR composites at various Si69 contents are shown in Figure 4.37- 4.41 and summarized in Table 4.10.

From Figure 4.37, it can be seen that scorch time of ST/NR composites was longer than that of ALT/NR composites. This may be due the enhancement of rubber-filler interaction. Si69 coated on RHF surface reduced hydrophobicity of RHF resulting in the reduction of filler agglomeration and the improvement of compatibility between RHF and NR matrix. In addition, the increased scorch time of ST/NR composites was probably because tri-ethoxysilylpropyl groups of Si69 delayed crosslinking reaction of NR (Poh and Ng, 1998). With increasing Si69 content, scorch times of ST/NR composites were stable while cure time was significantly changed as shown in Figure 4.38. Cure time of ST/NR composites showed the longest value at Si69 content of 5 wt% and tended to decrease with increasing Si69 content. This was attributed to the adsorption of rubber activator and accelerator by hydroxyl groups of polysiloxane on RHF surface (Thongpin, Sangnil, Suerkong, Pongpilaiprertti and Sombatsompop, 2009). The increment of scorch time and cure time by adding Si69 was also reported by De, *et al.*, (2004), Lopattananon, *et al.*, (2011), Poh and Ng, (1998) and Thongsang and Sombatsompop, (2006) in systems of grass fiber/NR, cellulosefiber/silica/NR and fly ash silica/NR composites.

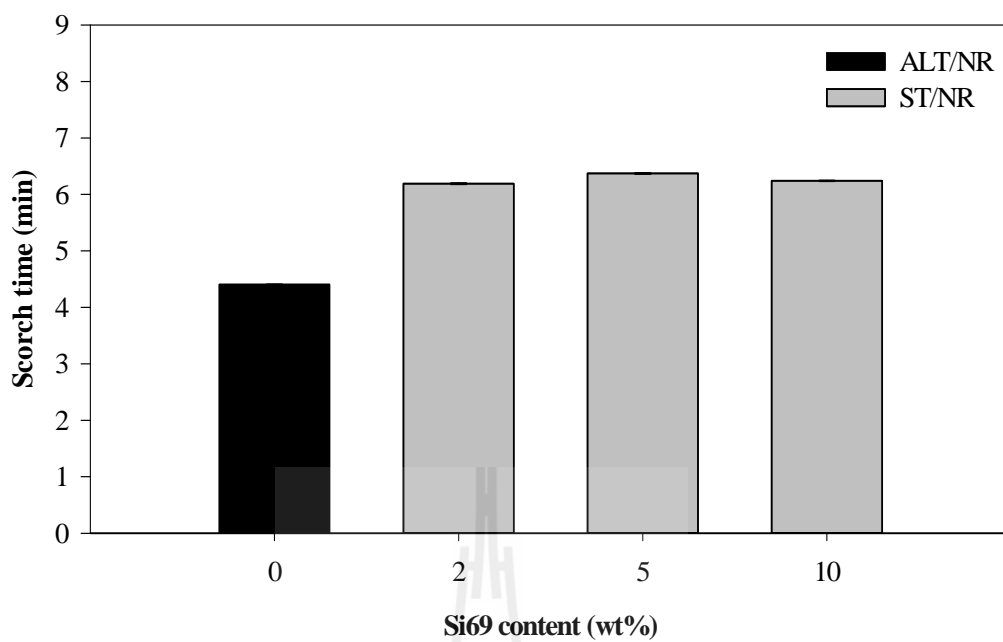


Figure 4.37 Scorch time of ALT/NR and ST/NR composites at various Si69 contents.

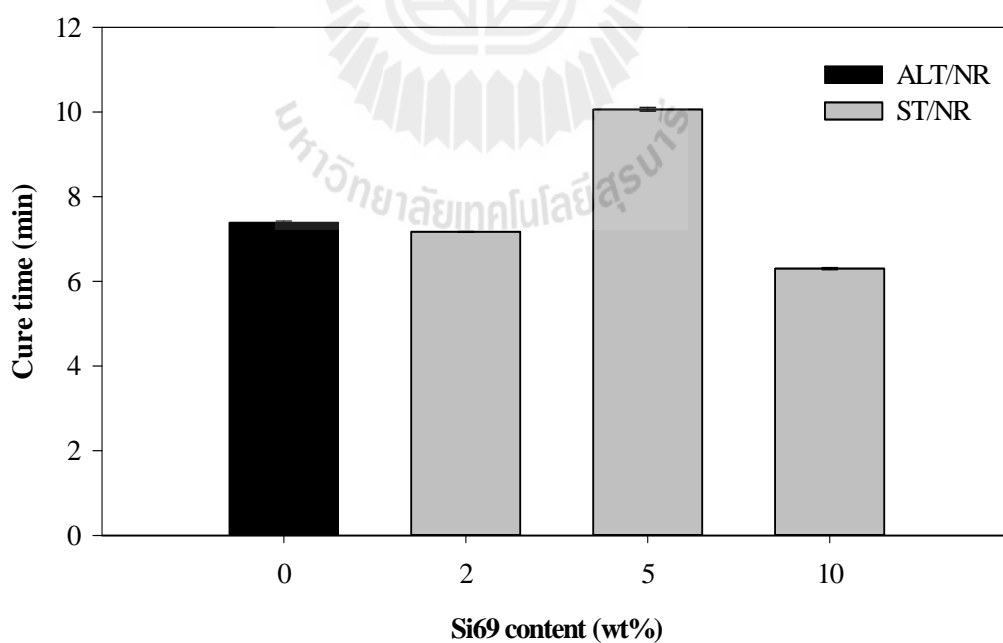


Figure 4.38 Cure time of ALT/NR and ST/NR composites at various Si69 contents.

Minimum torque and maximum torque of ALT/NR and ST/NR composites at various Si69 contents are presented in Figure 4.39 - 4.40, respectively. As seen, minimum torques of ST/NR composites were lower than that of ALT/NR composites. The minimum torque of ST/NR composites slightly decreased with increasing Si69 content. The decrement of minimum torque of ST/NR composites was because the low polarity of Si69 enhanced filler dispersion in NR matrix. Similar trend was found in maximum torque of NR composites (Figure 4.40). The maximum torque of ST/NR composites gradually decreased as compared to that of ALT/NR composites. With increasing Si69 content, maximum torque of ST/NR composites significantly decreased. This was because the excessive silane at high Si69 content performed as a plasticizer in NR matrix leading to the decrement of viscosity of NR composites (Sae-oui, Sirisinha, Hatthapanit and Thepsuwan, 2005). The similar result was found by Thongpin, *et al.*, (2009) in precipitated silica/NR composites. However, they suggested that the reduction of maximum torque of NR composites associated with the agglomeration of polysiloxane on silica surface. The agglomerated polysiloxane adsorbed rubber additives leading to the retardation for crosslink reaction of rubber. This resulted in the increment of scorch time and cure time and the decrement of maximum torque of rubber composites.

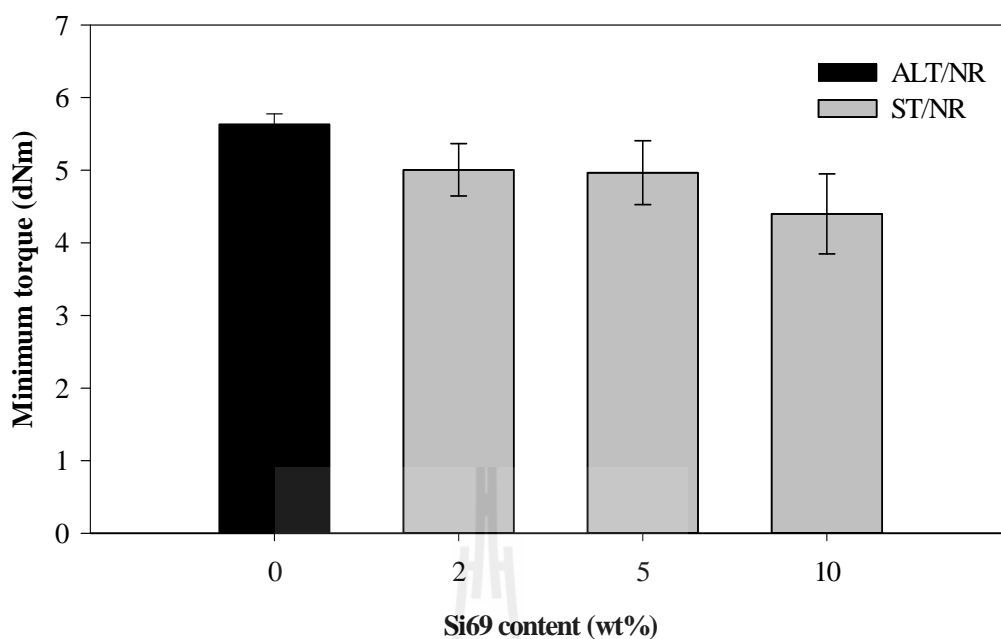


Figure 4.39 Minimum torque of ALT/NR and ST/NR composites at various Si69 contents.

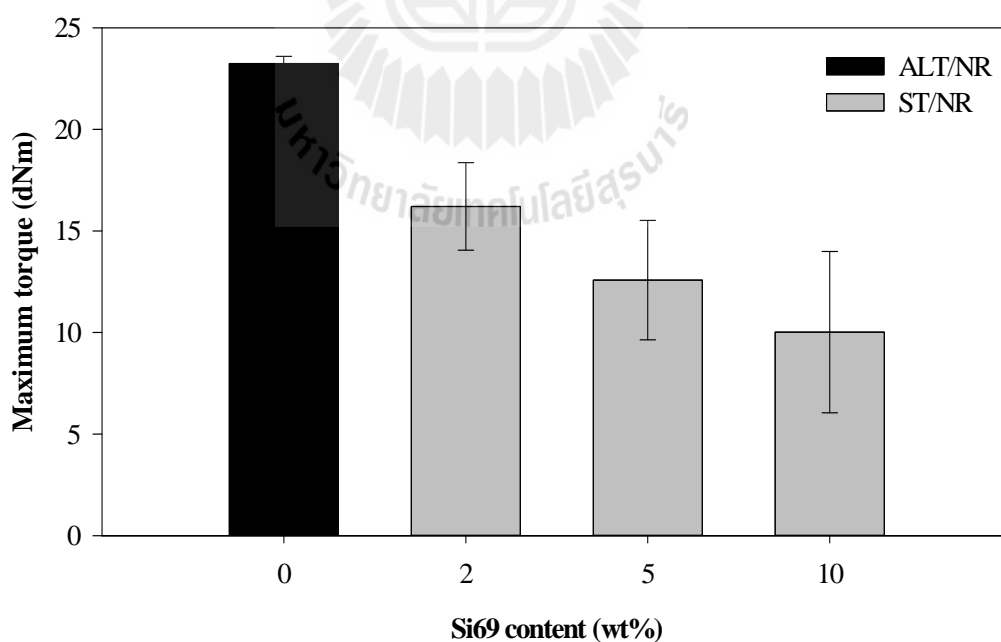


Figure 4.40 Maximum torque of ALT/NR and ST/NR composites at various Si69 contents.

Torque difference of ALT/NR and ST/NR composites at various Si69 contents is shown in Figure 4.41. Torque difference of ST/NR composites decreased as compared with that of ALT/NR composites. As Si69 content increased, torque difference of ST/NR composites gradually decreased. Thongpin, *et al.*, (2009) studied the effect of Si69 on cure characteristics of precipitated silica/NR composites and reported that the torques of NR composites decreased with increasing Si69 content. They suggested that the reduction of torques of NR composites was because the polylayers of Si69 on filler surface adsorbed rubber additives leading to the reduction of crosslink density of NR composites. However, there was no difference in crosslink density of ALT/NR and ST/NR composites in this study. Therefore, the reduction of torque difference of ST/NR composites may be because of plasticizing effect of the excessive silane leading to the decrement of viscosity of NR composites (Sae-oui, *et al.*, 2005).

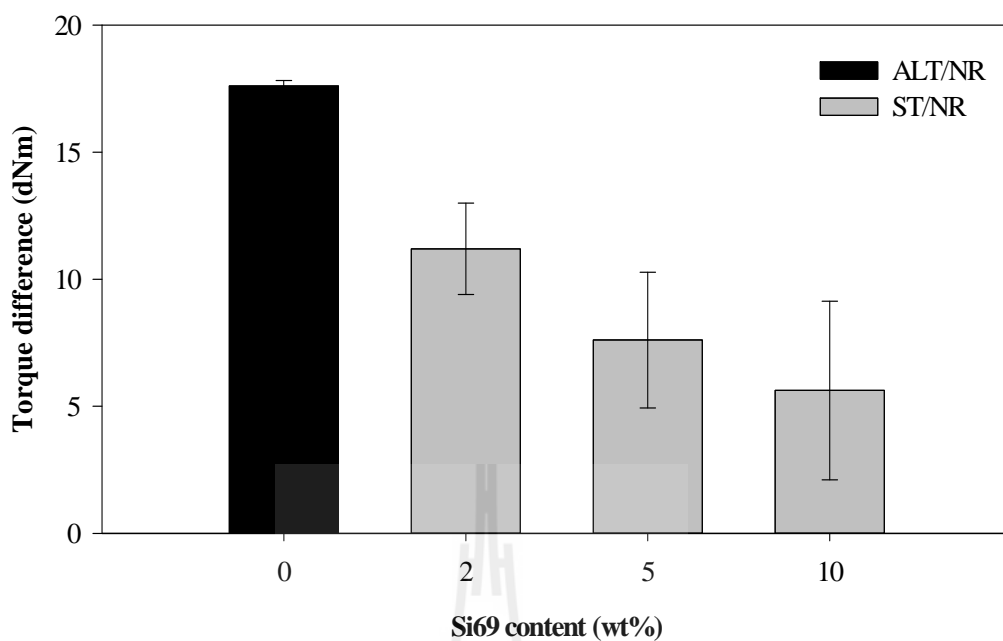


Figure 4.41 Torque difference of ALT/NR and ST/NR composites at various Si69 contents.

Table 4.10 Cure characteristics of ALT/NR and ST/NR composites at various Si69 contents.

Designation	Scorch time (min)	Cure time (min)	S_{\max} (dNm)	S_{\min} (dNm)	$S_{\max}-S_{\min}$ (dNm)
2AL/NR	4.41	7.39	23.24	5.63	17.61
2ST/NR	6.19	7.17	16.20	5.00	11.20
5ST/NR	6.37	10.06	12.58	4.97	7.60
10ST/NR	6.24	6.30	10.02	4.40	5.62

4.3.2.2 Mechanical properties and crosslink density

Modulus at 100% strain (M100), modulus at 300% strain (M300), elongation at break, tensile strength, tear strength and crosslink density of alkali treated RHF (ALT)/NR and silane treated RHF (ST)/NR composites at various Si69 contents are shown in Figure 4.42 – 4.47 and summarized in Table 4.11.

4.3.2.2.1 Tensile properties

Figure 4.42 and 4.43 show modulus at 100% strain (M100) and modulus at 300% strain (M300) of ALT/NR and ST/NR composites at various Si69 contents. Both M100 and M300 showed the maximum value at Si69 content of 5 wt% and began to decrease with further increasing Si69 content. The change in modulus of NR composites involved rubber-filler interaction and filler dispersion. At low Si69 content, the agglomeration of ST in NR was low while at high amount of Si69, Si69 acted as a plasticizer and caused the decrement of M100 and M300 of NR composites (Thongsang and Sombatsompop, 2006). However, several research works found that the addition of Si69 treated fiber increased modulus of rubber composites due to the improvement of interfacial adhesion between filler and rubber matrix. This result was found in system of hemp hurd powder/styrene butadiene rubber (SBR) composites (Wang, *et al.*, 2011), rice husk powder/NR composites (Nordin, Said and Ismail, 2006), rattan powder/NR composites (Ismail, *et al.*, 2012) and cotton fiber/NR composites (Zeng, *et al.*, 2009).

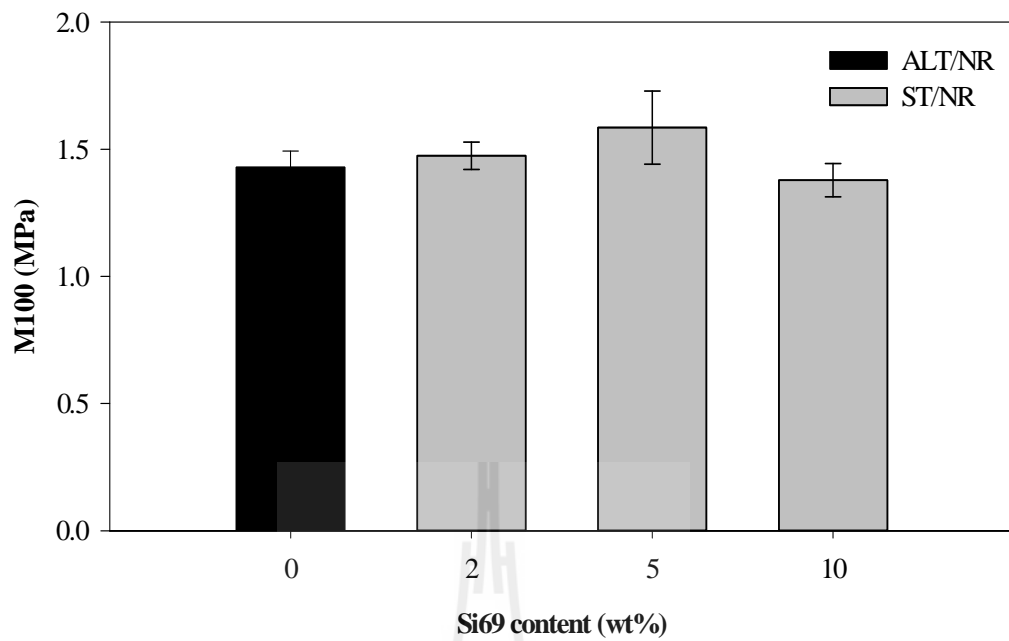


Figure 4.42 Modulus at 100% strain (M100) of ALT/NR and ST/NR composites at various Si69 contents.

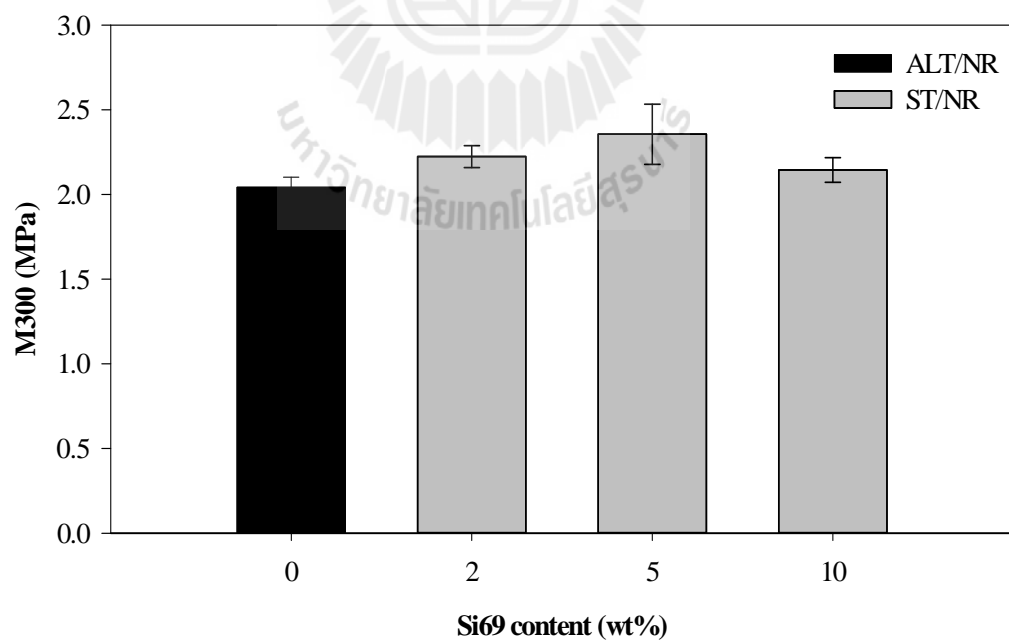


Figure 4.43 Modulus at 300% strain (M300) of ALT/NR and ST/NR composites at various Si69 contents.

Elongation at break of ALT/NR and ST/NR composites at various Si69 contents is shown in Figure 4.44. Elongation at break of ST/NR composites insignificantly increased as compared with ALT/NR composites. Elongation at break of ST/NR composites showed the maximum value at Si69 content of 2 wt% and then became stable with increasing Si69 content. The result was due to the plasticization effect of polysiloxane on RHF surface. The similar observation was found in wood sawdust/carbon black/NR and cotton fiber NR composites (Prachid Saramolee and Bunloy, 2009; Zeng, *et al.*, 2009).

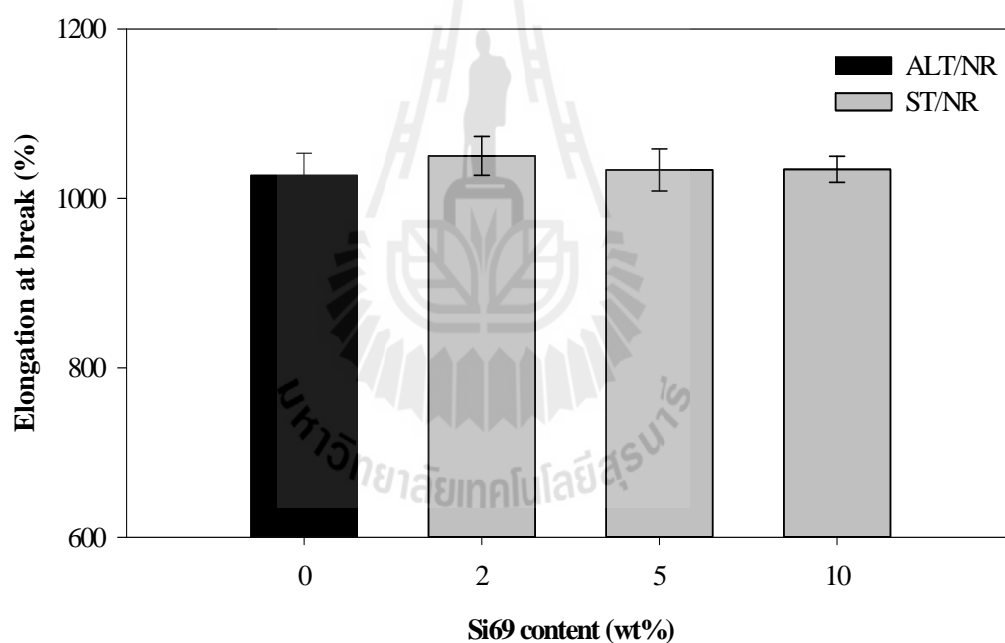


Figure 4.44 Elongation at break of ALT/NR and ST/NR composites at various Si69 contents.

From Figure 4.45, it can be seen that tensile strength of ST/NR composites was slightly higher than that of ALT/NR composite. Tensile strength of ST/NR composites showed maximum value at Si69 content of 5 wt% and tended to decrease with increasing Si69 content. At low Si69 content, the increment of tensile strength was attributed to the combination between the enhanced rubber-filler interaction and the better filler dispersion (Sae-oui, *et al.*, 2005). This result well agreed with SEM micrographs of ST/NR composites as shown in Figure 4.50 – 4.51. At high Si69 content, the reduction of tensile strength caused from polylayers of polysiloxane on RHF surface resulting from self condensation of Si69 molecules performed as a plasticizer between RHF and NR matrix (Thongpin, *et al.*, 2009; Thongsang and Sombatsompop, 2006).

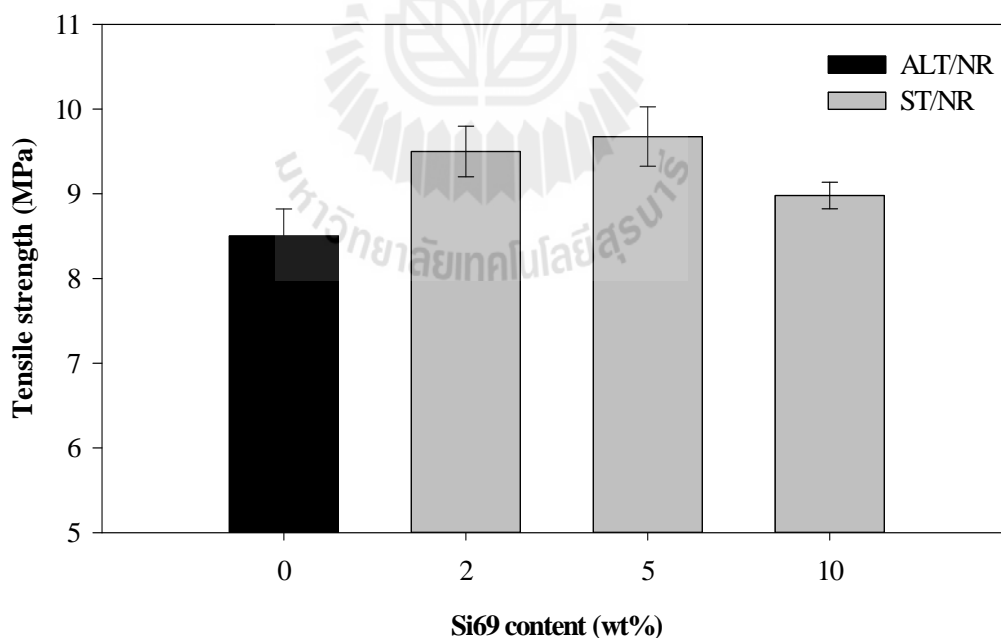


Figure 4.45 Tensile strength of ALT/NR and ST/NR composites at various Si69 contents.

4.3.2.2.2 Tear properties

Tear strength of ALT/NR and ST/NR composites at various Si 69 contents is shown in Figure 4.46. Tear strength of ST/NR composites was higher than that of ST/NR composites. The tear strength of ST/NR composites reached the highest value at Si69 content of 5 %wt and began to decrease with increasing Si69 content. An increase in tear strength of the ST/NR composites was attributed to the improvement of interfacial adhesion between RHF and rubber matrix (Mathew and Joseph, 2007). In contrast, the reduction of tear strength of ST/NR composites at high Si69 content was due to the plasticization effect of Si69.

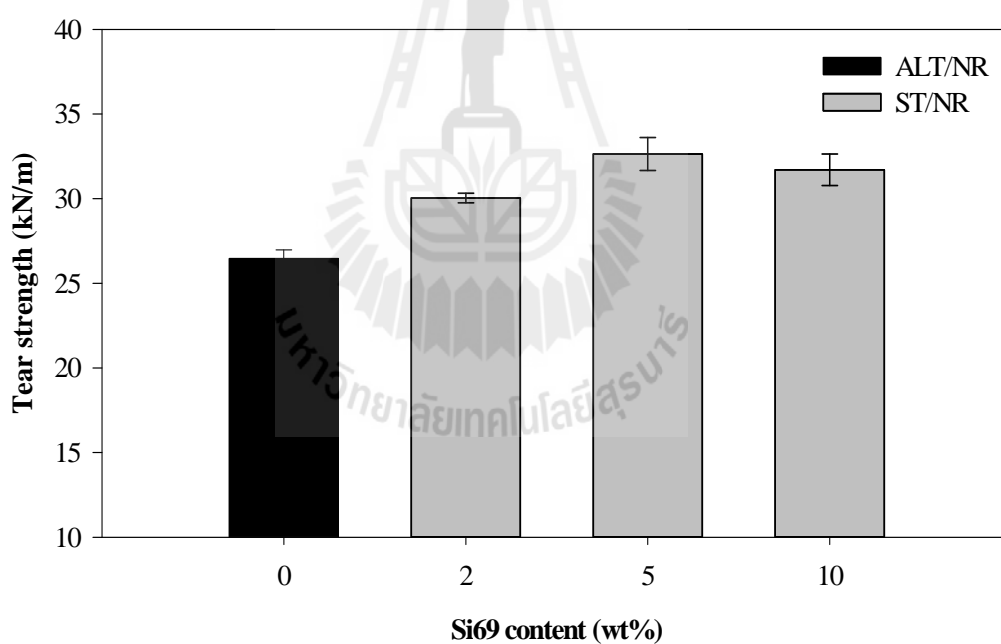


Figure 4.46 Tear strength of ALT/NR and ST/NR composites at various Si69 contents.

4.3.2.2.3 Crosslink density

Crosslink density of ALT/NR and ST/NR composites at various Si69 contents is shown in Figure 4.47. Crosslink density of ST/NR composites insignificantly changed as compared with that of ALT/NR composite. The crosslink density of ST/NR composites had the maximum value at Si69 content of 5 wt% and tended to level off with increasing Si69 content. It is well known that the crosslink formation of NR composites containing Si69 can occur via two vulcanization reactions, i.e., (1) NR molecules and sulfur crosslink agent and (2) NR molecules and sulfur from Si69 (Thongsang and Sombatsompop, 2006). However, the crosslink formation occurred in this system may follow only the first vulcanization path since the crosslink density of the NR composites did not change with increasing Si69 content. This was attributed to the sulfur distribution effect. Si69 owned four sulfur atoms in its molecule. The sulfurs could be drawn into NR matrix by active accelerator during vulcanization reaction. Consequently, Si69 was more active in system having large amounts of highly active accelerators with small amount of free sulfur, i.e., efficient vulcanization system (Sae-oui, Thepsuwan and Hatthapanit, 2004). In this study, a conventional sulfur vulcanization, which high amount of sulfur was added, was used to cure NR composites resulting in the less effective of Si69 and leading to the insignificant change of crosslink density of NR composites. From crosslink density result, it can be concluded that the improvement of mechanical properties of ST/NR composites was attributed to the increased rubber-filler interaction and filler dispersion.

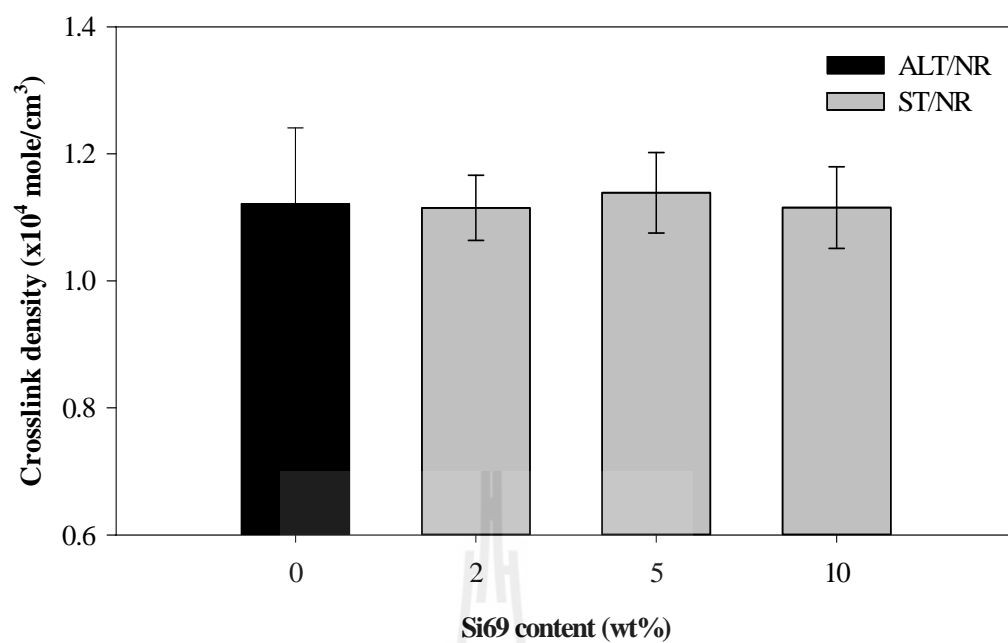


Figure 4.47 Crosslink density of ALT/NR and ST/NR composites at various Si69 contents.

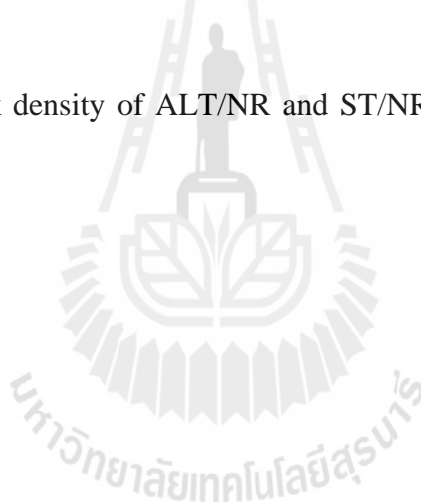


Table 4.11 Mechanical properties and crosslink density of ALT/NR and ST/NR composites at various Si69 contents.

Designation	M100 (MPa)	M300 (MPa)	Elongation at break (%)	Tensile strength (MPa)	Tear strength (kN/m)	Crosslink density ($\times 10^4$ mole/cm³)
2ALT/NR	1.43 \pm 0.06	2.07 \pm 0.06	1027.24 \pm 26.08	8.50 \pm 0.32	26.46 \pm 0.51	1.12 \pm 0.12
2ST/NR	1.47 \pm 0.04	2.22 \pm 0.06	1050.16 \pm 22.99	9.49 \pm 0.32	30.04 \pm 0.28	1.11 \pm 0.05
5ST/NR	1.61 \pm 0.13	2.35 \pm 0.18	1033.62 \pm 24.92	9.67 \pm 0.29	32.64 \pm 0.98	1.14 \pm 0.06
10ST/NR	1.38 \pm 0.06	2.14 \pm 0.07	1034.35 \pm 15.48	8.98 \pm 0.16	31.71 \pm 0.94	1.12 \pm 0.06



4.3.2.3 Morphological properties

SEM micrographs of ALT/NR and ST/NR composites at various Si69 contents are shown in Figure 4.48 (a-d). From Figure 4.48 (a), 2ALT/NR composites showed the holes after filler was pulled out and filler agglomeration in NR matrix. This indicated the weak interfacial adhesion between RHF and NR matrix and the poor dispersion of RHF in NR matrix. For ST/NR composites (Figure 4.48 (b-d)), the composites showed fewer holes after filler was pulled out from matrix and the better filler dispersion in NR matrix. In addition, ST/NR composites showed smaller gap between RHF and NR matrix than 2ALT/NR composites. This implied that Si69 increased rubber-filler interaction and decreased filler agglomeration in matrix. With increasing Si69 content, the fiber full out and small gap between RHF and NR matrix were still observed. This result implied the less rubber-filler interaction improvement resulting in the insignificant improvement of mechanical properties of ST/NR composites.

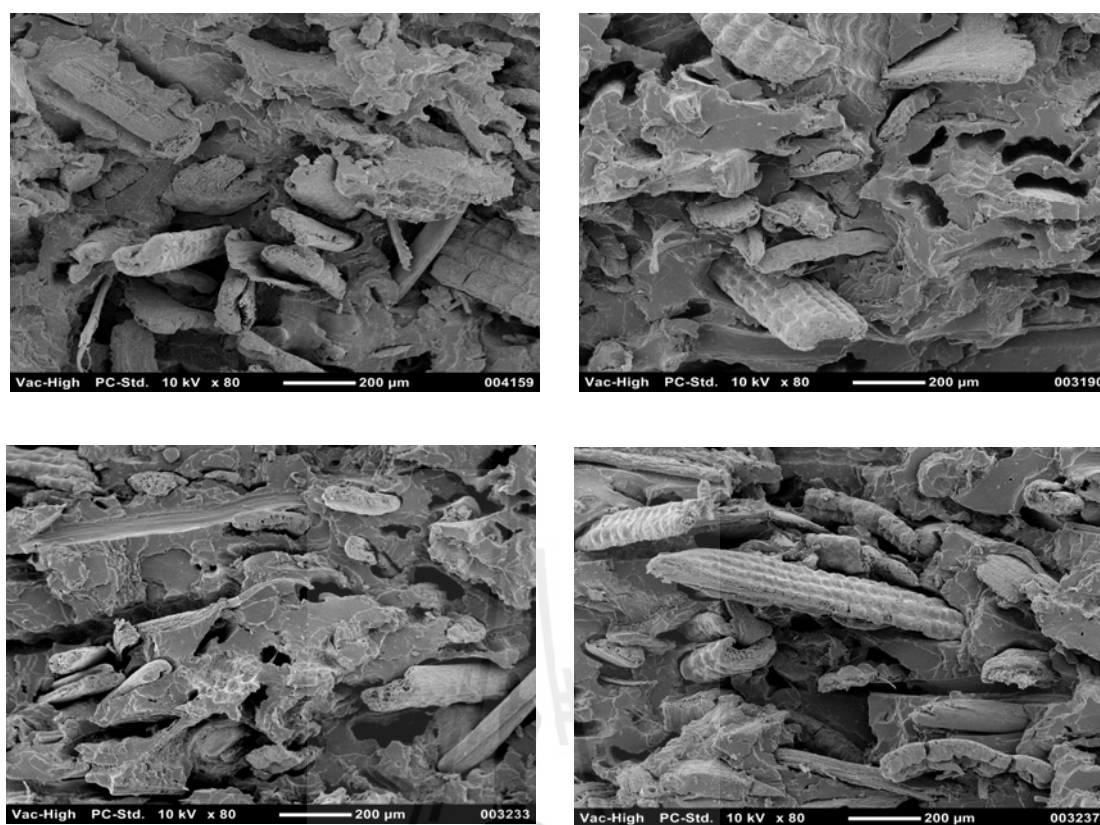


Figure 4.48 SEM micrographs of (a) 2ALT/NR, (b) 2ST/NR, (c) 5ST/NR (d) 10ST/NR composites.

4.3.2.4 L/D ratio

L/D ratio before and after mixing of UT/NR, 2ALT/NR and 5ST/NR composites are illustrated in Table 4.12. In general, fiber breakage after milling process involved types of fiber, the initial aspect ratio, the magnitude of stress and strain experience (Jacob, *et al.*, 2004). L/D ratio of UT/NR composite insignificantly decreased after mixing. This was because of the high stiffness of RHF resisted the breaking from shear force during milling. In contrast, 2ALT/NR composites showed reduction of L/D ratio after mixing due to the lower stiffness of ALT samples. The elimination of hemicellulose, lignin and wax on RHF surface during alkali treatment resulted in the decrement of stiffness of ALT leading the fiber breaking during compounding. However, for 5ST/NR composites, L/D ratio after mixing insignificantly changed. The result was because Si69 improved interfacial adhesion between RHF and NR resulting in transfer of shear force from filler to matrix leading to the less breaking of 5ST. From this result, the change in L/D ratio may be one factor affecting the change in mechanical properties of NR composites.

Table 4.12 L/D ratio before and after mixing of UT/NR, 2ALT/NR and 5ST/NR composites.

Designation	L/D	
	Before	After
UT/NR	4.48±1.43	4.00±1.36
2ALT/NR	6.58±3.36	4.44±1.92
5ST/NR	6.30±2.81	5.42±2.31

From the result, it was found that Si69 content affected the mechanical properties of ST/NR composites. NR composites containing Si69 content of 5 wt% had the highest tensile strength, M100, M300 and tear strength. This was because the enhancement of rubber-filler interaction and the good filler dispersion in NR matrix.

CHAPTER V

CONCLUSIONS

Effect of rice husk fiber (RHF) content on cure characteristics, mechanical properties and morphological properties of RHF/natural rubber (NR) composites was investigated. The addition of RHF into NR decreased scorch time and cure time of NR composites. Modulus at 100% strain (M100) and modulus at 300% strain (M300) of RHF/NR composites increased with increasing RHF content while elongation at break, tensile strength and tear strength decreased. SEM micrographs of RHF/NR composites showed RHF agglomeration in NR matrix and many holes left after RHF pull out from NR matrix indicating the poor interfacial adhesion between RHF and NR matrix. Based on the mechanical properties and material cost of NR composites, the optimum content of RHF was 40 phr.

Effect of acid and alkali treatments on physical properties of RHF was examined. Thermal decomposition patterns of acid treated RHF (ACT) were similar to that of untreated RHF (UT). On the other hand, TGA thermograms of alkali treated RHF (ALT) showed the disappearance of hemicellulose and lignin decompositions. With increasing treatment time, thermal decomposition patterns of ACT were not changed whereas those of ALT showed the reduction of silica content. FTIR spectra of ACT were similar to that of UT as treatment time increased. On the other hand, FTIR spectra of ALT showed the disappearance of absorption band at 1727 cm^{-1}

indicating the removal of hemicellulose and lignin in RHF during alkali treatment. The absorption bands of ALT had insignificant difference as treatment time increased. With increasing treatment time, the outer surface of ACT showed an insignificant change while ALT showed surface roughness. However, the inner surfaces of ACT and ALT were not changed with treatment time. Scorch time of ALT/NR composites was longer than that of ACT/NR composites. Nonetheless, treatment methods and treatment times exhibited no effect on cure time of NR composites. Elongation at break and tensile strength of ACT/NR and ALT/NR composites slightly decreased with increasing treatment time. M100, M300 and tear strength of ACT/NR and ALT/NR composites were insignificant difference. NR composites containing ALT at treatment time of 2 h (2ALT) had the highest tensile properties due to the improvement of interfacial adhesion between RHF and NR. Based on mechanical properties, alkali treatment at treatment time of 2 h was selected to pretreat RHF before silane treatment.

Effect of Si69 content on physical properties of RHF was studied. RHF was pretreated with alkali treatment for 2 h before treating RHF surface with Si69. Silane treated RHF (ST) had lower moisture adsorption on ST surface when compared with 2ALT. With increasing Si69 content, thermal decomposition patterns of ST were not changed. FTIR spectra of ST exhibited the small shoulder at $2972\text{--}2969\text{ cm}^{-1}$ assigned to -CH_2 and -CH_3 stretching of Si69 treated on RHF surface. The absorption band of ST was not changed with increasing Si69 content. Moreover, Si69 content exhibited no effect on the outer and inner surfaces of ST. Scorch time of ST/NR composites was longer than that of ALT/NR composites. With increasing Si69 content, there was no change in scorch time of NR composites. ST/NR composites showed the maximum

values of M100, M300, tensile strength and tear strength at Si69 content of 5 wt%.
due to the improvement of rubber-filler interaction and filler dispersion in NR matrix.



REFERENCES

- Adel, A. M., El-Wahab, Z. H. A., Ibrahim, A. A., and Al-Shemy, M. T. (2010). Characterization of microcrystalline cellulose prepared from lignocellulosic materials. Part I. Acid catalyzed hydrolysis. **Bioresource Technol.** 101: 4446-4455.
- Ahmad, I., Bakar, D. R. A., Mokhilas, S. N., and Raml, A. (2007). Direct usage of products of poly(ethylene terephthalate) glycolysis for manufacturing of rice husk/unsaturated polyester composite. **Iran Polym. J.** 16: 233-239.
- Ahmad, I., Lane, C. E., Mohd, D. H., and Abdullah, I. (2012). Electron-beam-irradiated rice husk powder as reinforcing filler in natural rubber/high-density polyethylene (NR/HDPE) composites. **Comp. Part B.** 43: 3069-3075.
- Ahmed, K., Nizami, S., Raza, N., and Mahmood, K. (2012). Mechanical, swelling, and thermal aging properties of marble sludge-natural rubber composites. **Int. J. Ind. Chem.** 3: 1-12.
- Attharangsarn, S., Ismail, H., Bakar, M. A., and Ismail, J. (2012). The effect of rice husk powder on standard malaysian natural rubber grade L (SMR L) and epoxidized natural rubber (ENR 50) composites. **Polym. Plast. Technol. Eng.** 51: 231-237.
- Bera, J., and Kale, D. D. (2008). Properties of polypropylene filled with chemically treated rice husk. **J. Appl. Polym. Sci.** 110: 1271-1279.

- Chandrasekhar, S., Satyanarayana, K. G., Pramada, P. N., Raghavan, P., and Gupta, T. N. (2003). Review processing, properties and applications of reactive silica from rice husk an overview. **J. Mater. Sci.** 38: 3159-3168.
- Ciannamea, E. M., Stefani, P. M., and Ruseckaite, R. A. (2010). Medium-density particleboards from modified rice husks and soybean protein concentrate-based adhesives. **Bioresource Technol.** 101: 818-825.
- De, D., De, D., and Adhikari, B. (2004). The effect of grass fiber filler on curing characteristics and mechanical properties of natural rubber. **Polym. Adv. Technol.** 15: 708-715.
- Fávaro, S. L., Lopes, M. S., Vieira de Carvalho Neto, A. G., Rogério de Santana, R., and Radovanovic, E. (2010). Chemical, morphological, and mechanical analysis of rice husk/post-consumer polyethylene composites. **Comp. Part A.** 41: 154-160.
- Flory, P. J. (1953). **Principles of polymer chemistry**. Ithaca, New York: Cornell University Press. p. 576.
- Geethamma, V. G., Joseph, R., and Thomas, S. (1995). Short coir fiber-reinforced natural rubber composites: Effects of fiber length, orientation, and alkali treatment. **J. Appl. Polym. Sci.** 55: 583-594.
- Genieva, S. D., Turmanova, S. C., Dimitrova, A. S., and Vlaev, L. T. (2008). Characterization of rice husks and the products of its thermal degradation in air or nitrogen atmosphere. **J. Therm. Anal. Calorim.** 93: 387-396.
- Hong, H., He, H., Jia, D., and Zhang, H. (2011). Effect of wood flour on the curing behavior, mechanical properties, and water absorption of natural rubber/wood flour composites. **J. Macromol. Sci. B.** 50: 1625-1636.

- Hornsby, P. R., Hinrichsen, E., and Tarverdi, K. (1997). Preparation and properties of polypropylene composites reinforced with wheat and flax straw fibres: Part I Fiber characterization. **J. Mater. Sci.** 32: 443-449.
- Hussain, A. I., Abdel-Kader, A. H., and Ibrahim, A. A. (2010). Effect of modified linen fiber waste on physico-mechanical properties of polar and non-polar rubber. **Nature Sci.** 8: 82-91.
- Ichazo, M. N., Hernández, M., Albano, C., and González, J. (2006). Curing and physical properties of natural rubber/wood flour composites. **Macromol. Symp.** 239: 192-200.
- Ismail, H., and Chia, H. H. (1998). The effects of multifunctional additive and epoxidation in silica filled natural rubber compounds. **Polym. Test.** 17: 199-210.
- Ismail, H., Edyham, M. R., and Wirjosentono, B. (2002). Bamboo fiber filled natural rubber composites: the effects of filler loading and bonding agent. **Polym. Test.** 21: 139-144.
- Ismail, H., Mohamad, Z., and Bakar, A. A. (2004). The effect of dynamic vulcanization on properties of rice husk powder filled polystyrene/styrene butadiene rubber blends. **Iran Polym. J.** 13: 11-19.
- Ismail, H., Norjulia, A. M., and Ahmad, Z. (2010). The effects of untreated and treated kenaf loading on the properties of kenaf fibre-filled natural rubber compounds. **Polym. Plast. Technol. Eng.** 49: 519-524.
- Ismail, H., Othman, N., and Komethi, M. (2012). Curing characteristics and mechanical properties of rattan-powder-filled natural rubber composites as a

- function of filler loading and silane coupling agent. **J. Appl. Polym. Sci.** 123: 2805-2811.
- Ismail, H., Ragunathan, S., and Hussin, K. (2011). Tensile properties, swelling, and water absorption behavior of rice-husk-powder-filled polypropylene/(recycled acrylonitrile-butadiene rubber) composites. **J. Vinyl Addit. Technol.** 17: 190-197.
- Ismail, H., Rosnah, N., and Rozman, H. D. (1997). Curing characteristics and mechanical properties of short oil palm fibre reinforced rubber composites. **Polymer**. 38: 4059-4064.
- Ismail, H., Rozman, H. D., Jaffri, R. M., and Ishak, Z. A. M. (1997). Oil palm wood flour reinforced epoxidized natural rubber composites: The effect of filler content and size. **Eur. Polym. J.** 33: 1627-1632.
- Jacob, M., Thomas, S., and Varughese, K. T. (2004). Mechanical properties of sisal/oil palm hybrid fiber reinforced natural rubber composites. **Compos. Sci. Technol.** 64: 955-965
- Jamil, M., Ahmad, I., and Abdullah, I. (2006). Effects of rice husk filler on the mechanical and thermal properties of liquid natural rubber compatibilized high-density polyethylene/natural rubber blends. **J. Polym. Res.** 13: 315-321.
- Jauberthie, R., Rendell, F., Tamba, S., and Cisse, I. (2000). Origin of the pozzolanic effect of rice husks. **Construct. Build. Mater.** 14: 419-423.
- Juliano, B. O. (1985). Rice Chemistry and Technology. In B. O. Juliano and D. B. Bechtel (eds.). **The rice grain and its gross composition** (pp 18-19). USA: The American Association of Cereal Chemists.

- Juliano, B. O. (1985). Rice Chemistry and Technology. In B. O. Juliano (ed.). **Rice hulls and rice straw** (pp. 691). USA: The American Association of Cereal Chemists.
- Kim, H. J., and Eom, Y. G. (2001). Thermogravimetric analysis of rice husk flour for a new raw material of lignocellulosic fiber-thermoplastic polymer composites. **Mokchae Kongha**. 29: 59-67.
- Kim, H. S., Kim, S., and Kim, H. J. (2006). Enhanced interfacial adhesion of bioflour-filled poly(propylene) biocomposites by electron-beam irradiation. **Macromol. Mater. Eng.** 291: 762-772.
- Kim, H. S., Kim, S., Kim, H. J., and Yang, H. S. (2006). Thermal properties of bio-flour-filled polyolefin composites with different compatibilizing agent type and content. **Thermochim. Acta**. 451: 181-188.
- Kim, H. S., Yang, H. S., and Kim, H. J. (2005). Biodegradability and mechanical properties of agro-flour-filled polybutylene succinate biocomposites. **J. Appl. Polym. Sci.** 97: 1513-1521.
- Kim, H. S., Kim, S., Kim, H. J., and Yang, H. S. (2006). Thermal properties of bio-flour-filled polyolefin composites with different compatibilizing agent type and content. **Thermochim. Acta**: 451: 181-188.
- Kim, H. S., Lee, B. H., Choi, S. W., Kim, S., and Kim, H. J. (2007). The effect of types of maleic anhydride-grafted polypropylene (MAPP) on the interfacial adhesion properties of bio-flour-filled polypropylene composites. **Comp. Part A**. 38: 1473-1482.
- Kohjiya, S., and Ikeda, Y. (2003). In situ formation of particulate silica in natural rubber matrix by the sol-gel reaction. **J. Sol-Gel Sci. Techn.** 26: 495-498.

- Lane, C. E., Ahmad, I., Mohd, D. H., and Abdullah, I. (2011). Effects of rice husk modification with liquid natural rubber and exposure to electron beam radiation on the mechanical properties of NR/HDPE/rice husk composites. **Sain Malaysia**. 40: 985-992.
- Li, X., Tabil, L., and Panigrahi, S. (2007). Chemical treatments of natural fiber for use in natural fiber-reinforced composites: a review. **J. Polym. Environ.** 15: 25-33.
- Lopattananon, N., Jitkalong, D., and Seadan, M. (2011). Hybridized reinforcement of natural rubber with silane-modified short cellulose fibers and silica. **J. Appl. Polym. Sci.** 120: 3242-3254.
- Lopattananon, N., Panawarangkul, K., Sahakaro, K., and Ellis, B. (2006). Performance of pineapple leaf fiber–natural rubber composites: the effect of fiber surface treatments. **J. Appl. Polym. Sci.** 102: 1974-1984.
- Luduenä, L., Fasce, D., Alvarez, V. A., and Stefani, P. M. (2011). Nanocellulose from rice husk following alkali treatment to remove silica. **BioRes.** 6:1440-1453.
- Ludueña, L., Vázquez, A., and Alvarez, V. (2012). Effect of lignocellulosic filler type and content on the behavior of polycaprolactone based eco-composites for packaging applications. **Carbohydr. Polym.** 87: 411-421.
- Luh, B. S. (1991). Rice Utilization. In B. S. Luh (ed). **Rice hull** (pp. 269-278). New York: Van Nostrand Reinhad.
- Mansaray, K. G., and Ghaly, A. E. (1998). Thermal degradation of rice husks in nitrogen atmosphere. **Bioresource Technol.** 65: 13-20.

- Mansaray, K. G., and Ghaly, A. E. (1999). Determination of kinetic parameters of rice husks in oxygen using thermogravimetric analysis. **Biomass Bioenerg.** 17: 19-31.
- Markovska, I., and Lyubchev, L. (2007). A study on the thermal destruction of rice husk in air and nitrogen atmosphere. **J. Therm. Anal. Calorim.** 89: 809-814.
- Martí-Ferrer, F., Vilaplana, F., Ribes-Greus, A., Benedito-Borrás, A., and Sanz-Box, C. (2006). Flour rice husk as filler in block copolymer polypropylene: effect of different coupling agents. **J. Appl. Polym. Sci.** 99: 1823-1831.
- Mathew, L., and Joseph, R. (2007). Mechanical properties of short-isora-fiber-reinforced natural rubber composites: effects of fiber length, orientation, and loading; alkali treatment; and bonding agent. **J. Appl. Polym. Sci.** 103: 1640-1650.
- Maziad, N. A., El-Nashar, D. E., and Sadek, E. M. (2009). The effects of a silane coupling agent on properties of rice husk-filled maleic acid anhydride compatibilized natural rubber/low-density polyethylene blend. **J. Mater. Sci.** 44: 2665-2673.
- Mishra, S., Mohanty, A. K., Drzal, L. T., Misra, M., and Hinrichsen, G. (2004). A review on pineapple leaf fibers, sisal fibers and their biocomposites. **Macromol. Mater. Eng.** 289: 955-974.
- Morsi, S. M., Pakzad, A., Amin, A., Yassar, R. S., and Heiden, P. A. (2011). Chemical and nanomechanical analysis of rice husk modified by ATRP-grafted oligomer. **J. Colloid Interf. Sci.** 360: 377-385.

- Muniandy, K., Ismail, H., and Othman, N. (2012). Biodegradation, morphological and FTIR study of rattan powder filled natural rubber composites as a function of filler loading and a silane coupling agent. **BioRes.** 7: 957-971.
- Mustapa, M. S. E., Hassan, A., and Rahmant, A. R. (2005). Preliminary study on the mechanical properties of polypropylene/rice husk composites. In **Proceeding of the Symposium Polimer Kebangsaan Ke-V**, Universiti Tenaga Nasional.
- Ndazi, B. S., Karlsson, S., Tesha, J. V., and Nyahumwa, C. W. (2007). Chemical and physical modifications of rice husks for use as composite panels. **Comp. Part A.** 38: 925-935.
- Ndazi, B. S., and Tesha, C. W. N. J. (2007). Chemical and thermal stability of rice husks against alkali treatment. **BioRes.** 3: 1267-1277.
- Nguyen, M. H., Kim, B. S., Ha, J. R., and Song, J. I. (2011). Effect of plasma and NaOH treatment for rice husk/PP Composites. **Adv. Compos. Mater.** 20: 435- 442.
- Nordin, R., Said, C. M. S., and Ismail, H. (2007). Properties of rice husk powder/natural rubber composites. **Solid State Sci. Technol.** 15: 83-91.
- Nordin, R., Said, C. S., and Ismail, H. (2006). The effect of filler loading and silane coupling agent on cure characteristics and mechanical properties of ric husk powder filled natural rubber compounds. In **Proceedings of the Technology and Innovation for Sustainable Development Conference**, Khon Kaen, Thailand.
- Ostad-Movahed, S., Yasin, K. A., Ansarifar, A., Song, M., and Hameed, S. (2008). Comparing effects of silanized silica nanofiller on the crosslinking and

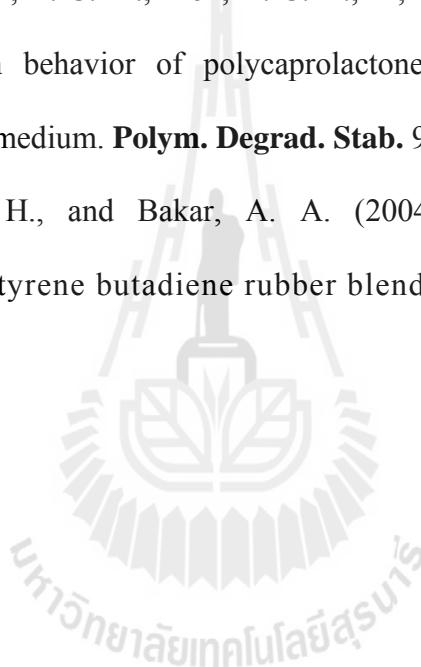
- mechanical properties of natural rubber and synthetic polyisoprene. **J. Appl. Polym. Sci.** 109: 869-881.
- Panthapulakkal, S., Law, S., and Sain, M. (2005). Enhancement of processability of rice husk filled high-density polyethylene composite profiles. **J. Thermoplas. Compos.** 18: 445-458.
- Panthapulakkal, S., Sain, M., and Law, S. (2005). Effect of coupling agents on rice-husk-filled HDPE extruded profiles. **Polym. Int.** 54: 137-142.
- Park, B.-D., Wi, S. G., Lee, K. H., Singh, A. P., Yoon, T.-H., and Kim, Y. S. (2004). X-ray photoelectron spectroscopy of rice husk surface modified with maleated polypropylene and silane. **Biomass Bioenerg.** 27: 353-363.
- Pires de Carvalho, F., Isabel Felisberti, M., Soto Oviedo, M. A., Davila Vargas, M., Farah, M., and Fortes Ferreira, M. P. (2012). Rice husk/poly(propylene-co-ethylene) composites: effect of different coupling agents on mechanical, thermal, and morphological properties. **J. Appl. Polym. Sci.** 123: 3337-3344.
- Poh, B. T., and Ng, C. C. (1998). Effect of silane coupling agents on the mooney scorch time of silica-filled natural rubber compound. **Eur. Polym. J.** 34: 975-979.
- Radovanović, B., Marković, G., and Radovanovic, A. (2008). Wood flour as a secondary filler in carbon black filled of styrene butadiene/chlorosulphonated polyethylene rubber blend. **Polym. Compos.** 29: 692-697.
- Rahman, I. A., Ismail, J., and Osman, H. (1997). Effect of nitric acid digestion on organic materials and silica in rice husk. **J. Mater. Chem.** 7: 1505-1509.
- Rangel-Vázquez, N. A., and Leal-García, T. (2010). Spectroscopy analysis of chemical modification of cellulose fibers. **J. Mex. Chem. Soc.** 54: 192-197.

- Razavi-Nouri, M., Fatemeh Jafarzadeh-Dogouri, Oromiehie, A., and Langroudi, A. E. (2006). Mechanical properties and water absorption behavior of chopped rice husk filled polypropylene composites. **Iran Polym. J.** 15: 757-766.
- Rozman, H. D., Musa, L., and Abubakar, A. (2005). The mechanical and dimensional properties of rice husk-unsaturated polyester composites. **Polym. Plast. Technol. Eng.** 44: 489-500.
- Rozman, H. D., Musa, L., and Abubakar, A. (2005). Rice husk–polyester composites: The effect of chemical modification of rice husk on the mechanical and dimensional stability properties. **J. Appl. Polym. Sci.** 97: 1237-1247.
- Sae-oui, P., Sirisinha, C., Hatthapanit, K., and Thepsuwan, U. (2005). Comparison of reinforcing efficiency between Si-69 and Si-264 in an efficient vulcanization system. **Polym. Test.** 24: 439-446.
- Sae-oui, P., Sirisinha, C., Thepsuwan, U., and Hatthapanit, K. (2004). Comparison of reinforcing efficiency between Si-69 and Si-264 in a conventional vulcanization system. **Polym. Test.** 23: 871-879.
- Sae-oui, P., Thepsuwan, U., and Hatthapanit, K. (2004). Effect of curing system on reinforcing efficiency of silane coupling agent. **Polym. Test.** 23: 397-403.
- Saramolee, P., and Bunloy, S. (2009). The curing characteristics and mechanical properties of wood sawdust/carbon black filled ethylene propylene diene rubber composites. **Walailak J. Sci. Tech.** 6: 255-271.
- Saramolee, P., Lertsuriwat, P., Hunyek, A., and Sirisathitkul, C. (2010). Cure and mechanical properties of recycled NdFeB-natural rubber composites. **Bull. Mater. Sci.** 33: 597-601.

- Sareena, C., Ramesan, M. T., and Purushothaman, E. (2012). Utilization of peanut shell powder as a novel filler in natural rubber. **J. Appl. Polym. Sci.** 125: 2322-2334.
- Sarkawi, S. S., and Aziz, Y. (2003). Ground rice husk as filler in rubber compounding **Jurnal Teknologi.** 39:135-148.
- Singha, A. S., and Thakur, V. K. (2009). Morphological, thermal, and physicochemical characterization of surface modified pinus fibers. **Int. J. Polym. Anal.** 14: 271-289.
- Syafri, R., Ahmad, I., and Abdullah, I. (2011). Effect of rice husk surface modification by LENR the on mechanical properties of NR/HDPE reinforced rice husk composite. **Sain Malaysia.** 40: 749-756.
- Thongpin, C., Sangnil, C., Suerkong, P., Pongpilaiprerti, A., and Sombatsompop, N. (2009). The effect of excess silane-69 used for surface modification on cure characteristic and mechanical properties of precipitated silica filled natural rubber (PSi/NR). **Adv. Compos. Mater.** : 2171-2174.
- Thongsang, S., and Sombatsompop, N. (2006). Effect of NaOH and Si69 treatments on the properties of fly ash/natural rubber composites. **Polym. Compos.** 27: 30-40.
- Vempati, R. K., Musthyala, S. C., Mollah, M. Y. A., and Cocke, D. L. (1995). Surface analyses of pyrolysed rice husk using scanning force microscopy. **Fuel.** 74: 1722-1725.
- Wang, J., Wu, W., Wang, W., and Zhang, J. (2011). Effect of a coupling agent on the properties of hemp-hurd-powder-filled styrene-butadiene rubber. **J. Appl. Polym. Sci.** 121: 681-689.

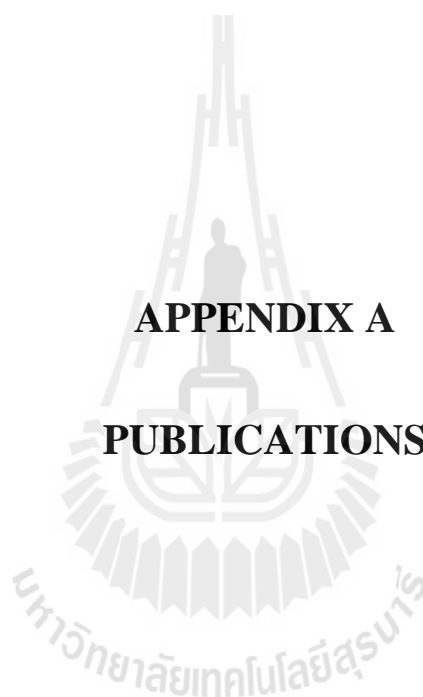
- Wolff, S. (1996). Chemical aspects of rubber reinforcement by fillers. **Rubber Chem. Technol.** 69: 325-346.
- Wongsorat, W. (2009). **Effect of surface modification on physical properties of sisal fiber/natural rubber composites.** M. Eng. thesis, Suranaree University of Technology, Thailand.
- Yang, H. S., Kim, H. J., Park, H. J., Lee, B. J., and Hwang, T. S. (2006). Water absorption behavior and mechanical properties of lignocellulosic filler–polyolefin bio-composites. **Compos. Struct.** 72: 429-437.
- Yang, H. S., Kim, H. J., Son, J., Park, H. J., Lee, B. J., and Hwang, T. S. (2004). Rice husk flour filled polypropylene composites; mechanical and morphological study. **Compos. Struct.** 63: 305-312.
- Yang, H. S., Kim, H. J., Park, H. J., Lee, B. J., and Hwang, T. S. (2007). Effect of compatibilizing agents on rice-husk flour reinforced polypropylene composites. **Compos. Struct.** 77: 45-55.
- Yang, H. S., Wolcott, M. P., Kim, H. S., Kim, S., and Kim, H. J. (2007). Effect of different compatibilizing agents on the mechanical properties of lignocellulosic material filled polyethylene bio-composites. **Compos. Struct.** 79: 369-375.
- Yin, C. Y., and Goh, B. M. (2011). Thermal degradation of rice husks in air and nitrogen: thermogravimetric and kinetic analyses. **Energ. Source Part A.** 34: 246-252.
- Yoshida, S., Ohnishi, Y., and Kitagishi, K. (1962). Histochemistry of silicon in rice plant. **Soil Sci. Plant. Nutr.** 8: 30-35.

- Zeng, Z., Ren, W., Xu, C., Lu, W., Zhang, Y., and Zhang, Y. (2009). Effect of bis(3-triethoxysilylpropyl) tetrasulfide on the crosslink structure, interfacial adhesion and mechanical properties of natural rubber/cotton fiber composites. **J. Appl. Polym. Sci.** 111: 437-443.
- Zhao, F., Bi, W., and Zhao, S. (2011). Influence of crosslink density on mechanical properties of natural rubber vulcanizates. **J. Macromol. Sci. B.** 50: 1460-1469.
- Zhao, Q., Tao, J., Yam, R. C. M., Mok, A. C. K., Li, R. K. Y., and Song, C. (2008). Biodegradation behavior of polycaprolactone/rice husk ecomposites in simulated soil medium. **Polym. Degrad. Stab.** 93: 1571-1576.
- Zurina, M., Ismail, H., and Bakar, A. A. (2004). Rice husk powder-filled polystyrene/styrene butadiene rubber blends. **J. Appl. Polym. Sci.** 92: 3320-3332.



APPENDIX A

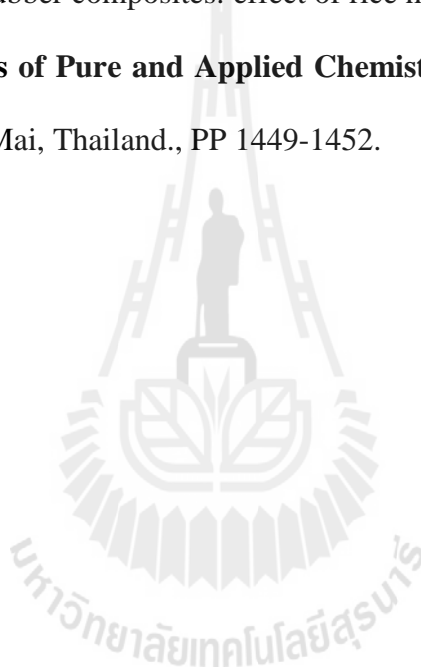
PUBLICATIONS



List of publications

Srisuwan, L., Jarukumjorn, K., and Suppakarn, N. (2012). Physical properties of rice husk fiber/natural rubber composites. **Adv. Mater. Res.** 410: 90-93.

Srisuwan, L., Jarukumjorn, K., and Suppakarn, N. (2012). Properties of rice husk fiber /natural rubber composites: effect of rice husk fiber surface modification. In **Proceedings of Pure and Applied Chemistry International Conference** 2012. Chiang Mai, Thailand., PP 1449-1452.



Advanced Materials Research Vol. 410 (2012) pp 90-93
Online available since 2011/Nov/29 at www.scientific.net
 © (2012) Trans Tech Publications, Switzerland
 doi:10.4028/www.scientific.net/AMR.410.90

Physical Properties of Rice Husk Fiber/Natural Rubber Composites

Ladawan Srisuwan^{1,2,a}, Kamasa Jarukumjorn^{1,2,b} and Nitinat Suppakarn^{1,2,c}

¹School of Polymer Engineering, Institute of Engineering,
 Suranaree University of Technology, Nakhon Ratchasima 30000, Thailand

²Center for Petroleum, Petrochemicals and Advanced Materials,
 Chulalongkorn University, Bangkok 10330, Thailand

^aladawan_sri@hotmail.com, ^bkasama@sut.ac.th, ^cnitinat@sut.ac.th

Keywords: Rice husk, natural rubber, rubber composites, physical properties

Abstract. In this study, rice husk fiber (RHF) was used as a reinforcing filler for natural rubber (NR). NR composites were prepared at various RHF contents, *i.e.*, 10, 20, 30, 40 and 50 phr. Sulfur conventional vulcanization was used. Effect of RHF content on cure characteristics, mechanical properties and morphological properties of NR composites were investigated. The results showed that scorch and cure times of RHF/NR composites were not affected by increasing RHF content. Crosslink density, tensile strength, elongation at break and tear strength of NR composites slightly decreased with increasing RHF content whereas M100 and M300 of the composites slightly increased with increasing RHF content.

Introduction

Rice husk (RH) is abundantly available in Thailand as a byproduct from the rice milling process. Only a minor portion of the rice husk is reserved as animal feed, bedding material or household fuel while the huge quantities are burned in fields leading to environmental pollution. Various researches attempted to expand the utilization of RH in industries, *e.g.* as pozzolanic material to enhance the lime treatment of degraded soil, as filler to increase compressive strength in cement, particleboard material and as a source for activated carbon [1]. In addition, RH can be used as reinforcing filler for natural rubber (NR). RH contains 45% cellulose, 19% hemicelluloses, 19.5% lignin and 15% silica by weight [2,3]. Besides cellulose, RH has high silica content as compared with other natural fibers [3]. Both cellulose and silica in RH can provide strength to the fiber as well as improve mechanical properties of NR. In addition, RH has many advantages similar to other natural fibers such as low density, low price, high strength, stiffness and non abrasiveness [4]. The utilization of RH as reinforcing filler for NR is an approach to obtain value added products from an agricultural waste.

Materials and Methods

Materials

Natural rubber (STR 5L) was purchased from Thai Hoa Rubber Public Co., Ltd. Rice husk (RH) was purchased from a local rice mill in Nakhon Ratchasima, Thailand. N-cyclohexyl-2-benzothiazole-2-sulphenamide (CBS), stearic acid, zinc oxide (ZnO), and sulfur (S) were supplied by Channel Chemicals Co., Ltd.

Preparation of rice husk fiber (RHF)

RH was washed thoroughly with tap water to remove the adhered soil and dust, and then dried in open air. The dried rice husk was ground using a grinding machine (RETSCH/SR200) and sieved with a sieve shaker (RETSCH/AS200). The rice husk fiber (RHF) retained in sieve size ranging between 150-300 μ m was used. The RHF was dried in an air oven at 80°C overnight to discharge the moisture before compounding.

Preparation and characterization of RHF/NR composites

To prepare NR composites, NR was masticated for 5 min on a two-roll mill (CHAICHAREON) to reduce its viscosity. Then, stearic acid, zinc oxide, CBS, RHF, and sulfur were added, respectively. Total mixing time was 20 min.

Cure characteristics of RHF/NR composites were determined using a moving die rheometer (MDR) (GOTECH/GT-M200F) at a temperature of 150 °C. Scorch time (T_s) and cure time (T_{c90}) of the RHF/NR composites were determined.

RHF/NR composites were vulcanized using a compression molding machine (LAB TECH/L320) at 150 °C. The vulcanized time was based on the cure time obtained from MDR. The composite sheet was cut into dumbbell shaped specimens with a die cutter (Type C). Tensile and tear properties of RHF/NR composites were determined according to ASTM D 412–06a and ASTM D 624, respectively.

Crosslink density of RHF/NR composites was measured according to ASTM D 6814. The vulcanized NR composites were swollen in toluene at 27° C for 72 h to obtain equilibrium swelling stage. Crosslink density was calculated by the Flory-Rhener equation [5].

Dispersion of RHF in RHF/NR composites and surface morphologies of tensile fracture surfaces of the composites were characterized using a scanning electron microscope (SEM) (JEOL/JSM-6400) at 10 kV. Samples were coated with gold before analysis.

Result and discussions

Cure characteristics and crosslink density

Cure characteristics and crosslink density of NR and RHF/NR composites are shown in Table 1. NR showed longer scorch and cure times than NR composites. The incorporation of RHF in NR matrix slightly decreased scorch and cure times of NR composites. The similar results were observed by Jacob *et al* [6], Ismail and Khalil [7] and Geetham *et al* [8]. They suggested that the addition of fiber in rubber increased the mixing time of rubber compounds leading to the high heat buildup during compounding and the formation of premature crosslinking in rubber composites. However, increasing RHF content in the NR composites had no effect on their scorch and cure times.

As shown in Table 1, gum NR had the highest crosslink density. With increasing RHF content, crosslink density of NR composites slightly decreased. Similar observation was reported by Zeng *et al* [9]. The decrement of crosslink density of NR composites was attributed to the adsorption of the accelerator by hydroxyl group of the fiber. RHF content had slightly effect on crosslink density of the NR composites. The NR composites containing RHF of 20 phr provided the lowest crosslink density.

Table 1 Cure characteristics of NR and RHF/NR composite

Samples	T_s (min)	T_{c90} (min)	Crosslink density (*10 ⁴ mol/cm ³)
NR	5.24	7.54	0.85
10RHF/NR	4.06	7.24	0.76
20RHF/NR	3.53	7.48	0.66
30RHF/NR	4.06	7.17	0.73
40RHF/NR	4.11	7.16	0.71
50RHF/NR	4.17	7.25	0.79

Mechanical properties

Properties of natural fiber reinforced rubber composites depend on fiber dispersion, fiber-rubber adhesion, fiber orientation, fiber aspect ratio and fiber content, *etc.* The incorporation of natural fiber in rubber improved modulus of the rubber composites while the composites maintained elasticity of the rubber matrix [10]. Tensile strength and elongation at break of NR and RHF/NR composites are shown in Fig. 1. Gum NR represented the highest tensile strength and elongation at break. The high strength of NR was because of the high crosslink density of the vulcanized NR as well as its strain-induced crystallization behavior [6]. For RHF/NR composites, tensile strength and elongation at break of NR composites slightly decreased with increasing RHF content. This was because RHF hindered the arrangement of rubber molecules leading to the reduction of strain-induced crystallization of NR. In addition, the reduction of both tensile strength and elongation at break of the composites was attributed to the incompatibility between hydrophilic RHF and hydrophobic NR.

Modulus at 100 %strain (M100) and modulus at 300% strain (M300) of NR and RHF/NR composites are shown in Fig. 2. Modulus of gum NR was lower than those of NR composites. In addition, M100 and M300 of RHF/NR composites slightly increased by adding RHF. This was because of the high stiffness of RHF.

Tear strength of NR and RHF/NR composites are shown in Fig. 3. NR represented the highest tear strength. The incorporation of RHF in NR reduced tear strength of RHF/NR composites. In addition, tear strength of the composites decreased as RHF content increased. This was because RHF obstructed strain-induced crystallization of NR leading to the decrement of tear properties of NR composites.

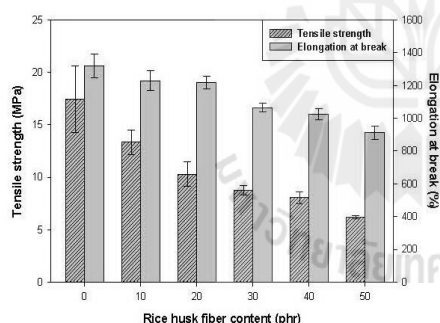


Figure 1 Tensile strength and elongation at break of NR and RHF/NR composites.

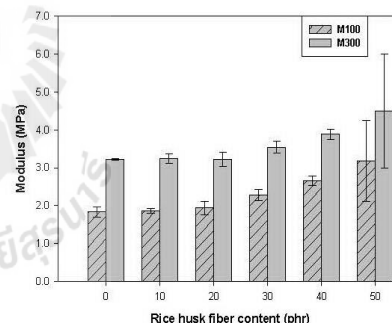


Figure 2 M100 and M300 of NR and RHF/NR composites.

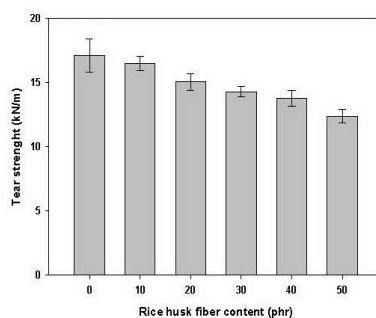


Figure 3 Tear strength of NR and RHF/NR composites.

Morphological properties

SEM micrograph of tensile fracture surface of NR and RHF/NR composites are shown in Fig. 4. Gum NR showed the smooth surface. NR composites exhibited a rough surface because of the presence of fiber. NR composites containing 10 phr RHF showed uniform dispersion of RHF while the composites containing 50 phr RHF illustrated agglomerated RHF in rubber matrix. In addition, all NR composites exhibited numerous holes due to the fiber pullout and large gap between RHF and NR matrix. These implied the poor interfacial adhesion between RHF and NR matrix. The SEM micrographs of NR composites were in good agreement with the reduction in tensile properties of NR composites.

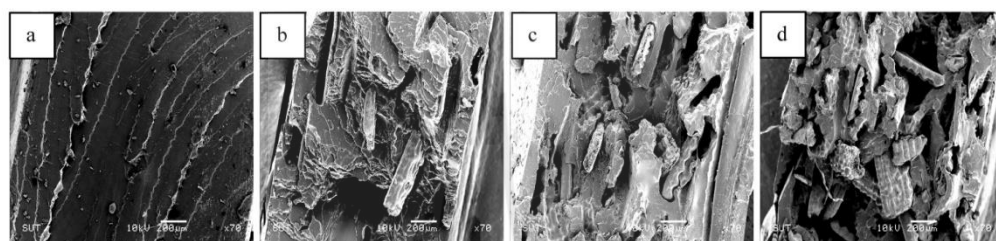


Figure 4 SEM micrographs of tensile fracture surface of (a) NR and (b) RHF/NR composites containing RHF of 10 phr, (c) 30 phr and (d) 50 phr.

Summary

Effect of RHF content on cure characteristics, mechanical properties and morphological of RHF/NR composites were studied. Gum NR showed the highest crosslink, tensile strength, elongation at break and tear strength. Tensile strength, elongation at break and tear strength of RHF/NR composites slightly decreased with increasing RHF content. RHF/NR composites with 50 phr RHF represented the highest M100 and M300. SEM micrographs showed that RHF and NR had poor interfacial adhesion which caused the decrement of mechanical properties of NR composites.

Acknowledgements

The authors would like to thank Suranaree University of Technology, Center for Petroleum, Petrochemicals, and Advanced Materials for financial supports and Channel Chemicals Co., Ltd. for rubber chemicals supports.

References

- [1] R.K. Vempati, S.C. Musthyala, A.Y.A. Mollah, and D.L. Coke: Fuel. Vol.74 (1995), p. 1722.
- [2] F. Marti-Ferre, F. Vilaplana, A. Ribes-Greus, A. Bennedito-Borras, and C. Sanz-Boz: J. Appl. Polym. Sci. Vol 99 (2006), p. 1823.
- [3] S. Panthapulakkal, M. Sain, and S. Law: Polym. Int. Vol. 54 (2005), p. 137.
- [4] R. Nordin, C.M.S. Said, and H. Ismail: Solid State Sci. Technol. Vol. 15 (2007), p. 83.
- [5] P.J. Flory: *Principle of polymer chemistry*. New York (1953): Cornell University Press.
- [6] M. Jacob, S. Thomas and K.T. Varughese: Compos Sci Technol. Vol. 64 (2004), p. 955.
- [7] H. Ismail and H. P. S. Abdul Khalil: Polym. Testing. Vol. 20 (2000), p. 33.
- [8] V.G. Geethamma, R. Joseph, and S. Thomas: J Appl. Polym. Sci. Vol. 55 (1995), p. 583.
- [9] Z. Zeng, W. Ren, C. Xu, W. Lu, Y. Zhang and Y. Zhang: J Appl. Polym. Sci. Vol. 111 (2009), p. 437.
- [10] P.L. Teh, Z.A. Mohd Ishak, A.S. Hashim, J. Karger-Kocsis and U.S. Ishiaku: Eur Polym J. Vol. 40 (2004), p. 2513.

PROPERTIES OF RICE HUSK FIBER/NATURAL RUBBER COMPOSITES: EFFECT OF RICE HUSK SURFACE MODIFICATION

Ladawan Srisuwan^{1,2}, Kasama Jarukumjorn^{1,2} and Nitinat Suppakarn^{1,2*}

¹ School of Polymer Engineering, Institute of Engineering, Suranaree University of Technology, Nakhon Ratchasima 30000, Thailand

² Center for Petroleum, Petrochemicals and Advanced Materials, Chulalongkorn University, Bangkok 10330, Thailand

* Author for correspondence: nitinat@sut.ac.th, Tel. +66 44 224439, Fax. +66 44 224605

Abstract: To improve compatibility between rice husk fiber (RHF) and natural rubber (NR), RHF surface was modified by treating with 1 M HCl or 1 M NaOH at various treatment times, i.e., 0, 1, 2, 6, 12 and 24 hours. Chemical compositions of untreated and treated RHF were characterized using thermogravimetric analysis. To prepare RHF/NR composites, 40 phr untreated or treated RHF was mixed with NR using a two roll-mill. Cure characteristics, tensile properties and morphological properties of untreated and treated RHF/NR composites were determined. RHF surface treatment methods and treatment times insignificantly affected scorch time, cure time and modulus of RHF/NR composites. Nonetheless, treating RHF surface with acid or alkali enhanced tensile strength and elongation at break of NR composites. As compared with acid treated RHF/NR composites, alkali treated RHF/NR composites had higher tensile strength and elongation at break. In addition, maximum values of tensile strength and elongation at break of NR composites was obtained when RHF was alkali treated for 2 hours.

1. Introduction

Rice husk (RH) is an agricultural waste obtained from rice milling industry. The majority of RH is disposed and burned in the fields leading to the environmental pollution. In order to solve this concern, rice husk fiber (RHF) is used as a reinforcing filler for natural rubber (NR). The main constituents of RHF are 32-35% cellulose, 19-25% hemicelluloses, 16-20% lignin and 13-17% silica [1-2]. The high contents of cellulose and silica in RHF could improve mechanical properties of NR composites. In addition, RHF has several advantages, i.e., low density, low cost, biodegradability and high stiffness [1-3]. However, the main drawback of RHF/NR composites is the incompatibility between RHF and NR. Hydrophilic character of RHF and hydrophobic character of NR lead to the weak interfacial adhesion between fiber and matrix as well as low mechanical properties of NR composites. Several studies have reported numerous methods to improve compatibility between RHF and NR, i.e., adding compatibilizer, matrix modification and fiber surface modification [4-6]. In this study, RHF surface modification using acid and alkali treatments are selected. Alkali treatment is conventional treatment for natural fibers. It can remove wax, fat, hemicelluloses and impurity on RHF

surface. The removal of these components enhances surface roughness of RHF leading to the improvement of interfacial adhesion between RHF and rubber matrix. However, alkali treatment removed silica in RHF. To preserve silica in RHF, acid treatment was used to modify RHF surface. The aim of this study was to investigate effect of RHF surface modifications and treatment times on cure characteristics and mechanical properties of RHF/NR composites.

2. Materials and Methods

2.1 Materials

Natural rubber (STR 5L) was purchased from Thai Hoa Rubber Public Co., Ltd. Rice husk (RH) was purchased from a local rice mill in Nakhon Ratchasima, Thailand. Hydrochloric acid (37%v/v HCl) and sodium hydroxide (NaOH) were purchased from Italma Co., Ltd. N-cyclohexyl-2-benzothiazole-2-sulphenamide (CBS), stearic acid, zinc oxide (ZnO), and sulfur (S) was supplied by Channel Chemicals Co., Ltd.

2.2 RHF Preparation

Rice husk was washed thoroughly with tap water to remove the adhered soil and dust, and then dried in open air. The dried rice husk was ground using a grinding machine (RETSCH/ZM200) and sieved with a sieve shaker (RETSCH/AS200). Rice husk fiber (RHF) retained in sieve size ranging between 150-300 μ m was used. Before compounding, RHF was dried in an oven at 80°C overnight to discharge the moisture.

2.3 RHF surface treatment

RHF was immersed in 1 M HCl or 1 M NaOH solution at room temperature and at a RHF to solution ratio of 1:25 (w/v). The treatment time was varied, i.e., 1, 2, 6, 12 and 24 hours. After that, RHF was filtered, rinsed with water several times to eliminate the residual and dried at 80 °C for 24 hours. According to the treatment time, HCl treated RHF was called 1ACT, 2ACT, 6ACT, 12ACT and 24ACT while NaOH treated RHF was called 1ALT, 2ALT, 6ALT, 12ALT and 24ALT.

2.4 RHF characterization

Thermal behaviors of untreated RHF and surface treated RHF were characterized by a thermogravimetric analyzer (TGA) (TA INSTRUMENT/SDT2960). TGA and its derivative weight loss (DTG) curves were acquired by heating a sample from 25°C to 800°C at a heating rate of 10°C/min under a nitrogen atmosphere.

2.5 RHF/NR composites preparation

To prepare NR composites, RHF was mixed with NR on a two-roll mill (CHAICHAREON) for 20 min. NR was masticated for 5 min to reduce its viscosity. Then, stearic acid, zinc oxide, CBS and 40 phr RHF were added, respectively, while sulfur was added lastly.

2.6 Cure characteristics

Cure characteristics of RHF/NR composites were determined using a moving die rheometer (MDR)(GOTECH/GT-M200F) at 150°C. Scorch time (T_s), cure time (T_{90}), maximum torque (S_{max}) and minimum torque (S_{min}) of the RHF/NR composites were determined.

2.7 Tensile properties

RHF/NR composites were vulcanized using a compression molding machine (LAB TECH/L320) at 150°C. The vulcanization time was based on the cure time obtained from MDR. The composite sheet was cut into dumbbell specimens with a die cutter (Type C). Tensile properties of RHF/NR composites were determined according to ASTM D 412-06a using a universal testing machine (UTM) (INSTRON/5569) with 5 kN load cell and 500 mm/min crosshead speed.

2.8 Morphological properties

Morphologies of tensile fracture surfaces of NR composites were characterized using a scanning electron microscope (SEM) (JEOL/JSM-6400) at 10 kV. The sample was coated with gold before analysis.

3. Results and discussion

3.1 Thermal properties of RHF

TGA and DTG thermograms of untreated RHF (UTRHF), acid treated RHF and alkali treated RHF are shown in Figures 1-2. All samples showed initial weight loss between 50 to 150°C attributing to the evaporation of water in RHF. Apart from this stage, several studies reported that rice husk has three decomposition stages according to the decompositions of hemicelluloses (150-300°C), celluloses (300-350°C) and lignin (400-500°C) [7-9]. Untreated and acid treated RHF showed hemicelluloses decomposition peak around 304-310°C. This decomposition peak was still observed even with increasing acid treatment time. This indicated that hemicelluloses could not be removed by treating RHF surface with HCl. Mishra *et.al.* also suggested that hemicelluloses and celluloses were slowly hydrolyzed in acid condition at low

temperature [8]. As compared with acid treated RHF, hemicelluloses decomposition peak of alkali treated RHF was slightly lower. With increasing alkali treatment time, hemicellulose decomposition peak disappeared. This indicated that alkali treatment effectively removed hemicelluloses, wax and fat on RHF surface. Residues remained after heating RHF at 700°C related to the presence of silica and char. The amounts of residues at 700°C of acid and alkali treated RHF were lower than that of untreated RHF. As compared with acid treated RHF, the alkali treated RHF had lower amount of residues and decreased more drastically with increasing treatment time. The reduction of residue of alkali treated RHF was because of the removal of silica during alkali treatment [10].

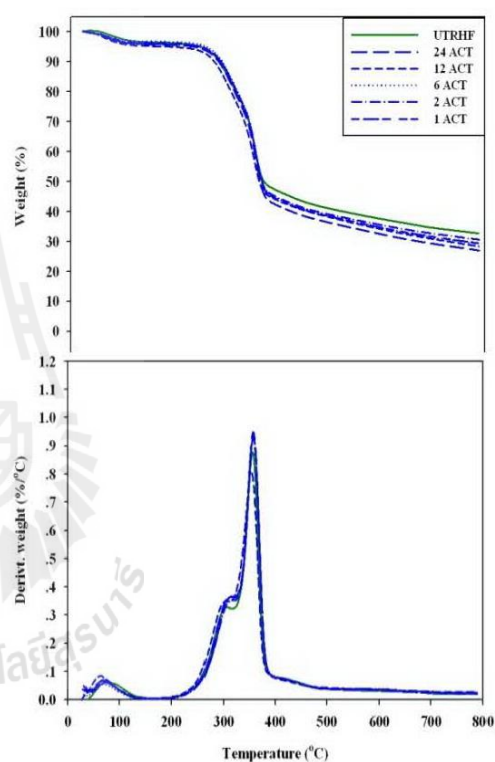


Figure 1. TGA and DTG curves of untreated RHF and acid treated RHF at various treatment times.

3.2 Cure characteristics of NR and NR composites

Cure characteristics of NR, untreated RHF/NR and treated RHF/NR composites are shown in Table 1. Scorch time and cure time of NR, untreated RHF/NR and treated RHF/NR composites insignificantly changed with various RHF surface treatment methods and treatment times. Torque difference was related to the extent of crosslink density of rubber composites and had similar trend to maximum torque [12]. Torque differences of NR, untreated RHF/NR and treated RHF/NR composites insignificantly changed with various RHF surface treatment methods and treatment

times. This implied the similar crosslink density of NR and NR composites.

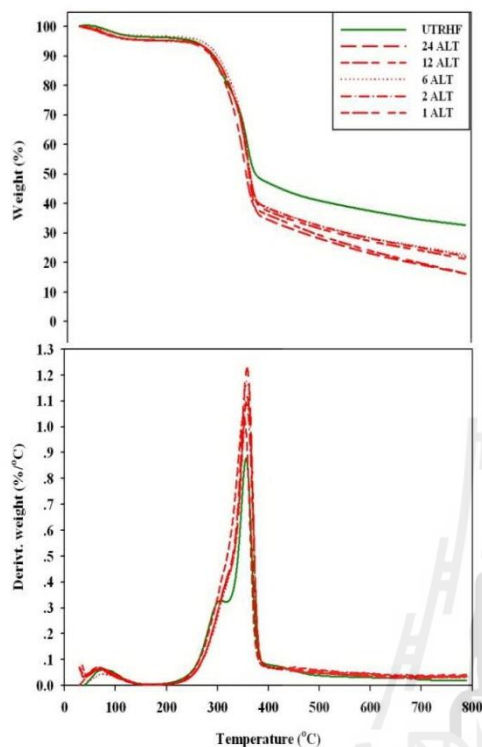


Figure 2. TGA and DTG of untreated RHF and alkali treated RHF at various treatment times.

3.3 Tensile properties of NR and NR composites

Tensile strength and elongation at break of NR, untreated RHF/NR and treated RHF/NR composites are shown in Figure 3. NR showed the highest tensile strength and elongation at break because of the strain-induced crystallization behaviors and the elasticity of NR [13]. After the incorporation of untreated RHF or treated RHF into NR, tensile strength and elongation at break of NR composites significantly decreased. This was because RHF restrained the arrangement of rubber chains leading to the decrement of strain-induced crystallization of NR. Tensile strength and elongation at break of both acid treated RHF/NR and alkali treated RHF/NR composites slightly higher than those of untreated RHF/NR composites. Moreover, their tensile strength and elongation at break slightly increased when the treatment time was increased up to 2 hours. As compared with acid treated RHF/NR composites, alkali treated RHF/NR composites had higher tensile strength and elongation at break. This was probably because alkali treatment removed hemicelluloses, wax and fat on RHF surface better than acid treatment leading to the high surface roughness and the mechanical interlocking between alkali treated RHF and NR. As the treatment time increased from 2 to 24 hours, tensile strength and

elongation at break of acid treated RHF/NR and alkali treated RHF/NR composites slightly decreased. This was because the amount of cellulose in RHF increased with increasing treatment time.

Modulus at 100% strain (M100) and 300% strain (M300) of NR, untreated RHF/NR and treated RHF/NR composites are shown in Figure 4. Modulus is related to stiffness of rubber composites and depends on crosslink density of the composites [13]. NR composites had higher M100 and M300 than NR. This was because of the high stiffness of RHF. M100 and M300 of acid treated RHF/NR and alkali treated RHF/NR composites were not affected by surface treatment time.

Table 1: Cure characteristics of NR, untreated RHF/NR and treated RHF/NR composites.

Sample	S_{max} (Nm)	S_{min} (Nm)	$S_{max} - S_{min}$ (Nm)	T_g (min)	T_{90} (min)
NR	23.74	5.91	17.84	4.27	7.45
UTRHF/NR	25.33	5.78	19.54	4.10	7.48
1ACT/NR	23.18	5.43	17.76	4.40	7.40
2ACT/NR	24.19	5.64	18.56	4.25	7.44
6ACT/NR	20.39	5.35	15.05	5.20	8.26
12ACT/NR	21.22	3.94	17.28	3.47	7.13
24ACT/NR	22.34	5.02	17.31	4.00	7.50
1ALT/NR	24.08	5.71	18.38	4.26	7.44
2ALT/NR	23.24	5.63	17.61	4.41	7.39
6ALT/NR	24.13	6.12	18.01	4.52	7.46
12ALT/NR	27.18	5.79	21.38	4.26	7.30
24ALT/NR	20.95	5.2	15.75	4.25	7.13

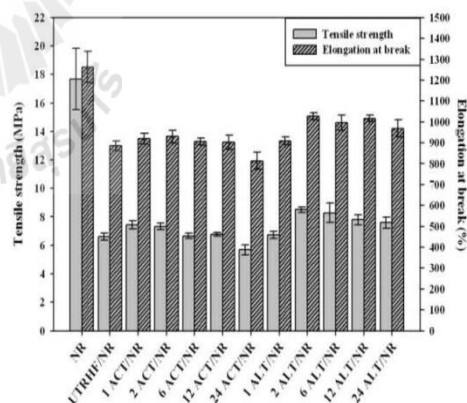


Figure 3. Tensile strength and elongation at break of untreated RHF/NR and treated RHF/NR composites.

3.4 Morphologies of NR and NR composites

Morphologies of tensile fracture surface of NR, untreated RHF/NR, 2ACT/NR and 2ALT/NR composites are shown in Figure 5. Untreated RHF/NR composites exhibited clean fiber surface and gap between fiber and NR indicating the weak interfacial adhesion between RHF and NR matrix. The gap

between fiber and NR matrix was still observed even in acid treated RHF/NR and alkali treated RHF/NR composites. However, surface of treated RHF seemed to be rougher than that of untreated RHF. The fiber surface roughness may help improve interfacial adhesion between RHF and NR leading to the enhancement of tensile properties of treated RHF/NR composites.

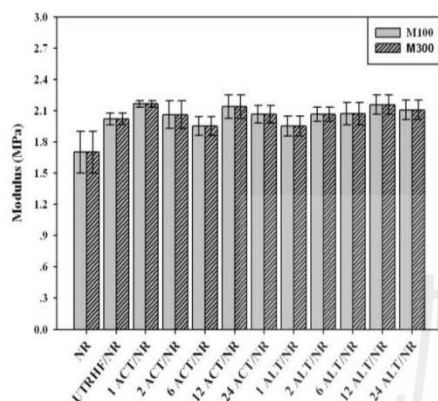


Figure 4. Tensile modulus at 100% strain and 300% strain of untreated RHF/NR and treated RHF/NR composites.

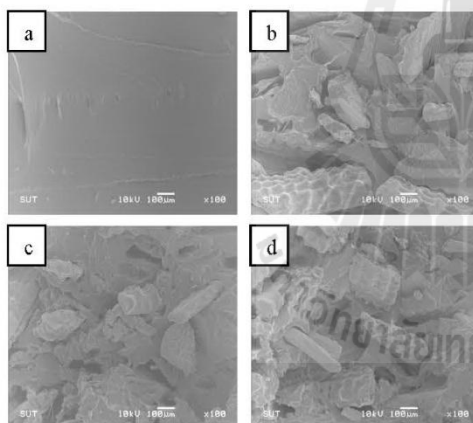


Figure 5. SEM micrographs of tensile fracture surface of (a) NR, (b) untreated RHF/NR, (c) 2ACT/NR and (d) 2ALT/NR composites.

4. Conclusions

Thermal properties of treated RHF suggested that alkali treatment removed hemicelluloses and impurities on RHF surfaces better than acid treatment. The treated and untreated RHF was used as fillers for producing NR composites. Effect of RHF surface treatments and treatment times on cure characteristics and mechanical properties of RHF/NR composites were determined. Scorch time and cure time of NR composites was not affected by RHF surface treatment

methods and treatment times. The fiber surface roughness led to the improved interfacial adhesion between the treated RHF and NR matrix and the improved tensile properties of treated RHF/NR composites. In addition, the optimum tensile strength and elongation at break of NR composites were obtained at 2 hours of alkali treatment.

Acknowledgements

The authors would like to thank Suranaree University of Technology, Center for Petroleum, Petrochemicals, and Advanced Materials for financial supports and Channel Chemicals Co., Ltd. for rubber chemicals supports.

References

- [1] R. Nordin, C. M. S. Said and H. Ismail, *Solid State Technol.* **15** (2007) 83-91.
- [2] R. Syafri, I. Ahmad and I. Abdullah, *Sain Malaysia.* **40** (2011) 749-756.
- [3] A. I. Khalf and A. A. Ward, *Mater Des.* **31** (2010) 2414-2421.
- [4] E. L. Chong, I. Ahmad, H. M. Dahlan and I. Abdullah, *Radi. Phys. Chem.* **79** (2010) 906-961.
- [5] N. A. Maziad, D. E. EL-Nashar and E. M. Sadek, *J. Mater Sci.* **44** (2009) 2665-2673.
- [6] J. Bera and D. D. Kale, *J Appl Polym Sci.* **110** (2008) 1271-1279.
- [7] L. Luduena, D. Fasce, V. A. Alvarez and P. M. Stefani, *Bioresour.* **6** (2011) 1440-1453.
- [8] S. Mishra, A. M. Mohanty, L. T. Drzal, M. Misra and G. Hinrichsen, *Macromol. Mater. Eng.* **289** (2004) 955-974.
- [9] K. G. Mansaray and A. E. Ghaly, *Bio Techn.* **65** (1998) 13-20.
- [10] B. S. Ndazi, C. Nyahumwa and J. Tesha, *BioResource.* **3** (2007) 1267-1277.
- [11] D. De, D. De and B. Aldhikari, *Polym. Adv. Technol.* **15** (2004) 708-715.
- [12] J. Wang, W. Wu, W. Wang and J. Zhang, *J Appl Polym Sci.* **121** (2011) 681-689.
- [13] M. Jacob, S. Thomas and K. T. Varughese, *Compost Sci Technol.* **64** (2004) 955-965.
- [14] H. Ismail and H. P. S. A. Khalil, *Polym. Test.* **20** (2001) 33-41.

BIOGRAPHY

Ladawan Srisuwan was born on September 24, 1986 in Chumphon, Thailand. She graduated from Maejo University in 2009 with Bachelor's degree in Material Science. She then continued her Master's degree in Polymer Engineering at School of Polymer Engineering, Institute of Engineering, Suranaree University of Technology. During her study, she presented two posters entitled **“Physical Properties of Rice Husk Fiber/Natural Rubber Composites”** in the 20th Processing and Fabrication of Advanced Materials (PFAM XX) in Hong Kong, China, and **Properties of Rice Husk Fiber/Natural Rubber Composites: Effect of Rice Husk Surface Modification** in Pure and Applied Chemistry International Conference 2012 (PACCON2012) in Chiang Mai, Thailand.